A STUDY AND IMPROVEMENT IN DESIGN OF ENGINE MOUNT OF THREE WHEELER VIKRAM

by

NALIN JOSHI

DEPARTMENT OF MECHANICAL ENGINEERING

INDIAN INSTITUTE OF TECHNOLOGY KANPUR

MAY, 1994

A STUDY AND IMPROVEMENT IN DESIGN OF ENGINE MOUNT OF THREE WHEELER VIKRAM

A Thesis Submitted

in Partial Fulfilment of the Requirements

for the degree of

MASTER OF TECHNOLOGY

by

NALIN JOSHI

to the

DEPARTMENT OF MECHANICAL ENGINEERING

INDIAN INSTITUTE OF TECHNOLOGY, KANPUR

May, 1994

C E R T I F I C A T E

It is certified that the work contained in this thesis, entitled " A Study and Improvement in Design of Engine Mount of Three Wheeler Vikram ", by *Nalin Joshi*, has been carried out under our supervision and that this work has not been submitted elsewhere for a degree.

Dr. N.N. Kishore
Professor
Department of Mech. Engg.
Indian Institute of Technology
Kanpur - 208016

Dr. Prashant Kumar
Professor
Department of Mech. Engg.
Indian Institute of Technology
Kanpur - 208016

May, 1994.

ABSTRACT

Rubber has been in use for the isolation of engine vibrations for a very long time from now. When, the engine is on a passenger vehicle, the isolation becomes very important. In the three wheeler " *Vikram* ", the power plant has been changed to 4-stroke diesel engine in place of original 2-stroke petrol engine. There are sharp distinct resonant conditions prevailing, resulting in large vibrations of the whole vehicle. The objective of the present work is to study the engine-mount system of Vikram and suggest modifications.

The engine mount system has been modelled as a rigid block supported on six inclined elastic members placed symmetrically about the longitudinal axis of the engine. The analysis results in six dominant natural frequencies corresponding to the six degrees of freedom of the system. The resonating natural frequencies are identified and a dependencies of these frequencies, on the geometrical location of the isolators is investigated.

The analysis required certain hardware properties of the engin-mount system such as moment of inertias of the engine, stiffnesses of the rubber isolator etc, which were experimentally determined.

From the parametric studies, two locations are identified, on the basis of which two designs are proposed. DESIGN 1, will considerably reduce vibrations at the idling, while DESIGN 2, will reduce the rocking of engine, thereby tackling the problem of exhaust pipe breakage, and will also curb the vibrations at the idling.

A finite element study of the Chassis is also undertaken to investigate its vibrational modes which reveals that present structure is satisfactory for vibrations at idling.

ACKNOWLEDGEMENT

I express my deep sense of gratitude and indebtedness to my thesis supervisors Dr. Prashant Kumar and Dr. N.N. Kishore for their invaluable guidance and constant encouragement through out the present work. Their attitude has been a constant source of inspiration to me. I am equally thankful to Dr. B. Sahay for introducing me to this project.

I am also grateful to Dr. A.Sahay, General Manager, Scooters India Limited Lucknow, for the great help rendered during the course of this project and also making one model of Vikram available for experimentation. My sincere thanks to Late Mr. Sarkar, Mr. Singh, Mr. Sen and Mr. Chakraborty for their cooperation and valuable suggestions.

My sincere thanks to Mr M.M Singh, incharge vibration lab,for helping me with my experimentation on the vehicle and Mr. Rao, incharge structures lab, for letting me avail the facilities at the lab.

I am grateful to all my friends in E.S.A lab for for their help given to me during my work. A special word of appreciation is due to Mr. Anurag Goel and Mr. R.C. Tiwari for their kind help in fabricating the experimental set up.

I am also thankful to wonderful company of dear friends, in particular, Ashok, Ashwani, Kailash, Kanu, Pathak, Rajesh, Sanjay, Vivek, Vikash, Venktesh and Virendra, who made my stay at IIT, Kanpur a memorable one.

Nalin Joshi

CONTENTS

NOMENCLATURE

a, a_i	Vertical distance of C.G. of the engine power pack from the center of the front and i^{th} isolator respectively.
b, b_i	Horizontal distance of C.G. of the engine power pack from the center of the front and the i^{th} isolator respectively, in X direction.
c_i	Horizontal distance of C.G. of the engine power pack from the center of the i^{th} isolator respectively, in Z direction.
E	Young's Modulus of elasticity.
F_p	Force developed in p direction.
F_{xy}	Force acting in X direction as a result of deflection of engine C.G. in Y direction.
$F_i(t)$	Force acting in X direction as a function of time.
G	Shear modulus of elasticity.
M	Mass of the engine.
$M_x(t)$	Moment acting on the engine about X axis as a function of time.
$(M_{xy})_i$	Couple acting about X axis due to deflection of i^{th} isolator in Y direction.
[M], [m]	Mass matrix, global and elemental.
K_{xy}	Force acting in X directon for unit displacement in Y direction.
[K], [k]	Stiffness matrix, global and elemantal.
I_x	Moment of inertia of the engine about X axis.
[N]	Shape functions.
u_0, v_0, w_0	Translation of C.G. of engine in X, Y,and Z directions respectively.
u_i, v_i, w_i	Deflection of the i^{th} isolator in X, Y, and Z direction respectively.
δ_p, δ_q	Deflection of rubber in p, q direction repectively

δ_x, δ_Y, δ_z	Deflection of rubber in X,Y, Z direction.
θ, θ_i	Angle of inclination made by the nornal of front isolator and the i^{th} isolator with the X direction.
θ_x, θ_y, θ_z	Angular displacement of the C.G.of the power pack about X, Y and Z axis.
ω_1	Natural frequency of the engine-mount system responsible for the rocking mode vibrattion of the engine about Z axis.
ω_2	Natural frequency of the engine-mount system responsible for vibratting the vehicle at idling.
ω_3	The third natural frequency of the engine-mount system that is observed it observed experimentally.

LIST OF FIGURES

LIST OF TABLES

CHAPTER 1

INTRODUCTION

.1 BACKGROUND:

n our country, one of the popular vehicles of city transport is hree wheeler, for reasons of economy. One such three wheeler *'Vikram"* is manufactured by Scooters India Limited Lucknow. This hree wheeler has a major share of market in Uttar Pradesh.

his vehicle was originally designed by the Italian Company *'iaggio*, with a two-stroke petrol engine. To suit Indian onditions, the three wheeler was modified by replacing petrol ngine with an indigenous diesel one and increasing the length of he chassis.

he two-stroke petrol engine on the three wheeler was very small n size, half the weight of the diesel engine and it runs at much ıigher engine speeds as compared to the present one. The engine ıounting of the petrol version were designed such that most of its ıatural frequencies pertaining to dominant mode, fell below the ıdling speed of the engine. Being a two stroke engine, the firing frequency(frequency of power stroke of engine) equaled the engine rotational speed. As a result the minimum forcing frequency which had to be taken care of while designing was the idling speed. Thus less weight, high speed of the engine and it being a two stroke engine, makes a good engine mounting system possible without designing the system very soft, which otherwise would have made the system unstable.

The present engine is single cylinder four- stroke diesel engine which was primarily designed for, agricultural needs such as pumping water, running the threshers etc. Because the engine has been designed to be anchored at one place and not for a vehicle, the unbalanced forces were not minimized.So at resonant conditions large forces are transmitted to the chassis.

Here as the engine is four-stroke, the minimum forcing frequency that has to taken care of, is the firing frequency, which in four stroke engine runs at half the engine running speed, and add to that the engine operating speed is low. Thus to escape resonant frequency of system, a very soft mounting system is required which would essentially make the system unstable with such a large mass on it accompanied by heavy forces and moments coming on it.

In the present vehicle, there are two major resonant phases, that are encountered during the entire engine speed range. First one is at idling, in which heavy vibrations are experienced by the vehicle. The vehicle, by the nature of it's use, has to come back to idling, quite frequently,for loading and unloading the passengers and at the traffic lights, thereby the vehicle stays at the resonant phase for some time.

Second resonant phase is encountered as the vehicle picks up speed, results in large rocking of the engine. These include large angular deflection θ_z about Z axis, as shown in Fig.1.1, is observed. Though this stage is transient as vehicle accelerates but this rocking causes frequent breakage of exhaust pipe. As shown in Fig. 1.1, the exhaust pipe is a single right angled bend pipe, whose one end is bolted rigidly to the engine and the far end (having a silencer) is parallel to the length of the vehicle. This end just hangs from the chassis through a flexible pad made of cotton sheets bonded together. The far end can not be rigidly mounted as it needs to allow the free movement of the exhaust pipe with the engine, while the later rocks. The exhaust comes out of exhaust pipe with a certain frequency governed by the engine speed. When this frequency matches with the natural frequency of the pipe, large axial movement of pipe, shown in Fig.1.1, occurs. Let pipe be divided in three parts P_1 , P_2 and P_3. At the resonant condition of pipe, P_3 vibrates axially. This axial movement results in torsional rotation of the hung pipe, leading to breakage of P_1 section of the pipe, at section P - P'. Under the rocking motion of the engine, the displacement of the

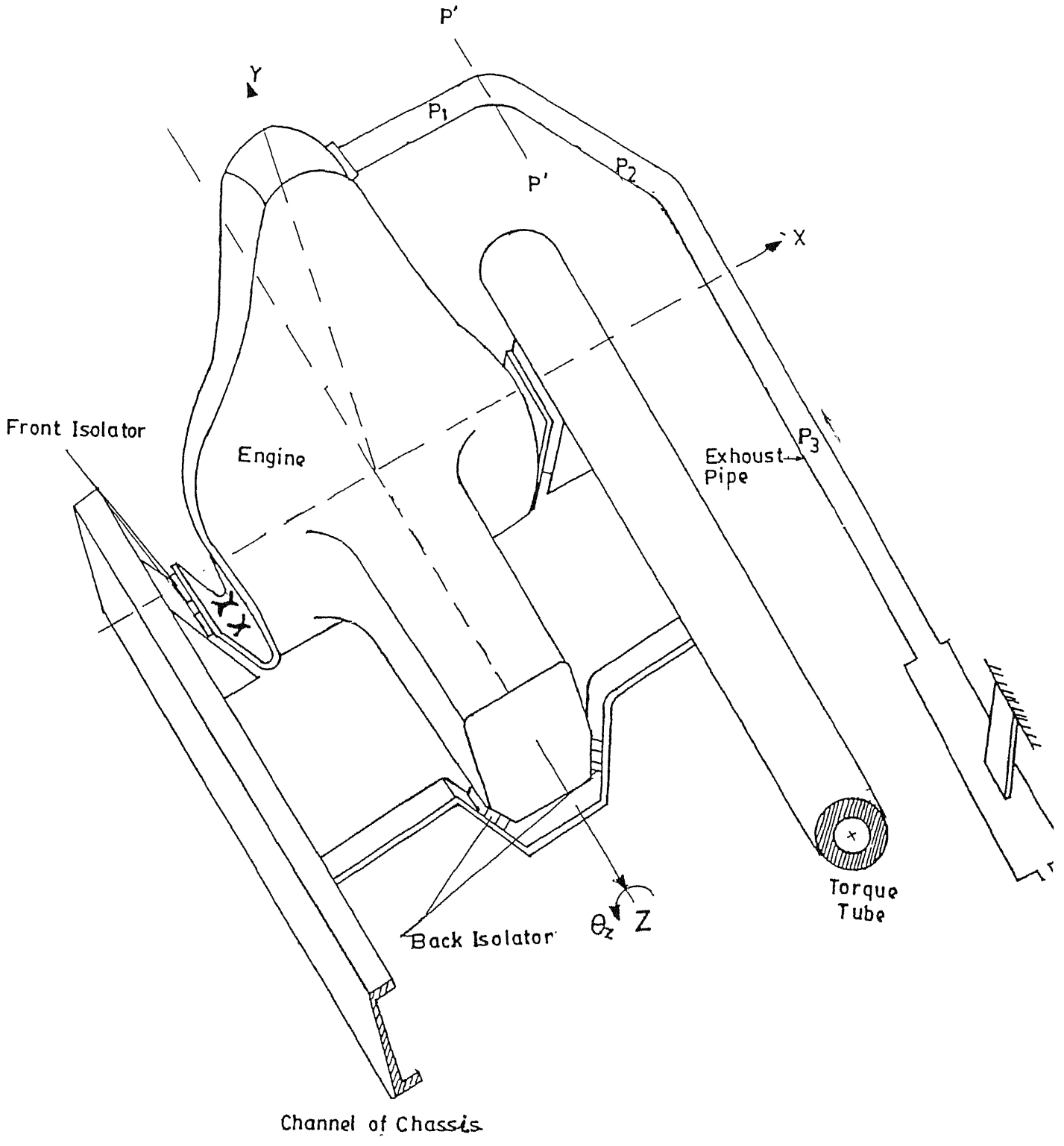

Fig.1.1 Schematic Diagram of Engine and Exhaust Pipe

exhaust pipe, resulting in bending of section P_1 and P_2, superimposed on the torsional movement of pipe, thereby aggravating the problem of pipe breakage. Besides that, the stud holding the pipe to the engine comes under axial forces as a result of inertia forces and the bending of pipe, resulting in it's frequent breakage also.

Thus the modified model of the three wheeler has two major problems. First, the ride is not smooth even at the idling conditions and as the vehicle picks up speed, it goes through one more resonant condition. Secondly, the exhaust pipe fails quite frequently because of the excessive vibrations resulting into maintenance discomforts in the field and unpopularity of the model.

1.2 LITERATURE SURVEY:

The automobile is subjected to vibrations from external sources such as from roads, winds etc. or from engine forces. For the passenger comfort and for longer life of the vehicle, structure needs to be isolated from these forces. Isolation of vibration in can be said to be temporary storage of energy and it's subsequent release with a certain time lag.

The vibrations can be controlled by three methods namely,

(i) Reduce the exciting force if possible by balancing.
(ii) Isolate by proper placement of resonant frequencies.
(iii) Provide damping to dissipate energy.

The isolation of rotating and reciprocating machinery to reduce the magnitude of oscillation forces transmitted to adjacent structure is a common practice.

The requirement for a successful machine installation is that the force transmitted to the supporting foundations be small. The above requirement may be met by adjusting the various natural frequencies of the system made of engine and it's supporting springs or rubber pad. The problem is resolved by controlling the natural frequencies.

In the year 1920 , the rubber was introduced as isolators for the mounting of the machines and engines. Stewart & Hull [1] first introduced the analytical modeling for bottom mounted bodies, using rubber isolators. The problem in mechanical sinusoidal motion was solved for steady state conditions by equivalent analogous electrical circuit, solving for complex quantities.

From 1940s, the designers have been trying to decouple the natural modes of vibration of a body, one from another, by adjusting orientation and location of the isolators. Each mode of vibration then exist independently of the other, i.e vibration in one mode doesn't excite the other. Each natural frequencies can then analyzed and controlled independently.

Crede [2] suggests that, locating the isolators in a horizontal plane passing through the center of gravity of the mounted body, such that the distance between the isolators, mounted either side of C.G., be twice the radius of gyration of the mounted body and the shear and normal stiffness of the isolators be equal, will result in decoupling the various modes. Crede and Walsh [3] suggests that, as many as possible, the various coupled frequency be made equal, by proper adjustment of the stiffness of isolators and its location, resulting in a single frequency that needs to be handled.

The above method of mounting was used, however locating isolators in a horizontal plane through center of gravity was not possible for very heavy machine, and therefore bottom mounting was required. To augment the above problem Crede suggested isolators be inclined. The inclination should be such that elastic axis (a line through which the application of force cause translation without rotation) and the center of gravity coincide, resulting in decoupling of translatory and rotary modes. Besides the decoupling inclining the isolators put the isolators both in compression and shear loading from just compression loading in non-inclined one. Inclination makes the system softer and results in increased stability of the mounted body. Scooter's India Limited, Lucknow, while designing the engine mount had gone by the

above practice.
Decoupling is very difficult and options available to the designer are limited to a few possibilities. These days, not many designers design for this condition. As most of the times, it is not possible to get all the desired natural frequencies, out of the range of forcing frequency resulting a large vibration of a particular mode, coupling up the various modes is beneficial.

During the running of the vehicle some natural frequencies have to be encountered, it is desirable that some form of damping should be present in the system, otherwise the amplitude of vibrating body would be very high. This damping is provided by a dashpot or a pad made of a flexible material. After investigating several possible materials, Hull [4] suggests rubber as the material, for this purpose. The relevant properties for various rubber materials, for a rectangular slab, under compression and shear loading are presented and discussed by DownieSmith [5].

A finite element study of the chassis structure has been undertaken assuming chassis as a space frame and proceeding on as suggested by Krishnamoorthy [11] and Weaver and Johnston [12].

1.3 SUMMARY OF THE PRESENT WORK:

The present work aims at bringing out an improved design of the engine-mounting system which encounters least number of resonating phases as possible during its operation and thus look for a design that results in less breakage of the exhaust pipe.

Chapter 2 deals with the modelling of engine mount system. The system parameters required in modelling such as rubber stiffnesses, weight of engine and it's inertia's are determined experimentally in Chapter 3 and the procedure is explained. The analytical results from the modelling are stated and discussed in Chapter 4 and the results obtained are verified by experimental observation in Chapter 5. Finally the improved designs are proposed in Chapter 6 and Chapter 7 recommends the further work that can be undertaken on the vehicle.

CHAPTER 2

FORMULATION OF THE PROBLEM

2.1 INTRODUCTION:

In this chapter, the constitutive equations of the engine and rubber mount system have been described in detail. They are modelled as a rigid block mounted on six rubber isolators. The modelled rigid block comprises of the engine except the fuel above piston, piston, connecting rod and the crank.

2.2 FORMULATION:

Rubber springs are made from highly elastic long-chain molecular material referred to as high polymers. The effective elasticity of rubber can be varied greatly, by shape of rubber spring.

For designing a vibration isolator inclined at an angle θ (Fig.2.1), following stiffness parameters are important,

- K_{xx} : force acting in X direction due to unit deflection in X direction of the isolator.
- K_{xy} : force acting in X direction due to unit deflection in Y direction of the isolator.
- K_{yy} : force acting in Y direction due to unit deflection in Y direction of the isolator.
- K_{yx} : force acting in Y direction due to unit deflection in X direction of the isolator.

For finding K_{xx}, let δ_p and δ_q are the deflection of the spring owing to F_p and F_q in P and Q directions respectively, as a result of δ_x deflection in X direction (Fig.2.1).

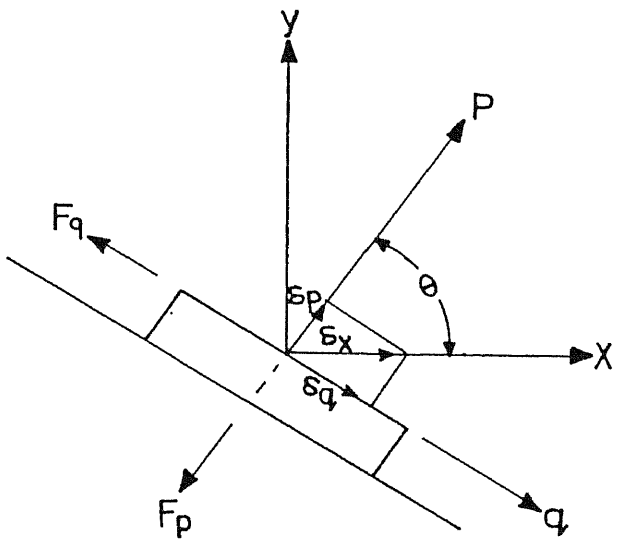

Fig. 2.1 Principal Elastic Axes of Inclined Isolator

δ_x can be expressed as,

$$\delta_p = \delta x \cos\theta$$
$$\delta_q = \delta x \sin\theta \qquad (2.1)$$

Due to these deflections forces F_p and F_q are developed in P and Q directions respectively, where

$$F_p = K_p \delta_p$$
and
$$F_q = K_q \delta_q \qquad (2.2)$$

Force acting in X direction, F_{xx}, becomes

$$F_{xx} = -(F_p \cos\theta + F_q \sin\theta)$$
$$= -(K_p \delta_p \cos\theta + K_q \delta_q \sin\theta)$$
$$= -(K_p \delta x \cos^2\theta + K_q \delta x \sin^2\theta) \qquad (2.3)$$

Thus, from the definition of K_{xx}, we have

$$K_{xx} = \frac{F_{xx}}{\delta x}$$
$$= -(K_p \cos^2\theta + K_q \sin^2\theta) \qquad (2.4)$$

Force acting in Y direction, F_{yx}, becomes

$$F_{yx} = - (F_p \sin\theta - F_q \cos\theta) \quad (2.5)$$
$$= - (K_p \delta x \cos\theta \sin\theta - K_q \delta x \sin\theta \cos\theta)$$

leading to,

$$K_{yx} = - (F_p \cos\theta \sin\theta - F_q \sin\theta \cos\theta) \quad (2.6)$$

Similarly the value of K_{yy} and K_{xy} are obtained.

$$K_{yy} = - (K_p \sin^2\theta + K_q \cos^2\theta) \quad (2.7)$$

$$K_{xy} = K_{yx} \quad (2.8)$$

As shown in Fig.2.2 the present engine is symmetrical with respect to a plane normal to X axis through center of gravity, from now on referred as X-plane.

The modelled rigid block experiences different transient forces and moments, resulting from the forces resulting from the explosion inside the cylinder. These forces have been dealt with, in chapter 3.

In the present vehicle the center of gravity of the engine power plant O is assumed to be on the crankshaft axis slightly in front of the plane of connecting rod movement (vertical plane through Q, (Fig.2.2). The forces and moments on the block come from the inertia forces of the piston, connecting rod and crank acting at Q and from the explosive force in the cylinder (the part of the block). Therefore the present model assumes to sustain two forces in X and Y directions acting at Q, resulting from inertia forces, and a couple about Z axis resulting from the explosive force generated inside the engine cylinder.

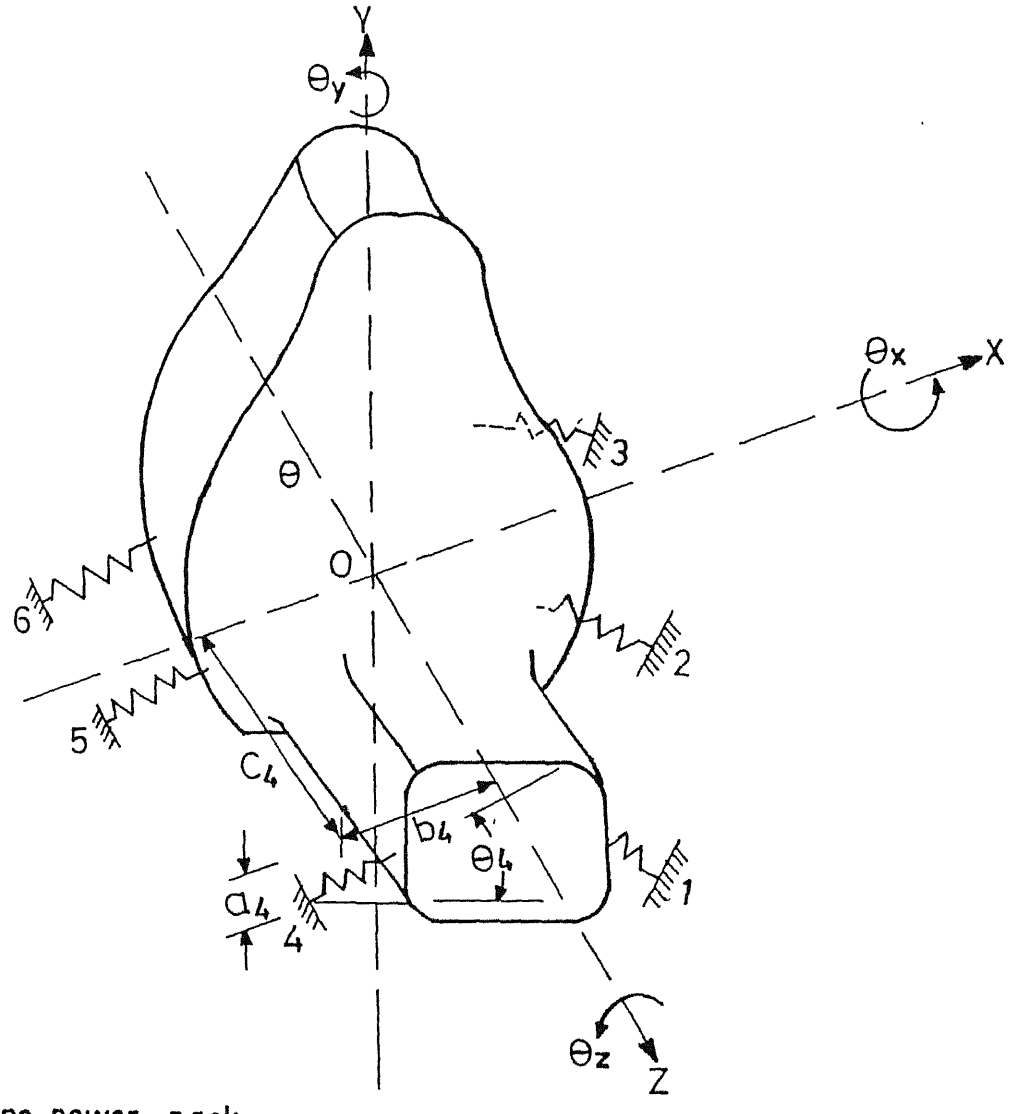

O : C.G of engine power pack

a_4 : Vertical distance of 4th isolator to C.G. axis

b_4 : Horizontal distance of 4th isolator to C.G. axis in X direction

C_4 : Horizontal distance of 4th isolator to C.G. in Z direction.

Fig. 2.2 Schematic Diagram of Modelled Engine

Thus, the engine mount system encounters following forces and moments.

$F_x(t)$:Forces acting in X direction, is a function of time.
$F_y(t)$:Forces acting in Y direction, is a function of time.
$M_z(t)$:Moment acting about Z axis , is a function of time.
$M_y(t)$:Moment acting about Y axis, due to $F_x(t)$ acting at Q.
$M_x(t)$:Moment acting about X axis, due to $F_y(t)$ acting at Q.

For developing the equations of motion, let u_0,v_0 and w_0 are translation in X,Y and Z directions and θ_x, θ_y and θ_z be the angular displacements of the engine about X,Y and Z axes.

Force balance along X axis can be written as,

$$M\ddot{u}_0 = \text{Forces acting in X direction}$$
$$= F_x(t) + \text{reaction of isolators in X dir.}$$

Deflection of i^{th}isolator in X direction is

$$u_i = u_0 + c_i\theta_y + a_i\theta_z \qquad (2.9)$$

Deflection of i^{th}isolator in Y direction is

$$v_i = v_0 + c_i\theta_x \qquad (2.10)$$

where,

a_i= vertical distance of the i^{th} isolator from C.G of the engine,

b_i= horizontal distance of i^{th} isolator from engine C.G along X direction,

c_i= horizontal distance of the engine C.G from the i^{th}isolator locations along Z axis(Fig. 2.2).

Reaction in X direction of isolators is given as

$$F_{xx} = \sum_{i=1}^{6} (K_{xx})_i u_i$$

where, $(K_{xx})_i$ is the stiffness and u_i is the deflection of the i^{th}isolator.

similarly,

$$F_{xy} = \sum_{i=1}^{6} (K_{xy})_i v_i$$

Thus, equation of motion along X axis, is given as,

$$M \ddot{u}_0 = F_x(t) + \sum_{i=1}^{6} (K_{xx})_i (u_0 + c_i\theta_y + a_i\theta_z) + \sum_{i=1}^{6} (K_{xy})_i (v_0 + c_i\theta_x) \qquad (2.11)$$

As the engine is symmetrical about X-plane, the vibrational modes in this plane are completely decoupled from the modes in the other planes. Hence two pairs of independent co-ordinates that is $(u_0, \theta_z \ \& \ \theta_y)$ and $(v_0, \theta_x \ \& \ w_0)$ are used, which amongst themselves are thoroughly coupled.

As a result, in equation 2.11

$$\sum_{i=1}^{6} (K_{xy})_i (v_0 + c_i\theta_x) = 0$$

Similarly equation of motion along Y axis,

$$M \ddot{v}_0 = F_y(t) + \sum_{i=1}^{6} (K_{yy})_i (v_0 + c_i \theta_x) \qquad (2.12)$$

And equation of motion along Z axis,

$$M \ddot{w}_0 = F_z(t) + (K_z) \sum_{i=1}^{6} (w_0 + a_i\theta_x) \qquad (2.13)$$

Equation of Motion of engine for rotation about Z axis,

$$I_z \ddot{\theta}_z = M_z(t) + \text{Couple acting about Z axis due to reactions of isolator.}$$

Couple acting about Z axis due to deflection in X direction at the i^{th} isolator,

$$(M_{zx})_i = (K_{xx})_i (u_0 + c_i\theta_y + a_i\theta_z) a_i + (K_{yx})_i (u_0 + c_i\theta_y + a_i\theta_z) b_i \qquad (2.14)$$

Couple acting about Z axis due to deflection in Y direction at the i^{th} isolator,

$$(M_{zy})_i = (K_{xy})_i (b_i \theta_z) a_i + (K_{yy})_i (b_i \theta_z) b_i \qquad (2.15)$$

Using $(M_{zy})_i$ and $(M_{zx})_i$, the equation of motion for rotation about Z axis,

$$I_z \ddot{\theta}_z = M_z(t) + \sum_{i=1}^{6} (M_{zx})_i + \sum_{i=1}^{6} (M_{zy})_i \qquad (2.16)$$

Similarly writing equation of motion for rotation of the engine about X axis,

$$I_x \ddot{\theta}_x = M_x(t) + \sum_{i=1}^{6} (M_{xy})_i + \sum_{i=1}^{6} (M_{xz})_i \qquad (2.17)$$

where,

M_{xy} :Couple acting about X axis due to Y directional deflection of each isolators.

M_{xz} :Couple acting about X axis due to Y directional deflection of each isolators.

And for any i^{th} isolator,

$$(M_{xy})_i = (K_{yy})_i (v_0 + c_i \theta_x) c_i$$

and

$$(M_{xz})_i = - (K_z)_i (w_0 + a_i \theta_x) a_i$$

And similarly rotation about Y axis is obtained as,

$$I_y \ddot{\theta}_y = M_y(t) + \sum_{i=1}^{6} (M_{yx})_i + \sum_{i=1}^{6} (M_{yy})_i \qquad (2.18)$$

where,

$$(M_{yx})_i = (K_{xx})_i(u_0 + a_i\theta_z + c_i\theta_y)\, c_i$$

$$(M_{yy})_i = (K_{xy})_i(\, b_i\theta_z)\, c_i$$

Writing equations 2.11, 2.12, 2.13, 2.16, 2.17 and 2.18 in matrix form, following form of matrix equation is obtained.

$$[\, M \,]\{\, \ddot{\phi} \,\} + [\, K \,]\{\, \phi \,\} = \{\, F(t) \,\} \qquad (2.19)$$

where,

[M] and [K] are 6 x 6 symmetric matrices given as,

$$[K] = \begin{bmatrix}
-\Sigma(K_{yy})_i & 0 & -\Sigma(K_{yy})_i c_i & 0 & 0 & 0 \\
 & -4\Sigma(K_z)_i & -4\Sigma(K_z)_i a_i & 0 & 0 & 0 \\
 & & -\Sigma(K_{yy})_i c_i^2 + -\Sigma(K_z)_i a_i^2 & 0 & 0 & 0 \\
 & & & -\Sigma(K_{xx})_i & -\Sigma(K_{xx})_i a_i + -\Sigma(K_{xy})_i b_i & -\Sigma(K_{xx})_i c_i \\
 & \text{Symmetric} & & & -\begin{pmatrix} \Sigma(K_{xx})_i\, a_i^2 \\ 2\Sigma(K_{xy})_i b_i a_i \\ \Sigma(K_{yy})_i\, b_i^2 \end{pmatrix} & \begin{matrix} -\Sigma(K_{xx})_i c_i a_i + \\ -\Sigma(K_{yx})_i c_i b_i \end{matrix} \\
 & & & & & -\Sigma(K_{xx})_i c_i^2
\end{bmatrix}$$

$$[M]=\begin{bmatrix} M & 0 & 0 & 0 & 0 & 0 \\ & M & 0 & 0 & 0 & 0 \\ & & I_x & 0 & 0 & 0 \\ & \text{Symmetric} & & M & 0 & 0 \\ & & & & I_z & 0 \\ & & & & & I_y \end{bmatrix}$$

$$\{\phi\} = \begin{Bmatrix} v_0 \\ w_0 \\ \theta_x \\ u_0 \\ \theta_z \\ \theta_y \end{Bmatrix}$$

$$\{F(t)\} = \begin{Bmatrix} F_y(t) \\ 0 \\ M_x(t) \\ F_x(t) \\ M_z(t) \\ M_y(t) \end{Bmatrix}$$

Thus equation-2.9 can be solved to obtain the eigenvalues and the steady state response. Eigenvalues so obtained are the natural frequencies of the engine-mount system.

CHAPTER 3

HARDWARE ELEMENTS

3.1 INTRODUCTION:

The formulation, as discussed in chapter 2, requires the inertias of the engine about its three principal inertia axes, the stiffnesses of the rubber isolators about its three principal elastic axes (about the planes of symmetry, Fig.3.1), the exact location of the isolators in space and the position of the center of gravity of the engine in space.

To know the frequency of the exciting forces and moments, the speed range of the engine is required and to study the dynamic analysis of the engine power pack, the unbalanced forces and moments associated with the engine must be known.

This chapter describes the methods of determining the various properties experimentally.

3.2 ENGINE SPECIFICATION:

Following are some particulars of the engine of VIKRAM.

Make	:	Greaves India Limited, Aurangabad
Type	:	Single Cylinder, 4-Stroke air cooled diesel engine
Cylinder Bore	:	85 mm
Stroke Length	:	90 mm
Cubic Capacity	:	510 cm^3
Max. Output	:	11 H.P at 3000 rpm
Max. Torque	:	3 Kg-m at 2000 rpm
Engine weight	:	102 Kg
Speed range of the engine	:	850-3200 rpm

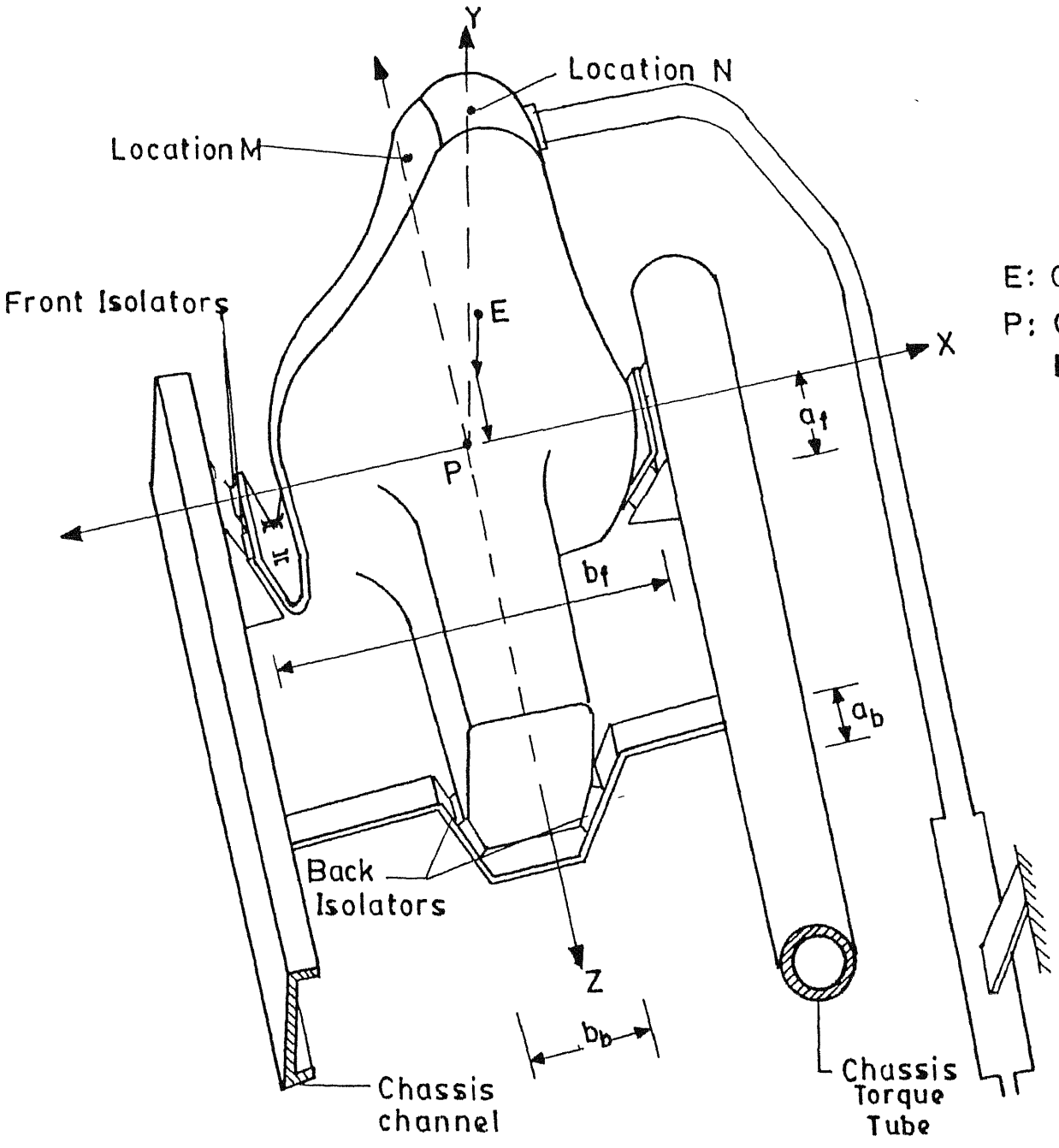

Fig.3.1 Schematic diagram of Engine-mount System

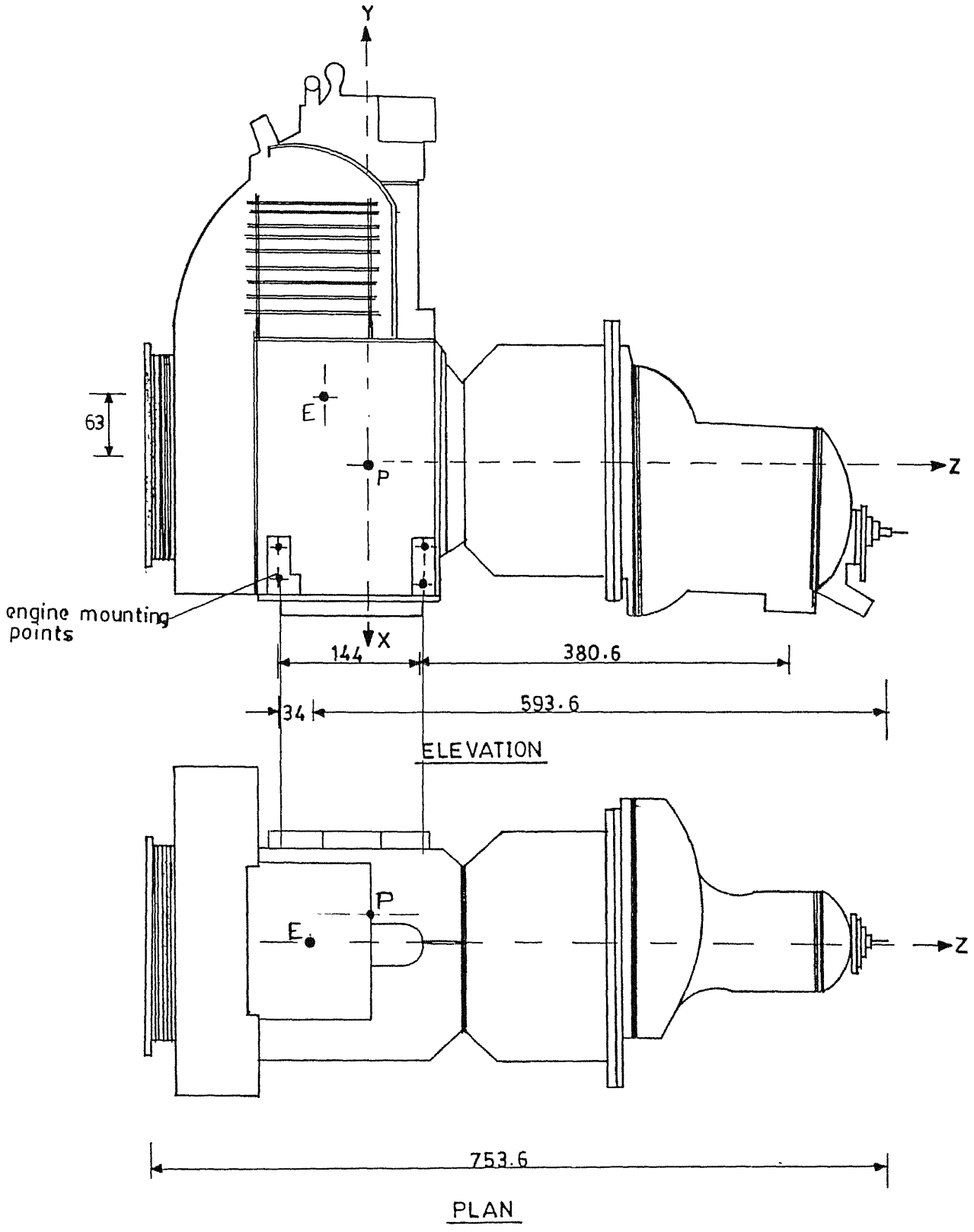

Fig. 3.2 Engine Assembly

(All dimensions in mm)

Engine Power Pack Dimensions:

Engine Height	:	562 mm
Engine Height	:	753.6 mm
Engine width	:	232 mm at mounting points (Fig.3.2)

3.2.1 ENGINE MOUNTING:

The engine and the clutch-gear system are mounted on six inclined rubber isolators as shown in Fig.3.1. Four of them are beneath the engine, named as front isolators and the remaining two are beneath the gear box (a part of power pack), called as back isolators. These isolators are fixed on the inclined rests on the chassis, one on the side channel of the chassis and other on the chassis torque tube. The front isolators are connected to the engine, through two brackets, one on each side (Appendix A), with each bracket housing two isolators attached to it.

Some of the important dimensions of the mounting system (Fig. 3.1) are :

b_f =403 mm (The horizontal distance between two mounting points of the front isolator)

b_b =162.5 mm (The horizontal distance of center of gravity from the mounting support of back isolator)

a_f =160 mm (The vertical distance of center of gravity from the mounting support of the front isolator)

a_b =155 mm (The vertical distance of center of gravity from the mounting support of the back isolator)

3.2.2 CENTER OF GRAVITY:

The center of gravity of the engine and engine-clutch-gear system is shown in the engineering drawing (Fig.3.2). Point E denotes the center of gravity of engine and point P denotes that of engine power pack (engine and clutch-gear system). The center of gravity of engine (P) lies in the vertical plane passing through the crank

shaft axis, 63 mm above the axis. The power pack's center of gravity is 21 mm off from the vertical plane passing through the crankshaft in positive X direction.

3.2.3 MOMENTS OF INERTIA: Theoretical Development

Because the moment of inertia of the engine, about its three principal axes could not be obtained by the supplier of the engine, they were determined experimentally.

Theory:

One method of determining moment of inertia is by using the concept of angular oscillations. The engine is placed on a platform which is hung by three wires (Fig.3.3). The rigid platform having a weight W Kgs, hangs by three long parallel steel ropes such that the axis about which moment of inertia is to be measured is vertical. The other end of the steel ropes are tied at three equidistant points on a supporting frame. When the suspending platform is given a small angular displacement about the vertical axis, tangential restoring force come into play and the platform begins to oscillate. Knowing the period of oscillation τ and the geometry of the torsional pendulum, the moment of inertia can be determined. For developing the relation between moment of inertia and the time period of oscillation, let α be a small angular displacement of the platform (Fig.3.3) at any particular instant of time and θ_i be the inclination of the rope from the vertical. Then the tangential restoring force F_i in the i^{th} rope is

$$\begin{aligned} F_i &= W_i \operatorname{Sin} \theta_i \\ &\cong W_i \theta_i \\ &= \frac{W_i \alpha r_i}{L} \end{aligned} \qquad 3.1a$$

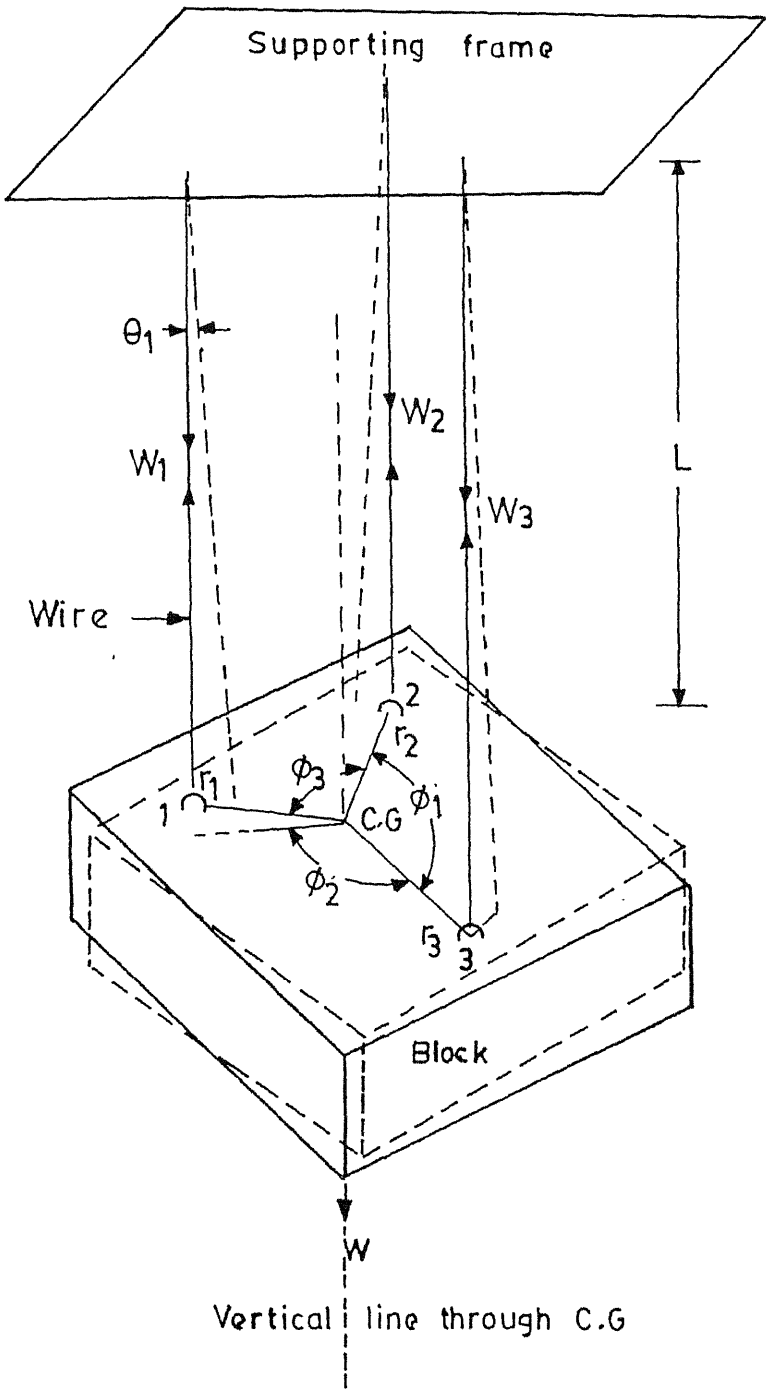

Fig. 3.3 Determination of moment of inertia

where L is the length of steel rope, W_i is the portion of the hanging weight taken by the i^{th} rope and r_i is the distance of the center of gravity from the i^{th} rope.

The torsional stiffness of the entire system is

$$K_\alpha = \sum_{i=1}^{3} \frac{F_i r_i}{\alpha} \qquad (3.1b)$$

knowing the time period, τ, of the torsional pendulum moment of inertia, I, can be calculated as

$$I = \frac{\tau^2 K_\alpha}{4\pi^2} \qquad (3.2)$$

Substituting the values of K_α from Eqs.3.1 in equation 3.2,

$$I = \frac{W r_1 r_2 r_3 \tau^2}{4\pi^2} \left[\frac{r_1 \sin\phi_1 + r_2 \sin\phi_2 + r_3 \sin\phi_3}{r_1 r_2 \sin\phi_3 + r_2 r_3 \sin\phi_1 + r_1 r_3 \sin\phi_2} \right] \qquad (3.3)$$

Where ϕ_1, ϕ_2 and ϕ_3 are angular displacements as shown in Fig.3.3. If the center of gravity is at such a position that $r_1 = r_2 = r_3$, equation 3.3 simplifies to

$$I = \frac{W r^2 \tau^2}{4\pi^2} \qquad (3.4)$$

Before the engine is placed over the platform the moment of inertia, I_1, is obtained for the hanging platform. Now when the engine is loaded on the the platform I_2, the combined moment of inertia, is obtained. Then, the moment of inertia of the engine is obtained by subtracting I_1 from I_2.

3.2.4 MOMENT OF INERTIA: Experimental Set-up

With the theory in the backdrop, an experiment was devised. The main elements for the experiment set-up were (Fig.3.4)

i) The supporting frame.

ii) The suspending steel rope.

iii) The platform.

Fig.3.4 Experimental Set-up

Experimental Set-up:

The experiment was done in Structures laboratory of Civil Engineering department, I.I.T Kanpur, as it had half meter thick roof with, through the thickness holes at regular intervals.

To the roof a frame was rigidly clamped, which in turn act as a rigid support for the base platform and the steel ropes. The base frame i.e the platform, is suspended through steel ropes. The different elements comprising the assembly are given as under:

(a) ROOF FRAME:

As shown in Appendix A,the roof frame is a rectangular frame, made out of angle irons, with four hole, one each at its four corners, for bolting it on to the roof. The frame has three additional holes, forming a equilateral triangle amongst themselves, for suspending a steel rope from one each.

(b) BASE FRAME:

Base frame is a triangular steel frame with the ends flattened as shown in Appendix A. It is made out of angle irons. On top of the frame a 6 mm thick mild steel plate frame is welded. The Base frame was tied to the hanging ropes at the three flattened ends.

(c) LONG STEEL BOLTS AND NUTS:

The Roof frame is fixed to the thick roof by long steel bolts specially made from 10 mm diameter mild steel rods. The head of the bolts was made by welding a nut to one end of the bar.

(d) ROOF WASHER:

The Roof washer are rectangular slabs, to act as base for tightening the nut on the long bolt that projects out of the top of the thick roof slab and to prevent the lateral movement of the bar in the hole as the bore of the hole is larger than the diameter of bar.

(e) STEEL ROPES:

The steel ropes of 4.5 mm diameter was chosen through which the platform could be hung. These ropes were preferred over steel wire for flexibility and safety.

3.2.5 EXPERIMENTAL RESULTS:

The axis about which inertias are desired, should be placed vertical on the platform of the torsional pendulum (Section 3.1.3). Hence, while calculating I_x, XX axis should be vertical,

and likewise for other axes. Thus engine can be put on the platform in three different positions, such that, any one of X, Y or Z axis is vertical. Fig. 3.5b shows, position A, i.e when Z axis is vertical, Fig. 3.6b shows position B, when Y axis is vertical and Fig 3.7b shows Position C when X axis is vertical.

To keep the steel ropes taut, initial weights are kept on the platform.

In all the three positions:

Mass of the platform + initial weights	W_i =	29.2	kg
Mass of the engine power pack	W_e =	102	kg
Mass of the engine power pack + platform + intialweights	W =	131.2	kg
Length of steel rope	L =	1760	mm

The experiment was done first by placing the engine and initial weights and finding out the period of oscillation, and then by off loading the engine and noting down the period of the oscillation. The time of at least 15 oscillation was recorded to determine the period of oscillation.

(i) MOMENT OF INERTIA ABOUT Z AXIS (I_z)

I_z is calculated, when the engine has been placed in Position A (Fig. 3.5). The engine is placed so that vertical axis through the center of gravity of platform passes through the center of gravity of the engine power pack. This has been ensured by placing the engine flywheel on a wooden circular base whose center passes through the centroid of the triangular platform.

The period of oscillation with engine loaded on the platform is found to be

$$\tau_1 = 1.475 \pm 0.01 \quad \text{sec}$$

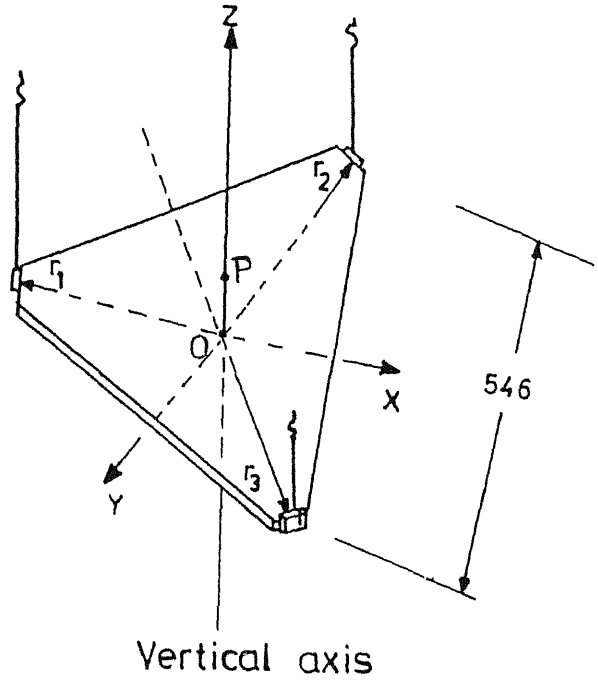

P: Engine C.G

O: platform C.G.

Fig.3.5a Vertical Axis through C.G.s in Position A

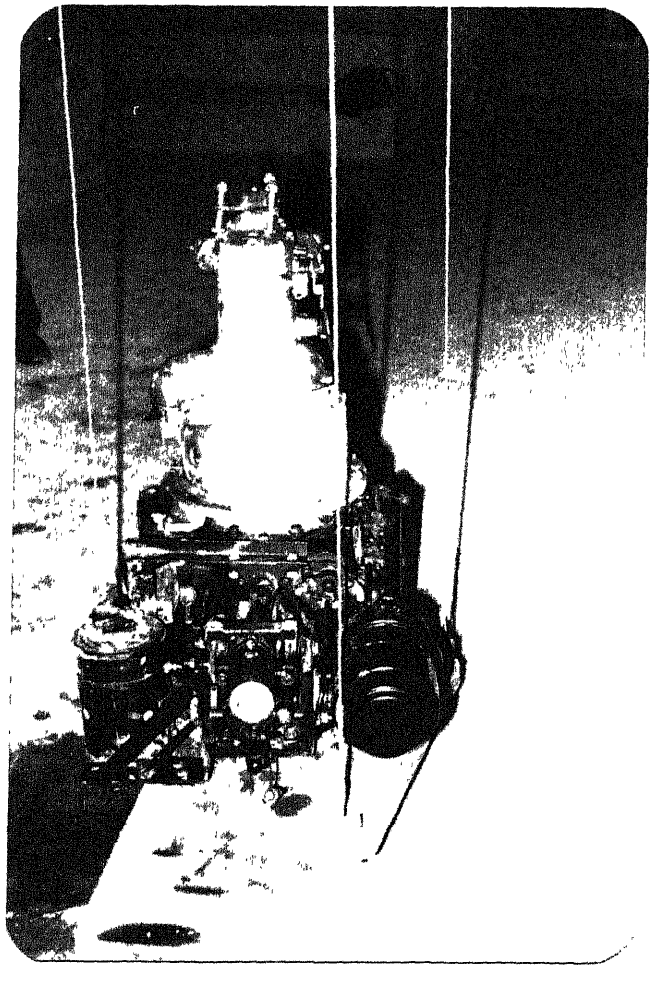

Fig.3.5b Engine Placed in Position A

The period of oscillation with the engine off loaded is found to be

$$\tau_2 = 1.939 \pm 0.01 \quad \text{sec}$$

From Fig.3.5b

$$r_1 = r_2 = r_3 = 0.313 \text{ m}$$

From equation 3.4, moment of inertia of engine and platform and initial weight together about Z axis is

$$I_{AA} = 3.948 \text{ kg-m}^2$$

Moment of inertia of platform and initial weights together about Z axis is

$$I_A = 1.52 \quad \text{kg-m}^2$$

Moment of inertia of the engine is

$$I_z = 2.42 \quad \text{kg-m}^2$$

The radius of gyration of the engine about Z axis is,

$$R_z = 0.154 \text{ m}$$

(ii) MOMENT OF INERTIA ABOUT Y AXIS (I_Y)

In Position B as shown in Fig. 3.6, the vertical axis through the center of gravity of the Base frame (P-P) and through the engine center of gravity (Y-Y) do not coincide. In such case, the C.G of the system (engine and platform combined) should be found. Vertical axis through system C.G., is shown as S-S in Fig.3.5a, with the following dimensions and angles.

$r_1 = 283$ mm, $r_2 = 315$ mm, $r_3 = 344.6$ mm,
$\phi_1 = 110.6°$; $\phi_2 = 123°$; $\phi_3 = 126.4°$.

The period of oscillations recorded with engine on the platform is found to be

$$\tau_1 = 1.753 \pm 0.02 \text{ sec}$$

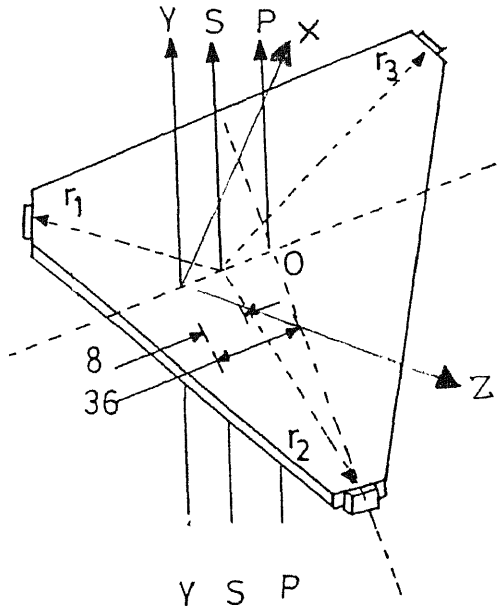

P-P : Vertical axis through C.G of platform.

S-S : Vertical axis through C.G of system.

Y-Y : Vertical axis through C.G of power pack.

Fig.3.6a Vertical Axis through C.G.s in Position B

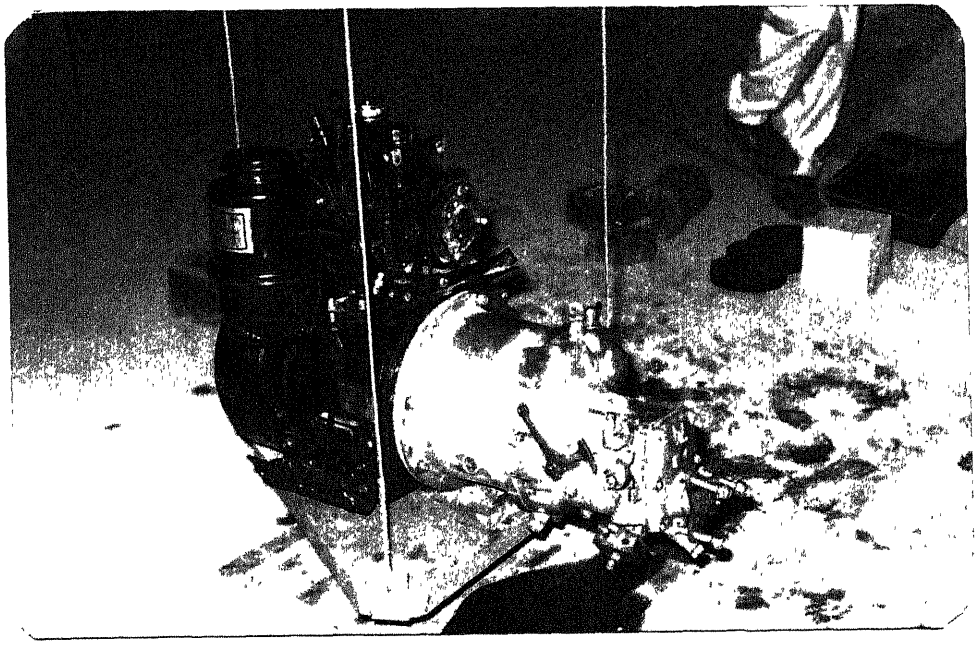

Fig.3.6b Engine Placed in Position B

The period of oscillation recorded without the engine is found to be

$$\tau_2 = 1.939 \pm 0.01 \text{ sec}$$

Thus using Eq.3.3, the combined Moment of inertia of the engine, platform and initial weights, about vertical axis S-S is determined as

$$I_S = 5.5 \text{ kg-m}^2$$

Moment of inertia of platform and weights has already been determined is

$$I_p = 1.52 \text{ kg-m}^2$$

To determine moment of inertia of the engine about the axis S-S, I_p of the platform is transformed to axis S-S and is subtracted from $I_S = 5.5$ kg-m^2. Finally, moment of inertias of the engine is determined about Y-Y axis, by transforming the moment of inertia of engine from S-S to Y-Y axis.

$$I_Y = 3.95 \text{ Kg-m}^2$$

Radius of gyration of the engine about Y axis is,

$$R_Y = 196 \text{ mm}$$

(iii) MOMENT OF INERTIA ABOUT X AXIS (I_x)

In position C (Fig.3.7), the X axis is vertical and the C.G of the platform and initial weights passes through the the combined C.G of the engine platform assembly.

From Fig.3.7a

$$r_1 = r_2 = r_3 = r = 0.313 \text{ m}$$

The period of oscillation with engine on the platform is found to be

$$\tau_1 = 1.87 \mp 0.01 \text{ sec.}$$

The period of oscillation without engine is

$$\tau_2 = 2.03 \mp 0.02 \text{ sec.}$$

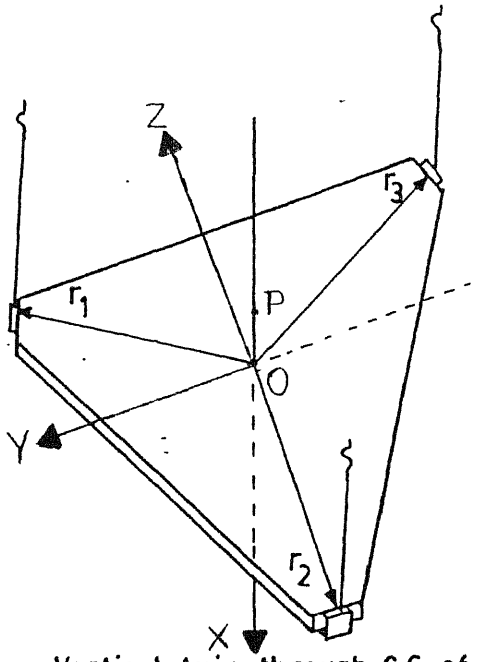

Vertical Axis through C.G of engine power pack

P: Engine C.G.
O: Platform C.G.

Fig3.7a Vertical Axis through C.G.s in Position C

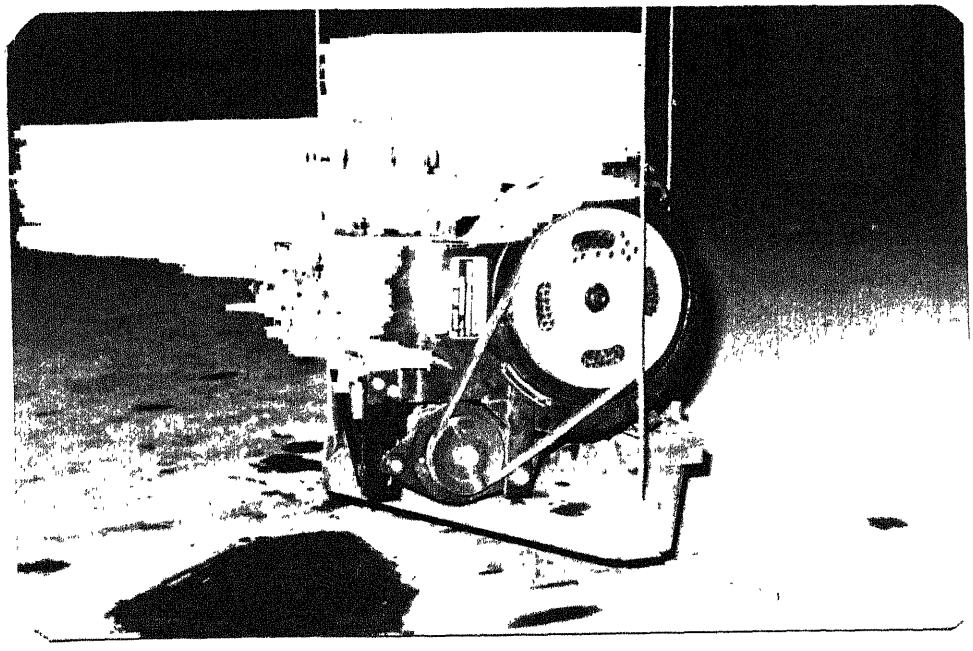

Fig.3.7b Engine placed in Position C

It may be noticed that the value of τ_2 here is different than taken previously because due to space restriction the orientation of the initial weights placed on the platform had to be changed in Position C. The moment of inertia of the engine platform assembly obtained from Position C is,

$$I_{cc} = 6.35 \text{ Kg-m}^2$$

The moment of inertia of the platform without engine is

$$I_c = 1.66 \text{ Kg-m}^2$$

The moment of inertia of the engine about X axis is,

$$I_x = I_{cc} - I_c$$
$$= 4.69 \text{ Kg-m}^2$$

Radius of gyration of the engine about X axis is,

$$R_x = 0.214 \text{ m}$$

3.2.6 ENGINE FORCES AND MOMENTS:

The engine mount system has to support the weights and moments associated with the engine. They are as follows.

(i) **Weight of the engine:**

The engine mass is 101 Kgs, as a result a load of 10 Kgs axial and 13 Kgs in shear comes on the four front isolators. But the magnitude of these forces are small as compared to the dynamic forces taken up by the isolators.

(ii) **Reciprocating inertia forces, F_{rec}, in the engine:**

These forces are given [10] as,

$$F_{rec} = M_{rec}\omega^2 r\{ \cos(\omega t) + \frac{\cos(2\omega t)}{n} \} \qquad (3.5)$$

where,

M_{rec} : reciprocating masses (mass of piston + mass of gudgeon pin + $\frac{1}{3}$ mass of con.rod)

ω : angular velocity of the engine crank shaft

r : radius of crank

n : connecting rod length / crank radius

A_p : Area of piston

l_p : connecting rod length

r : crank radius

n : $\frac{l_p}{r}$ (equal to 4 for diesel engine)

For Aluminum piston [10],

$$M_{piston} = 0.43 \ (\ 0.00415 \ D^3_{cylinder} \ )$$
$$= 1.095 \text{ kg.}$$

$$M_{con.rod} = 250 \ A_p$$
$$= 1.42 \text{ kg}$$

$$M_{rec} = 1.095 + \frac{1.42}{3}$$
$$= 1.568 \text{ kg}$$

This force in the present system acts vertically. In balanced engine, half of the magnitude of primary forces are balanced by placing the required counter weight on the crank shaft. But in doing this balancing, another force in horizontal direction is generated, given by,

$$F_{hori} = \frac{1}{2} M_{rec} \omega^2 r \sin(\omega t) \qquad (3.6)$$

(iii) Forces due to rotating masses, F_{rot}, of the engine:

It is assumed that the present engine is balanced to the extent that C.G of the crank shaft and the crank lies along its axis. So now the rotating forces, will stem from the portion of the mass of the connecting rod, M_{rot}, which can be assumed placed at the big end, will be responsible for centrifugal force.

$$M_{rot} = \frac{2}{3} M_{con.rod}$$
$$= 0.94 \text{ kg}$$

leading to,

$$F_{rot} = M_{rot} \omega^2 r \sin(\omega t) \qquad (3.7)$$

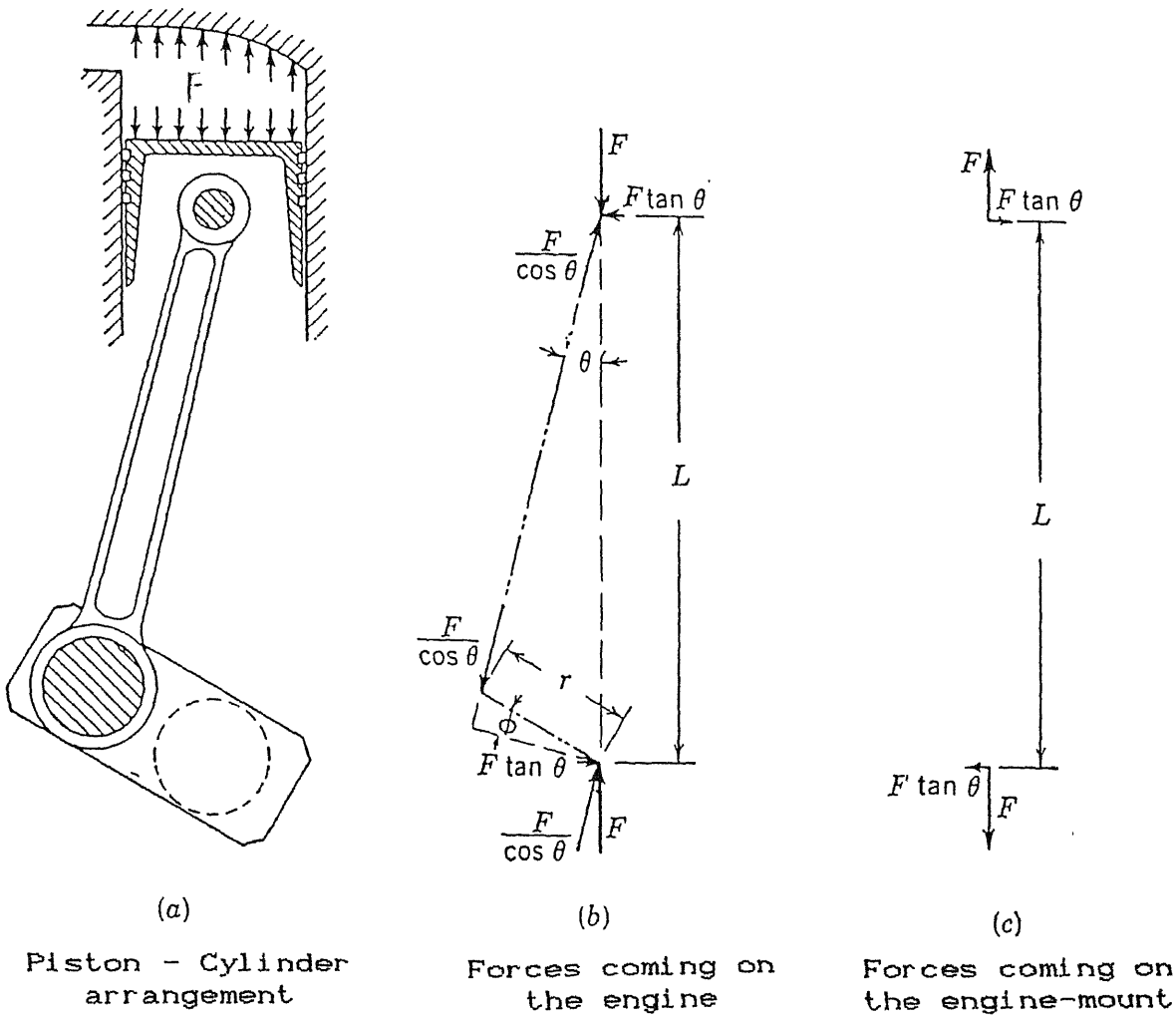

(a) Piston - Cylinder arrangement

(b) Forces coming on the engine

(c) Forces coming on the engine-mount

Fig. 3.6 Forces resulting from gas pressure

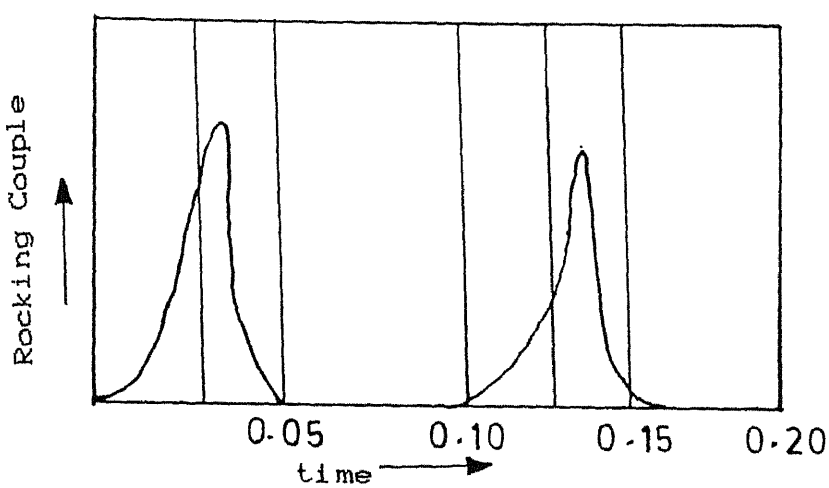

Fig. 3.6d Nature of rocking couple for a 4-stroke engine at 1200 rpm

(iv) Rocking Moment of the engine:

In the engine, at the end of compression stroke, due to explosion inside the cylinder, a lateral force normal to the cylinder axis acts on the piston, besides the thrust in the connecting rod. As a reaction to this lateral force, an opposing force acts on the cylinder walls. Figure 3.8 b and c shows the two forces F and Ftanθ acting on the engine and the engine mounting supports respectively. The force F acts upwardly on the cylinder head, is balanced by equal, downward directed force on the crankshaft bearing. The summation of vertical forces for a engine structure is thus zero. The lateral force Ftanθ, spaced L distance apart, results in a couple upon the engine mountings. This reaction results in a moment about crank shaft axis. As a result, whole of the engine rocks. The nature of this moment is shown in Fig.3.8d. This rocking moment is assumed to be composed of a constant component and a harmonic component. The engine being a 4 stroke engine, the frequency of harmonic component is half the engine speed, as this moment is dependent on the explosion frequency i.e firing frequency. The rocking moment is assumed to be maximum at 20° (assuming maximum pressure of about 60 bar inside the cylinder at around 20°, [10]) crank angle as the explosion pressure is maximum around that crank angle.

Maximum explosive force generated inside the engine,

$$F_{max} = p_{max} A_p$$
$$= (60.5 \times 10^5)\ 0.0056$$
$$= 34344 \text{ N}$$

Rocking moment,

$$M_z = \frac{1}{2} F_{max}\, l_{con} \tan(20^\circ) \left[1 + \sin\left(\frac{\omega t}{2}\right) \right]$$
$$= \frac{1}{2} (34344)\ 0.18 \tan(20^\circ) \left[1 + \sin\left(\frac{\omega t}{2}\right) \right]$$
$$= 1124.5 \left[1 + \sin\left(\frac{\omega t}{2}\right) \right] \qquad (3.8)$$

So the net vertical force,

$$F_Y = \left(\frac{1}{2} M_{rec} + M_{rot}\right) \omega^2 r \cos(\omega t) \qquad (3.9)$$
$$= 1.724\ \omega^2 r \cos(\omega t)$$

and the net horizontal force,

$$F_x = \left(M_{rot} - \frac{1}{2} M_{rec}\right) \omega^2 r \sin(\omega t)$$
$$= 0.16\ \omega^2 r \sin(\omega t) \qquad (3.10)$$

3.3 PROPERTIES OF ISOLATORS:

Natural Rubber isolators are extensively used for vibration and shock isolation. These are primarily used where small deflections are required to be small for isolating large forces. These can be placed in areas where placing a metal spring is not feasible due to space restrictions.

Its greatest utility is to give desired directional stiffness. Rubber isolators have inherent damping in it and can thus be used to pass over a resonant phase safely.

Steel spring are purposefully employed for lower frequency, up to 10 Hz and high loads, while rubber springs on the other hand are employed for frequencies over 10 Hz and under lower loads with a simultaneous noise reduction requirement.

3.3.1 RUBBER STIFFNESS:

The stiffness of rubber member is a function generally of

(i) The rubber compound and its curing method.

(ii) The size and shape of rubber.

The compound and the method of curing determine a property that bears some similarity to Young's Modulus for metals. This modulus is a function of hardness of the rubber. Normally isolator lies in the hardness range of 30-70 Shore Durometer. Stiffness of the isolator is function of the entire volume of rubber, but a

reasonably good indication is obtained by durometer.

Stiffness is also dependent on forcing frequency and aging. Change of stiffness with forcing frequency comes about beyond 50 Hz, at outdoor conditions in India. The harder the spring, higher the stiffness.

In the present vehicle, two kinds of rubber isolators are being put to use. One that is put at the front mountings of the engine (Fig.3.1), known as front isolators and the second type is at the rear mounting ends of the engine, called back isolators. The front one take the major share of load and are critical isolators. Therefore front isolators have been chosen from the Dunlop's range of antivibration rubber mounts. The Dunlop's isolator, chosen by Scooters India Limited Lucknow for the present vehicle is

Dunlop's Make 31/336 - 1 MN 50.

The back isolators play minor role and therefore are selected as less costly, locally made by Shivalik's Rubber Product Lucknow.

Figure 3.9 shows a rubber isolator fixed on an inclined rest. x-y-z axes are parallel to the X-Y-Z axes (attached to the engine power pack C.G, Fig.3.1) respectively. p - q_1 - q_2 are three principal elastic axes, of the isolator. Rubber stiffness can be defined along its three elastic axes.

Compressive Stiffness, K_p, is the force required, along p axis (Fig.3.10), for a unit deflection of the isolator in p direction.

Shear Stiffness, K_{q1}, is the force required in q_1 direction for a unity deflection of isolator along q_1 direction.

Shear Stiffness, K_{q2}, is the force required in q_2 direction for a unity deflection of isolator along q direction.

For the present analysis, values of K_p and K_{q1} are the major requirements as the engine vibration along Z axis is small compared to that along the other axes.

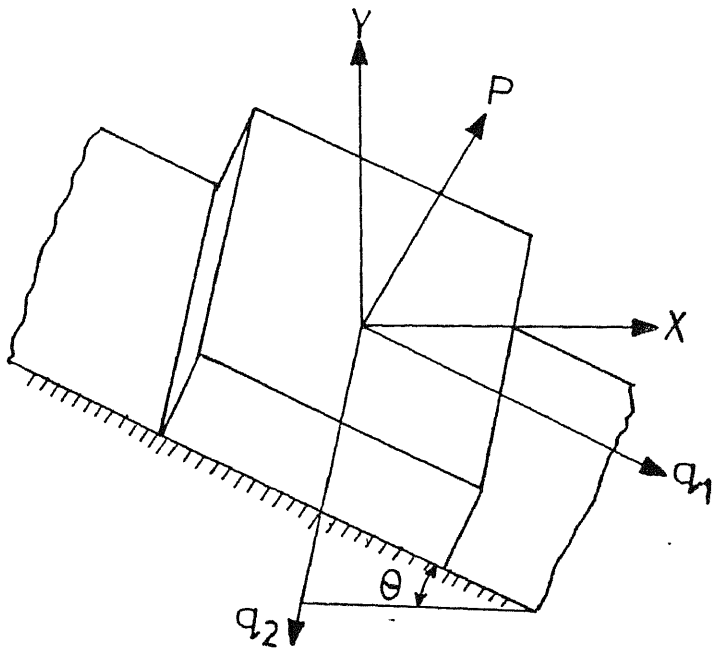

Fig.3.9 Elastic Axes Of the Isolator

(a) Compressive Stiffness (K_p)

Rubber is seldom allowed to go in tension because of the difficulty of obtaining suitable end connections and because rubber member under severe tensile stress may fail, if it experiences slight surface damage.

K_p for Dunlop's Isolator:

For Dunlop's Isolator, K_p, can be obtained from two sources,

(i) From the Dunlop's Catalogue

(ii) From the load-deflection curve obtained experimentally from compressive test on U.T.M.

Figure 3.10a shows the load-deflection curve for compressive loading obtained from the catalogue. Mean stiffness obtained for the entire range of loading comes out equal to 48.73 kg/mm. Figure 3.10a also shows, the load-deflection curve obtained from U.T.M. The mean stiffness that comes about is equal to 56.4 kg/mm.

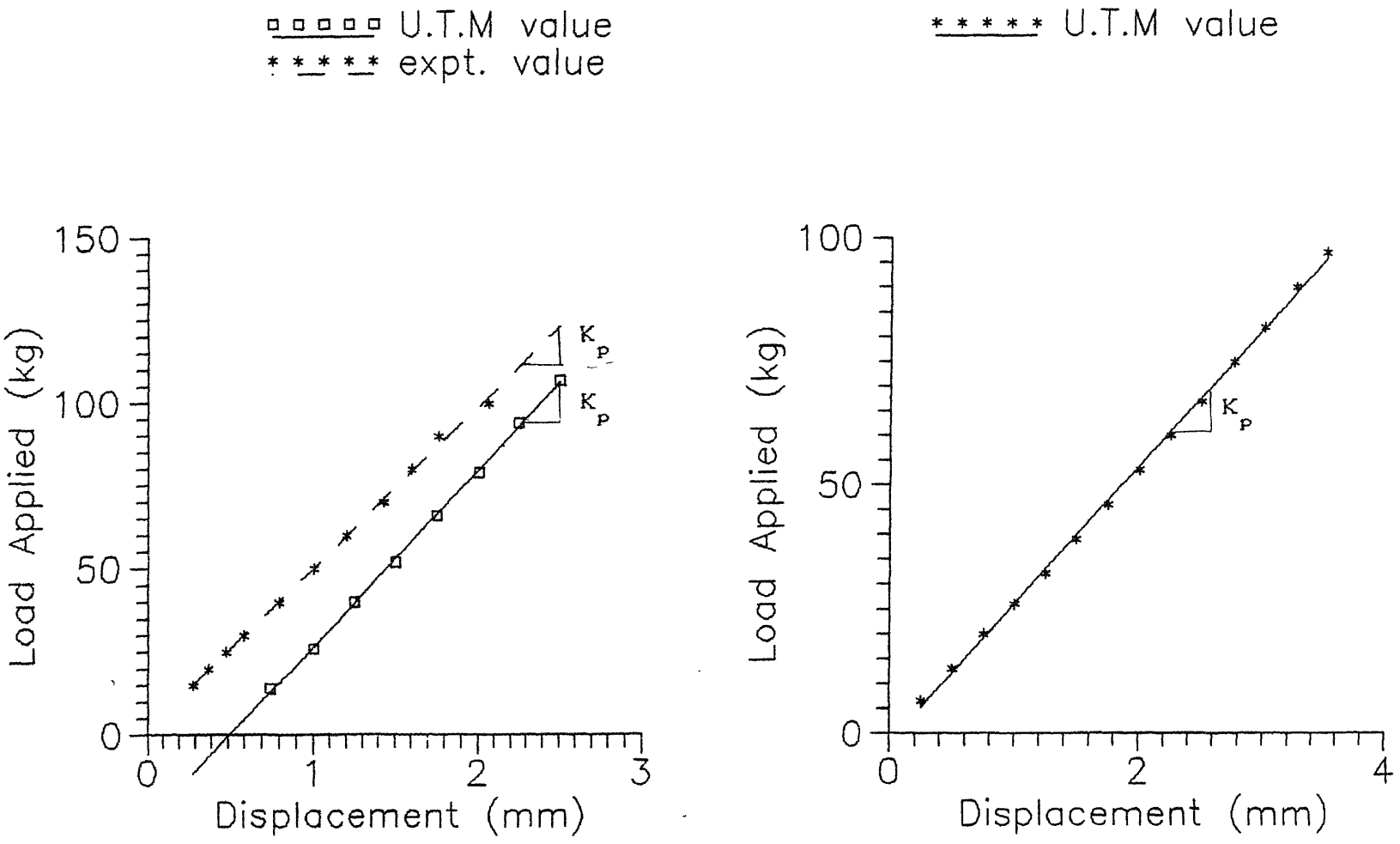

Fig. 3.10 Load-deflection Curve for compression loading of isolator

Thus, the value of K_p, for Dunlop's rubber is

From catalogue is : 48.73 Kg/mm

From the U.T.M's experiment : 56.40 kg/mm

The two obtained stiffnesses are close but for the analysis to follow in chapter 5, the experimentally obtained stiffness value of K_p will be picked up as the results of the U.T.M are bound to be more reliable.

K_p for Shivalik's Isolator:

When the engine is not running, these rubber isolator aren't loaded at all as the C.G. of the engine lies in between the four front isolators. At the time of running of the engine, the load coming over them would not be as high as compared to the Dunlop's isolator because of its location. The stiffness is measured by fitting a best fit curve over the load-deflection curve obtained from U.T.M as experiment (Fig.3.10b).

Compressive stiffness for Shivalik's isolator,

$$K_p = 27.2 \text{ Kgs/mm}$$

(b) Shear Stiffness (K_{q1} and K_{q2}):

As explained in Sec. 7.3.1, two shear stiffnesses result, depending on the direction of loading.

K_{q1} results for loading in q_1 direction while

K_{q2} results for loading in q_2 direction.

To determine experimentally these stiffnesses, a simple experiment was performed. Figure 3.11 shows the set-up for determining the shear stiffnesses. The isolator was clamped at its ends, and a shear load is applied along the direction q_1 or q_2 depending whether K_{q1} or K_{q2} needs to be calculated. If K_{q1} is being calculated the load is applied gradually along q_1 direction and the deflection noted down along the axis q_1. The load_deflection graph is plotted, the slope of which gives the required stiffness.

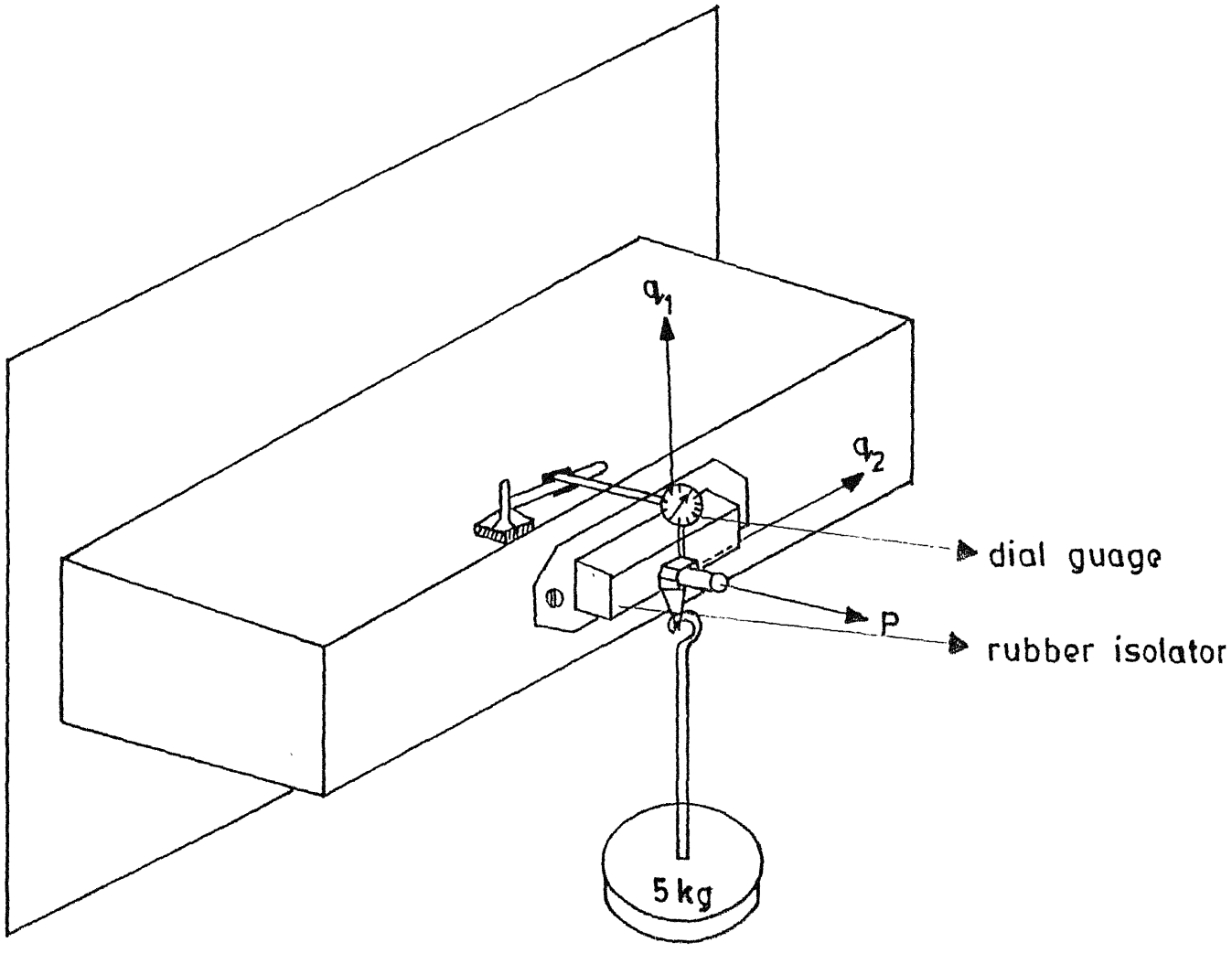

Fig.3.13 Experimental set-up for determining shear stiffness

K_{q1} for Dunlop's Isolators:

From the load-deflection curve for shear loading obtained from Dunlop's catalogue (Fig.3.12a),

$$K_{q1} = 4.19 \text{ Kgs/mm}$$

The stiffness obtained experimentally (Fig.3.12a) is,

$$K_{q1} = 3.33 \text{ Kgs/mm}$$

Here again the experimentally obtained value is relied upon for further analysis.

K_{q1} for Shivalik's Isolator:

Fig.3.12b, shows load-deflection curve for shear loading of Shivalik's rubber, with the shear load in q_1 direction. The stiffness thus calculated is,

$$K_{q1} = 2.91 \text{ Kgs/mm}$$

K_{q2} for Dunlop's Isolator:

Figure.3.12a, shows the load-deflection curve for shear loading of Dunlop's isolator as done previously, with load now acting in q_2 direction. The stiffness calculated is,

$$K_{q2} = 3.60 \text{ Kgs/mm.}$$

K_{q2} for Shivalik's Isolator:

The stiffness of Shivalik's rubber in shear, with load in q_2 direction, is calculated from Fig.3.12b as,

$$K_{q2} = 3.33 \text{ Kgs/mm}$$

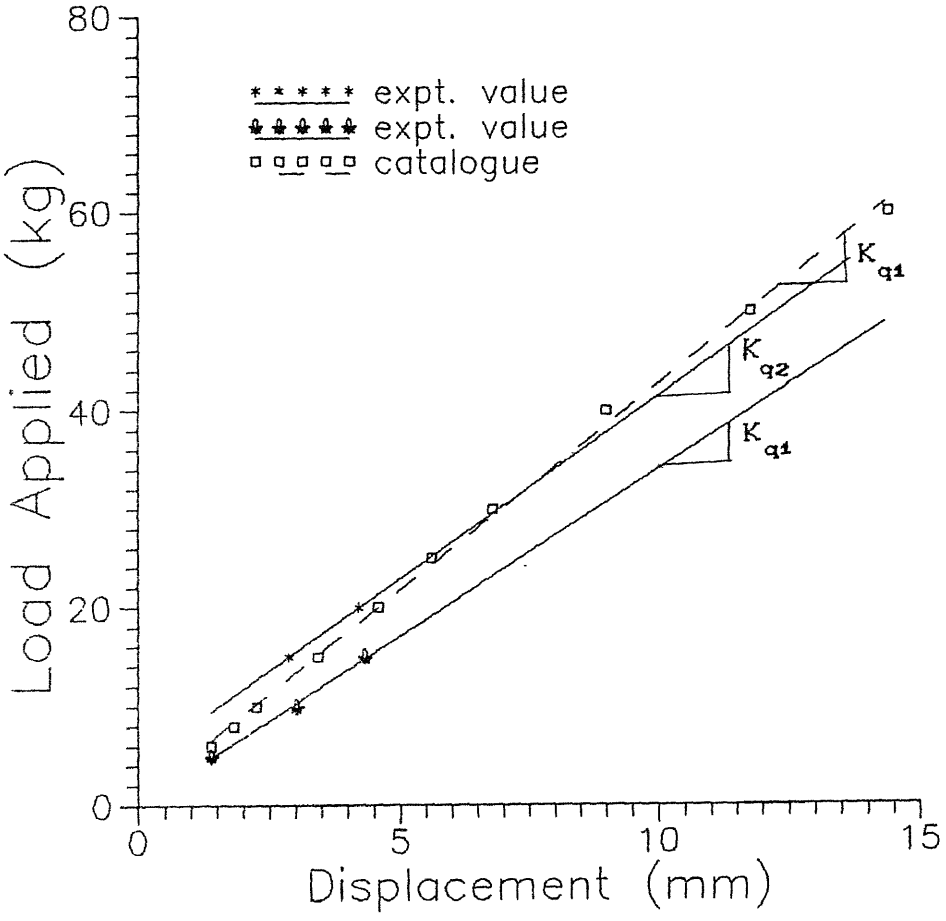

(a) For Dunlop's Rubber

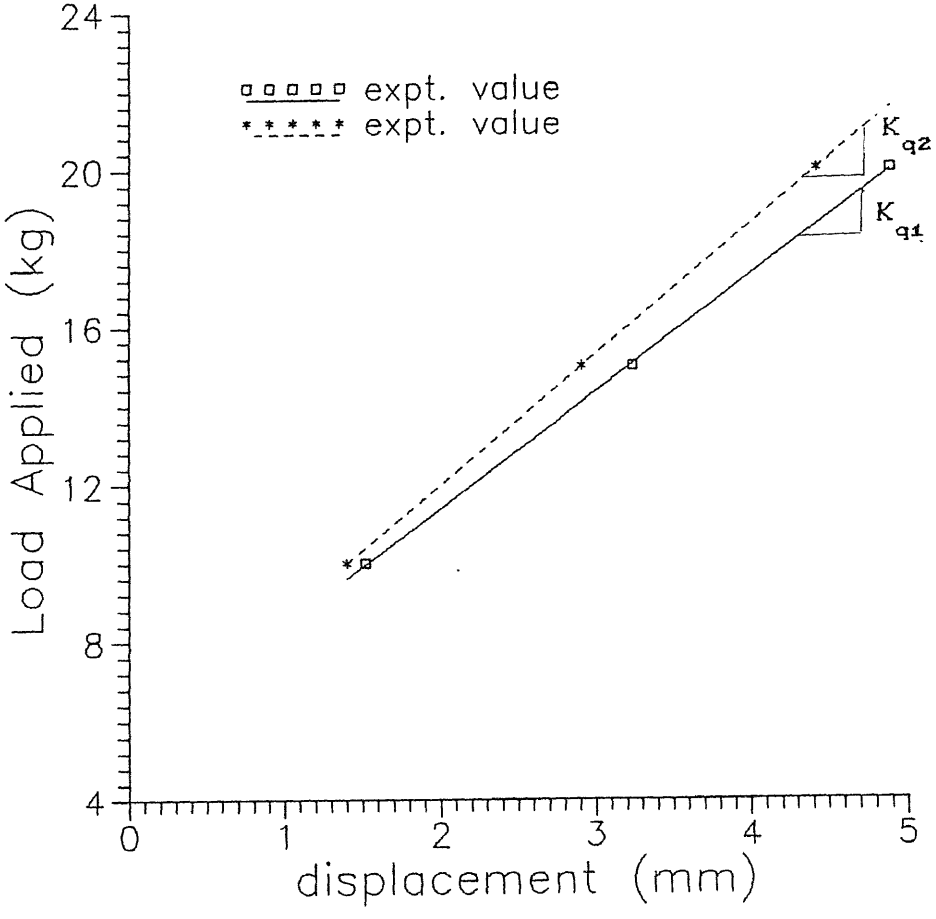

(b) For Shivalik's Rubber

Fig. 3.12 Load-deflection Curve for shear loading of isolator

The stiffnesses of the rubbers are tabulated here:

Table 1: Stiffnesses of Rubber Isolators

Rubber Type	K_p Kg/mm		K_{q1} Kg/mm		K_{q2} Kg/mm	
	EXPT.	CATLOG.	EXPT.	CATLOG.	EXPT.	CATLOG.
DUNLOP'S RUBBER 1	52.8	48.73	3.3	4.19	3.6	NA
SHIVALIK'S RUBBER 2	27.2	NA	2.91	NA	3.33	NA

NA : Data Not Available

CHAPTER 4

PARAMETRIC STUDY OF ENGINE - MOUNT SYSTEM

4.1 INTRODUCTION:

Based on the model developed in chapter 2, and the hardware properties like moment of inertia's, stiffnesses of rubber isolator etc obtained experimentally in chapter 3, an exhaustive study is undertaken to study the effect of the engine-mount parameters on various natural frequencies. In the end the natural frequencies of the existing mount system is found.

4.2 DETERMINATION OF NATURAL FREQUENCIES:

The mass matrix [M] and the stiffness matrix [K] required in equation 2.7 are obtained by putting the required stiffness values of each isolator, the inertia's of the engine and the correct location i.e. a_i's, b_i's and c_i as of the engine mounting system.

To get the natural frequencies, only the homogeneous part of equation 2.7 is taken up, i.e

$$[M]\{ \ddot{\phi} \} + [K]\{ \phi \} = \{ 0 \} \qquad 4.1$$

The above equation can be converted to an eigenvalue problem of the form

$$\left[[K] - \omega^2 [M] \right] \{ \phi \} = \{ 0 \}$$

and the eigenvalues are obtained giving [K] and [M] matrices as input, to any standard mathematical eigenvalue routine. The square root of the eigenvalue are the natural frequencies of the engine mount system. Presently the eigenvalue are being found out using eigenvalue routine F02AEFE.F, available in NAG library available here in Computer Center of IIT, Kanpur which require degree of freedom of the problem, the stiffness matrix and the mass matrix as the input.

4.3 ANALYTICAL RESULTS:

Before proceeding further, it may be recalled that the geometrical parameters that are required by the analysis. As shown in Fig.3.1, they are

a_i :Vertical distance of C.G of the engine power pack from the midpoint of i^{th} isolator.

b_i :Horizontal distance of C.G of the engine power pack from the midpoint of i^{th} isolator in X direction.

c_i :Horizontal distance of C.G of the power pack from the midpoint of i^{th} isolator in Y direction.

$a_1 = a_4 = 145$ mm, $a_2 = a_3 = a_5 = a_6 = 150$ mm.
$b_1 = -b_4 = 75$ mm, $b_2 = b_3 = -b_5 = -b_6 = 190$ mm.
$c_1 = c_4 = 480$ mm, $c_2 = c_5 = 48$ mm, $c_3 = c_6 = 76$ mm.
$\theta_1 = \theta_4 = 45^\circ$, $\theta_2 = \theta_3 = 142^\circ$, $\theta_5 = \theta_6 = 38^\circ$

The mass matrix and the stiffness matrix are built by putting in the geometrical parameters and the different stiffness calculated in chapter 3. The initial assumption while modelling was that the engine is symmetrical, about a vertical plane through Z axis (Fig.3.1), which results in two independent sets of coupled modes i.e (X, θ_y & θ_z) and (Y, Z & θ_x). As these sets are independent, each is solved separately providing 6 natural frequencies in all.

For the present system, the frequencies that come out are

: 6.75 Hz, 14.35 Hz, and 21.34 Hz in (Y, Z & θ_x) set.
: 9.24 Hz, 17.44 Hz, and 24.01 Hz in (X, θ_y & θ_z) set.

The lowest frequency is significant disturbing effect on the surrounding structure. The effect of subsequent natural frequency decreases. In the present system, the lowest frequency, 6.75 Hz, is passed over as the engine builds up to idling frequency of 14.25 Hz. The present system, is being disturbed by three natural frequencies, as will be discussed in the chapter to follow. The first frequency, 9.24 Hz of (X, θ_y & θ_z) set be called ω_1. The second frequency is 14.35 Hz of (Y, Z & θ_x) set, called ω_2 while

the third frequency is 21.34 Hz of (Y, Z & θ_x) set, called ω_3 for future reference.

4.3.1 Variation of Natural Frequencies with the Geometrical Parameters:

There are two variables that can be changed in the process of designing a better engine-mount system for " *Vikram* ". They are the geometrical variables (a_i, b_i, θ_i) and the stiffness variables of the isolating pads. Of the commercially available pads, the one from Dunlop can be relied upon. Dunlop has a range of anti vibration pads. The present one is the only one with lowest load requirements. Therefore only geometrical parameters will be changed, to have reduced vibrations at idling and a smooth ride during vehicle acceleration.

Before discussing further, the geometrical variables are minimized by equating them to independent variables so that variables that need to be handled are few. These are

$$\theta = \theta_5 = \theta_6 = \pi - \theta_2 = \pi - \theta_3$$

$$a = | a_i |, \; i = 2, 3, 5 \;\&, 6$$

$$b = b_2 = b_3 = - b_5 = - b_6$$

Only the location and orientation of front isolators are changed. The properties of the Dunlop isolators, among the few available ones, can be relied upon and also because they are the major load sharing parts, the change of rubber isolators has been ruled out.

Variation in ω_1

Figures 4.1a to 4.1c show surface curves obtained for natural frequency ω_1 with change in the vertical distance of C.G. from the rubber isolator(a), and inclination angle (θ). In the figure the frequency ω_1 has been represented as a surface, a function of a and θ for different b's.

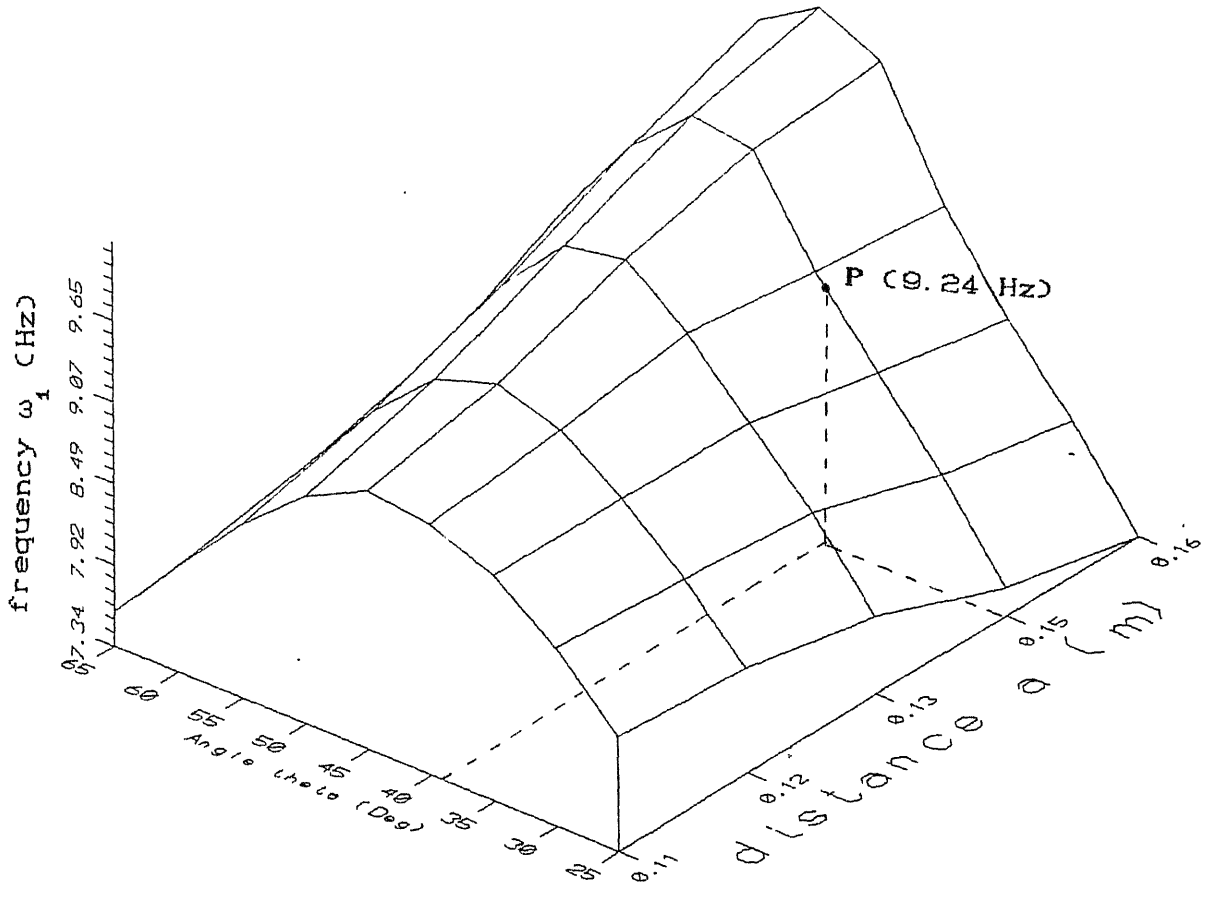

Fig. 4.1a Surface curve of ω_1 for b = 190 mm

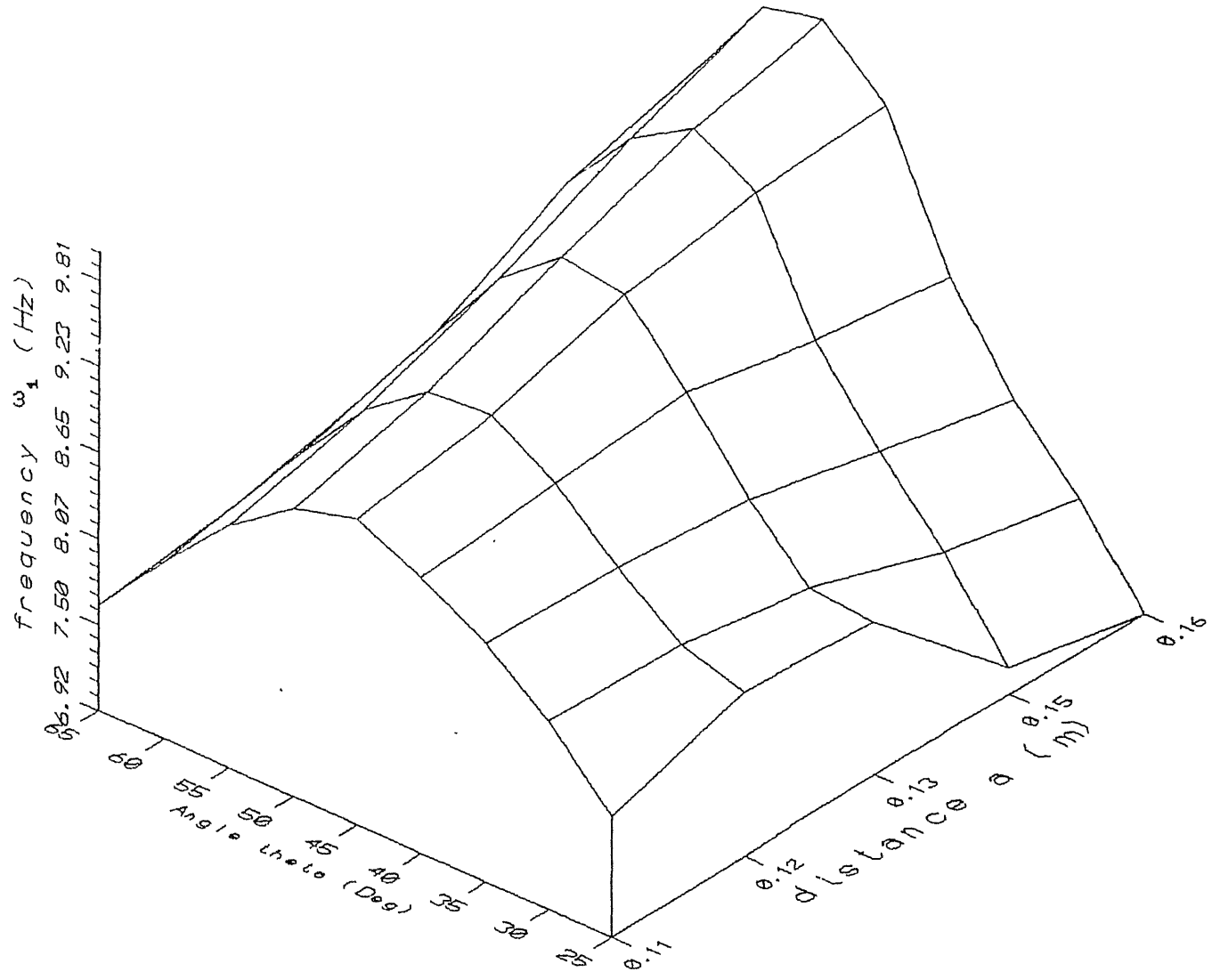

Fig. 4.1b Surface curve of ω_1 for b = 180 mm

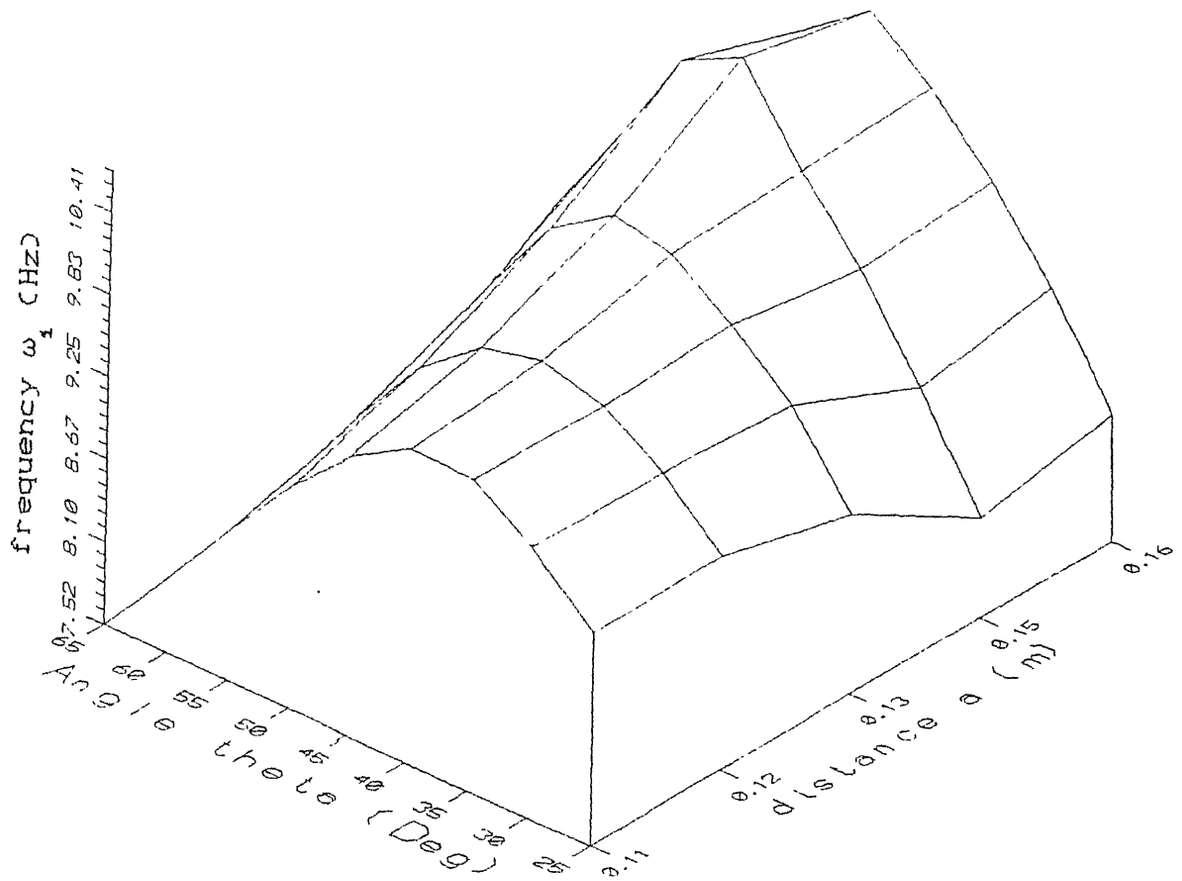

Fig. 4.1c Surface curve of ω_1 for b = 210 mm

Range a, b and θ, are decided by the geometrical constraints. These constraints are stated below.

b_{min} = 180 mm (restricted by mounting point on the engine).
b_{max} = 230 mm (restricted by the outer frame).
a_{min} = 130 mm (restricted by the channel).
a_{max} = 160 mm (restricted for fear of unstability).
θ = 25° (restricted to prevent isolators from excessive shear loading).
θ_{max} = 90°

Following observations can be made from the surface curve of ω_1.

(i) There exists a ridge in the frequency surface of ω_1. For b equal to 190 mm, Fig.4.1a, this ridge happens to be around 45°. Any change in inclination angle θ, to either side of 45° results in decrease in the value of ω_1 i.e. if the aim is to have low values of ω_1, the point chosen from the graph should be away from the ridge.

(ii) For a chosen value of θ, variation of ω_1 with a is gradual.

(iii) As b is increased ω_1 increases, goes up. Thus the lowest possible value of ω_1 also go up. The lowest obtainable ω_1, from the three surface plots in Fig.4.1 is 6.92 Hz at an inclination angle θ = 25°, a = 160 mm and b = 180 mm.

Variation of ω_2

Figure 4.2a shows surface of natural frequency ω_2, as a function of a and θ. Following observations are noted from this plot.

(i) There is a constant fall in ω_2, as the inclination angle θ is decreased. This fall is nearly linear. Thus when it comes to lowering ω_2, the inclination angle θ becomes the controlling parameter. The variation obtainable in ω_2 is from 18.2 Hz to 10.90 Hz with angular change in the inclination of the isolators from 65° to 25°.

(ii) At a constant angle θ, ω_2 changes only marginally with variation in a. For example at θ = 25°, there is a very gradual increase in ω_2 with increasing a, whereas at 40°, ω_2 first

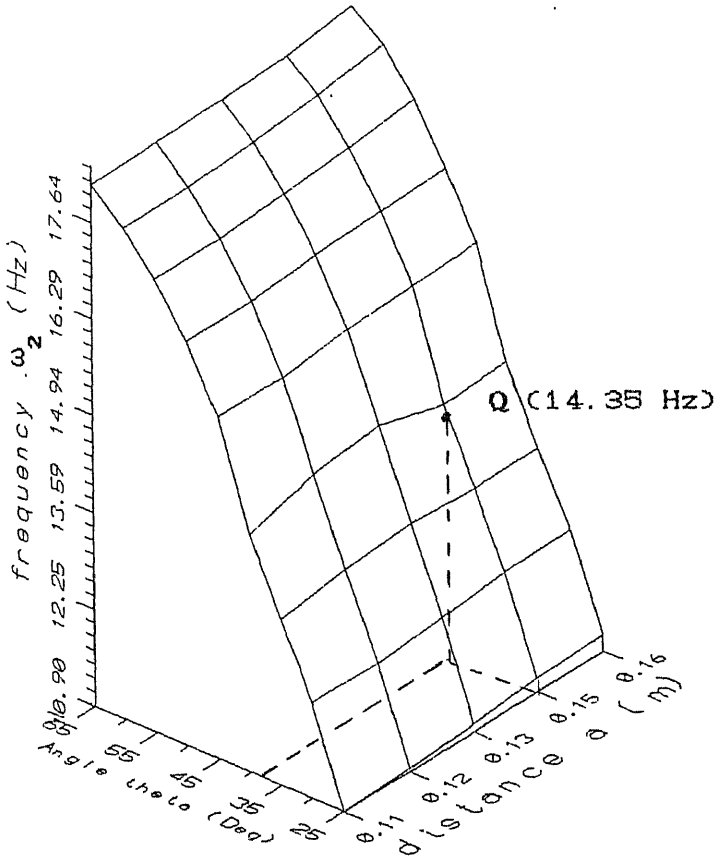

Fig. 4.2a Surface curve of ω_2

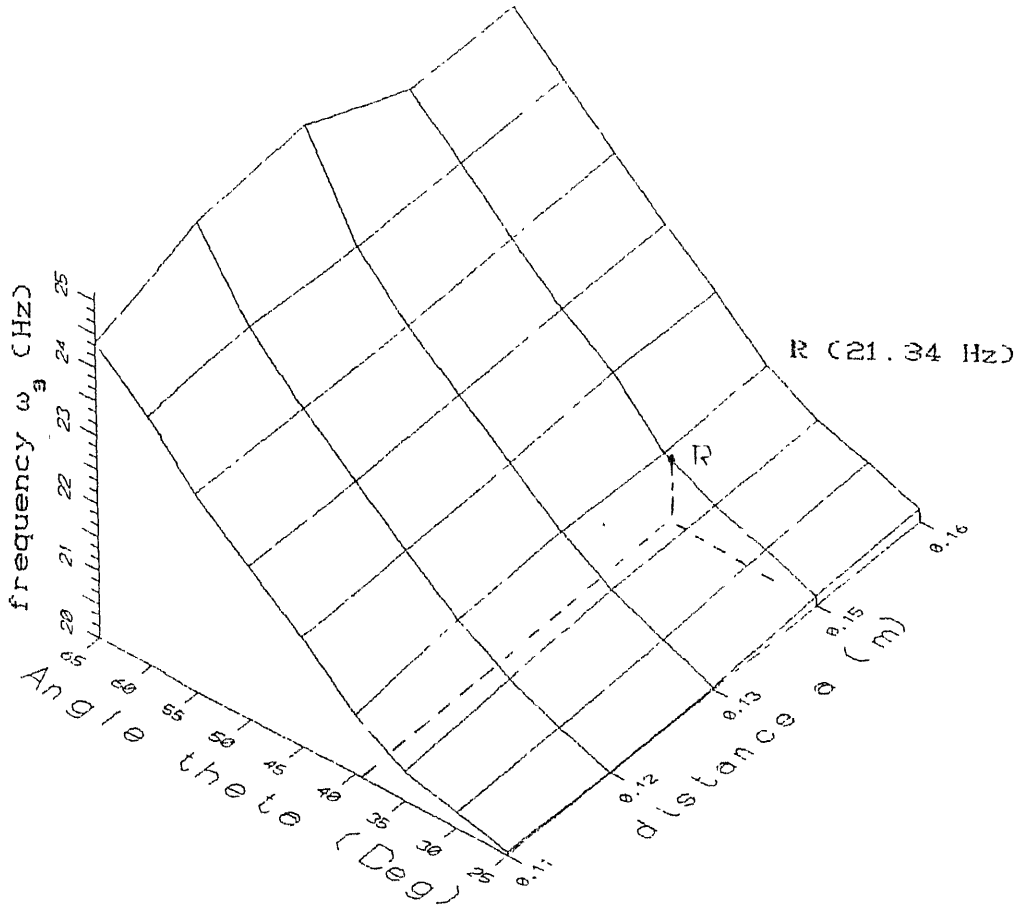

Fig. 4.2b Surface curve of ω_g

increases and then decreases. On the whole no major change in ω_2, can be brought about, with change in a.

(iii) As b is varied, it is found that the surface curve for ω_2 does not change i.e. b has just no influence on deciding the value of ω_2

Variation in ω_3

Figure 4.2b shows surface curve for ω_3, with θ and a. From the figure the following observations are made.

(i) As in the case of ω_2 , ω_3 also continuously decreases with decrease in inclination angle θ from 65° to 25°, although the rate with which ω_3 falls is far less as compared to that of ω_2. The overall drop observed in ω_3 is from 24 Hz to 20 Hz with an angular change in inclination of isolators from 65° to 25°.

(ii) The change in ω_3 brought about by change in a is marginal.

(iii) ω_3 also comes out independent of b. Both these quantities are primarily defined by angle θ.

4.4 NATURAL FREQUENCIES OF EXISTING ENGINE-MOUNT SYSTEM

For the existing engine mounting system, having geometrical variable as

b = 190 mm a = 150 mm θ = 38°

the natural frequencies of concern are:

referring to point P in Fig.4.1a,	ω_1 =	9.24 Hz
referring to point Q in Fig.4.2a,	ω_2 =	14.35 Hz
referring to point R in Fig.4.3a,	ω_3 =	21.34 Hz

The effect of these frequencies on the performance of engine will be discussed in the next chapter.

CHAPTER 5

PERFORMANCE OF THE EXISTING ENGINE-MOUNT SYSTEM

In this chapter, the results of investigations of resonant frequencies of the three wheeler *'Vikram'*, are presented. The frequencies are studied by visual observations of the engine vibrations and data from instruments. These observations are compared with those resulting from the analytical model.

5.1 VISUAL OBSERVATIONS:

When the engine is started at the idling speed (of around 14.3 Hz, 860 rpm) , the engine vibrates considerably, which decreases substantially as the engine speed is increased further. The ,mode of vibration of engine at idling is in vertical direction. This cause discomfort to the passenger, even when the vehicle is not moving. The vibrations at idling therefore suggests presence of resonance frequency

As the engine speed is increased beyond idling speed, one notices a very large rocking of the engine about its longitudinal axis (Z axis, Fig. 3.1). This engine speed, at which the rocking of the engine is maximum, from now on will be called as rocking speed or rocking frequency. At the rocking frequency, the vehicle's body again experiences high amplitude vibrations, resulting in considerable discomfort to the passenger sitting inside. The amplitude of rocking vibration increases further when the engine is loaded. The rocking last a little longer, engine frequency range (18-21 Hz), as compared to the vibrations at idling. But beyond this range the vibrations decrease substantially suggesting encounter with some natural frequency or its harmonics.

When the engine is further speeded up, beyond the engine speed of around 24 Hz (1440 r.p.m), the vehicle will be stable and free of vibrations.

From the visual observations, it can be inferred that there are two major resonating phases encountered during its speeding. It is clear that beyond the 24 Hz of the engine speed, the engine-mount system doesn't encounters any other prominent natural frequency.

5.2 OBSERVATIONS THROUGH ACCELEROMETERS:

During these observations, the engine was run and accelerometers were placed on the engine at different locations, to record the frequency components of the vibrational displacement, both at idling speed and at rocking speed of the engine. The displacement-time response is recorded by the accelerometers using a TAPE RECORDER. The fast fourier transform (FFT) of response is obtained on a Digital Oscilloscope with FFT capabilities (Model No. 4027, Larsen and Tubro Limited, Bombay).

The response of the accelerometers placed on the engine at Position M and Position N (Fig.3.1), are as follows:

At Position N : It records displacement in Y direction, which is caused by translation of the C.G. and rotation about X or Y axis.

At Position M : It records displacement in X direction, which is caused by translation of C.G. and of rotation about Z or Y axis.

In the forced vibrations, the body always vibrates with the frequencies present in the exciting force. The dominant ones come out as big peaks. The location from which response is picked up show frequencies dominating in that mode of vibration. The frequencies for which peaks are obtained in Fig.5.1, are same irrespective of the locations from which they are obtained. Only the height of peaks vary, at a frequency, from location M to N, suggesting coupling up of different modes of vibration of the engine.. Similar observations are made from Fig.5.2.

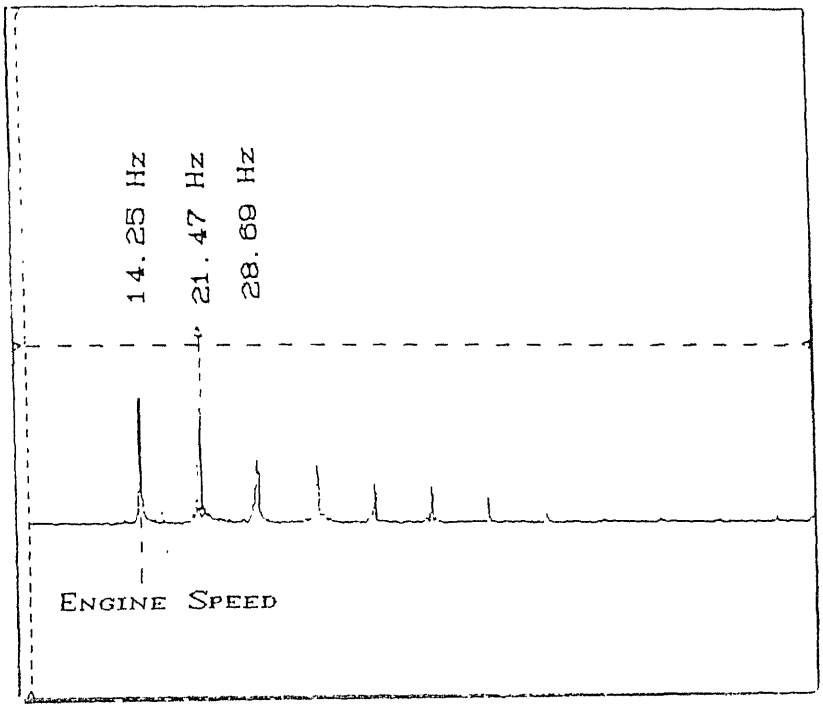

(a) FFT obtained from Location M at idling speed

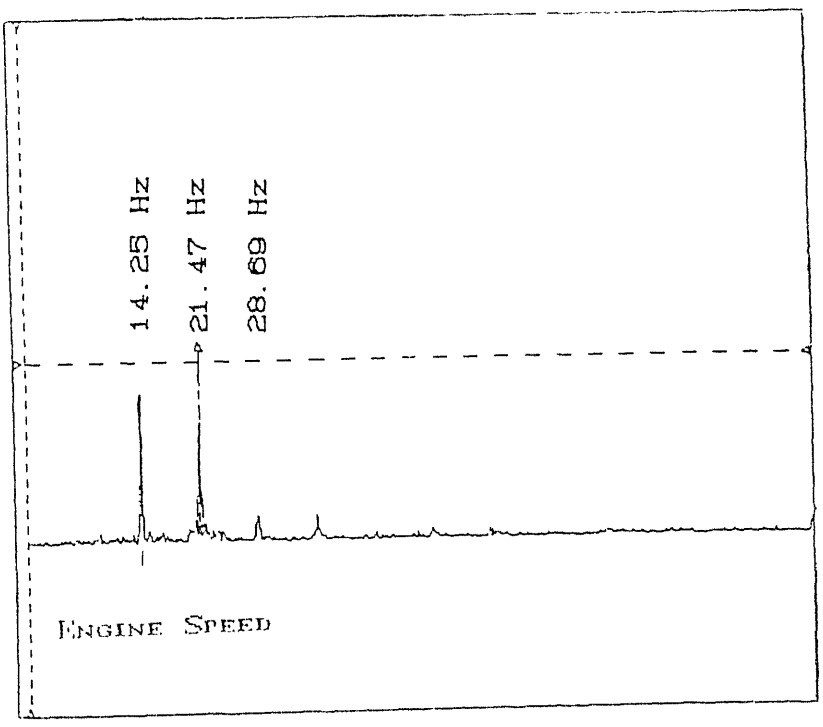

(b) FFT obtained from location N at idling speed

Fig.5.1 FFT Plots Of The Engine At idling speed

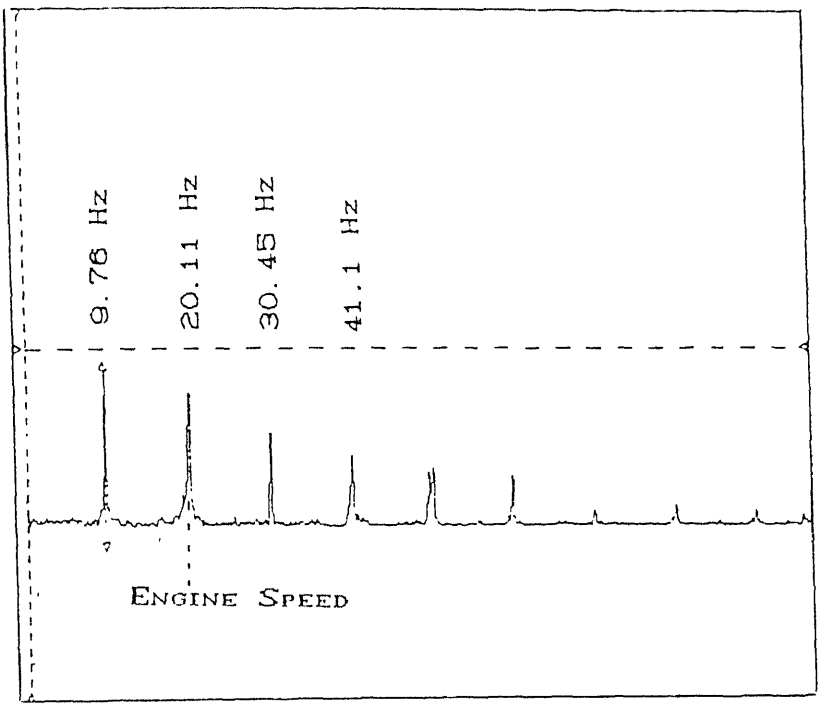

(a) FFT obtained from Location M at rocking speed

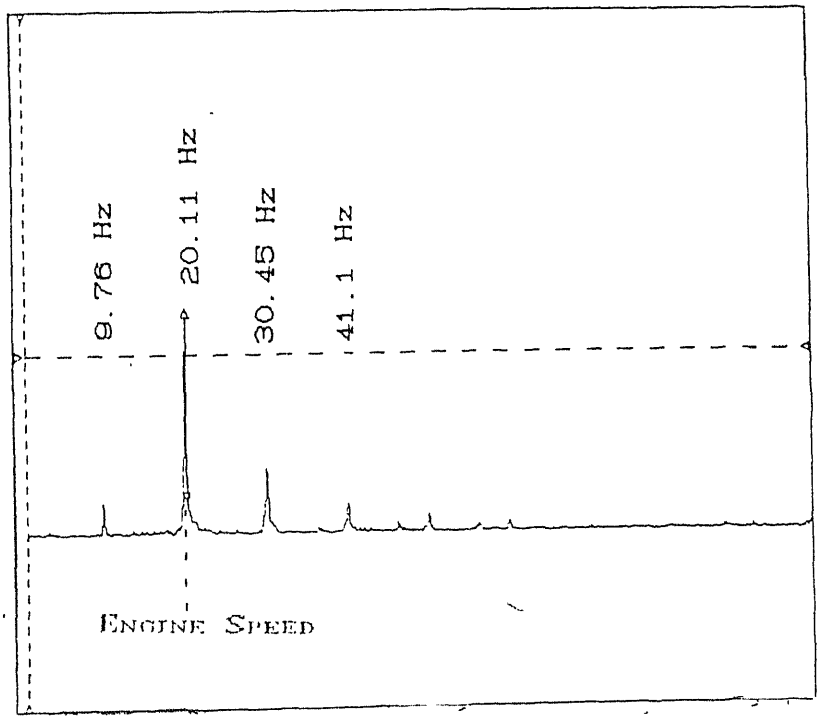

(b) FFT obtained from location N at rocking speed

Fig.5.2 FFT Plots Of The Engine At rocking speed

Figures 5.1a and 5.1b show FFT of time-displacement response of the accelerometers placed at location M and location N respectively, while engine is run at the idling speed of around 14.3 Hz. The peaks obtained from both the locations, whose value lie below 24 Hz are 14.25 Hz and 21.47 Hz. The engine is running at idling and here, the peak at 14.25 Hz, corresponds to engine speed of 14.25 Hz. The primary component of reciprocating forces and the rotating forces of the engine is the cause of peak at frequency of 14.25 Hz. The secondary component runs at twice the speed and hence the peak of 28.69 Hz. The frequency of 14.25 Hz may or may not be a natural frequency of the engine-mount system. The frequency of 21.47 Hz corresponding to another peak is not a multiple of the forcing frequency, and hence it can be either due to some kind of large force from some engine element or can be due to forcing frequency coinciding with the natural frequency of the system.

Fig. 5.2a and Fig. 5.2b shows FFT of time-displacement response of the accelerometers mounted at location M and N respectively, when the engine runs at rocking speed of 20 Hz (1200 rpm). The peaks obtained from both the locations, with frequency value below 24 Hz are 20.11 Hz. The peak of 20.11 Hz indicates that engine is running at 20.11 Hz. The difference in height, of peak at 9.76 Hz, at location N and M suggests that 9.76 Hz is associated with the rocking of engine resulting in the displacement of the engine in X direction either due to translation or rotation of the engine. As the recording is being done at maximum rocking of the engine condition, force components frequency responsible for the rocking is under resonant condition. Thus 9.76 Hz is the cause of resonant condition. Presently running speed of engine is 20.11 Hz The excitation of mode corresponding to natural frequency of 9.76 Hz, at the running speed can be attributed to some kind of forcing which runs at half the running speed of engine (as 9.76 X 2 $\cong$ 20 Hz).

The peak of 20.11 Hz suggests that the engine is vibrating at or around its one of the natural frequency of mount system, or a peak is resulting due to forcing from the primary forces of the engine which runs at the engine speed.

From the above experiments, two resonating frequencies of 9.24 Hz(the frequency responsible for rocking mode vibration of the engine), and 21.45 Hz (results in vibration of engine in vertical mode) are established. There are two more frequencies (14.25 Hz and 20.11 Hz) which can be suspected of being natural frequencies of the engine-mount system.

5.3 COMPARISON WITH ANALYTICAL MODEL:

Restating the results of the analytical model (Chapter 4), the six natural frequencies are,

ω_1 = 9.24 Hz, 17.44 Hz and 24.01 Hz (X, θ_z & θ_y)

6.75 Hz, ω_2 = 14.35 Hz and ω_3 = 21.34 Hz (Y, Z & θ_x)

Table 5.1 shows all the three amplitude of C.G. in direction X, Y and Z against the engine frequencies varying between 14 Hz and 24 Hz. It also shows all the three angular amplitudes for rotational vibrations, generated when the engine is varied between 14 and 24 Hz.

At ω_2 = 14.35 Hz, (Y, Z & θ_x) set gets excited. The large value of Y and Z displacement and of θ_x rotational amplitude are representative of resonance vibration. In the actual case, due to presence of damping the amplitude do not reach such large values. Theoretically at 14.35 Hz, there is a natural frequency. In the Sec.5.2 the frequency of 14.25 Hz was suspected to be a natural frequency. From the visual observations at idling as there are significant vibrations, it was deduced that there must exist some natural frequency or its harmonic. Co-relating the above observations at ω_2 = 14.25 Hz one of the natural frequency of the

Table 5.1: Transient Response Of The Center Of Gravity Of Engine

Forcing frequency (Hz)	Deflections Of C.G					
	θ_y	X mm	θ_z	Y mm	θ_x	Z mm
14.15	24.0	9.5	3.0	18.0	3.0	2.0
14.35*	25.3	9.7	3.4	220	46	39
15.00	28.1	10.0	3.87	3.0	0.9	0.56
15.50	30.5	11.9	4.1	1.4	0.6	0.4
16.00	34.0	12.7	4.8	0.7	0.5	0.3
16.50	35.6	16.2	5.7	0.5	0.48	0.28
17.00	48.6	18.0	6.9	0.5	0.48	0.26
17.30	63.4	22.4	9.88	0.5	0.46	0.26
17.60	85.0	31.5	11.4	0.5	0.52	0.24
18.48**	3048	1427	546	0.8	0.66	0.29
19.00	227	81.0	33	1.0	0.73	0.35
19.50	76.0	25.0	13	1.7	0.88	0.35
20.00	56.0	23.7	6.8	2.1	1.2	0.46
20.50	43.0	16.2	4.7	4.8	1.93	0.65
21.00	33.0	9.22	3.6	13.5	4.6	1.6
21.34†	31.5	7.79	4.87	597	197	5.8
22.00	26.2	8.5	4.1	8.41	2.5	0.65
23.92	28.0	54.5	29.77	0.59	0.5	0.13

* 14.35 Hz = 861 rpm

**18.48 Hz = 1109 rpm

† 21.34 Hz = 1280 rpm

engine -mount system exists which results mainly in vertical vibrational mode.

At a frequency of 18.48 Hz, (X, θ_z & θ_y) set gets excited. From the theoretical calculated natural frequencies, none appears at 18.48 Hz. But 18.48 Hz is twice of 9.24 Hz, suggesting that mode corresponding to ω_1= 9.76 Hz is being excited by some forcing frequency which runs at half the engine speed of 18.48 Hz. From the experimental observations, it is found that 9.76 Hz was some resonating frequency associated with rocking of engine. This frequency was also found to be excited by some forcing frequency running at half the rocking speed (20.11 Hz) of the engine. From Sec.3.8, it is known that frequency of rocking moment M_z matches with firing frequency of engine (half the engine speed). From the above statement, it is clear that rocking of engine is result of encounter with natural frequency ω_2(9.24 Hz) of the engine-mount system. When the engine is carrying load, rocking increases. A 1 Hz change in firing speed requires a change of 2 Hz in the engine speed. So if 9.24 ± 1 Hz is the range of resonance vibration, then the rocking would be present from 18 Hz and at around 21 Hz. This explains the high duration of rocking vibration as compared to vibrations at idling.

At frequency ω_3= 21.34 Hz, the (Y, Z & θ_x) set gets exited. This is shown by large amplitude displacements in Y and Z displacements of the C.G. and rotation about X axis (Table 5.1). The experiments also shows 21.47 Hz as one of the natural frequency. The mode of vibration at ω_3 natural frequency is in vertical direction. This mode gets excited when engine speed is around 21 Hz. But from visual observation at rocking speed of engine (18 - 21 Hz), rocking of engine is the major vibrational mode. The vibration at ω_3 mode is not visible through visual observation. This can be because the rocking is the result of excitation of ω_1 mode, which is the 2^{nd} natural frequency while ω_3 is the 4^{th} natural frequency of engine -mount system. As the order of natural frequency increases, its effect, when excited decreases. The other frequencies that were obtained by analytical modelling,

6.75 Hz is passed over as the vehicle builds up speed. The frequencies 17.44 Hz and 24.02 Hz are excited at engine speed twice their values. From visual observations one does not feel any resonance vibration at engine speed of 34 Hz or at 48 Hz (rarely reached), because these are still higher order natural frequencies having very little practical significance. So for further analysis one need not be concerned of these natural frequencies.

5.4 DISCUSSION ON EXISTING DESIGN

for the existing engine-mount design, the three natural frequencies of concern are

For the present engine- mount design, the three natural frequencies of concern are

ω_1 = 9.24 Hz (marked P in Fig.4.1a)

ω_2 = 14.35 Hz (marked Q in Fig.4.2a)

ω_3 = 21.34 Hz (marked R in Fig.4.2b)

The idling speed of engine is 14.25 Hz. As the idling speed is very close to ω_2, at idling the mode corresponding to natural frequency ω_2 gets excited. The heavy vibrations at idling are the result of this excitation. To have a system that never encounters this resonating mode, ω need to be placed below 14 Hz.

As the vehicle accelerates, at the running speed of around 10 Kmph, when the engine speed is 18.5 Hz, ω_1 gets excited by the frequency firing frequency of engine, (discussed in the next chapter of Experimental Observations), which is half the engine speed. To escape from disturbance due to ω_1, the value of ω_1 should be below the firing speed at idling i.e. 7 Hz.

With further acceleration, ω_3 is encountered when engine running speed is around 21.5 Hz. The effect of this is not dominant, and is not even observed by the visual observations.

5.5 Conclusion:

the existing engine-mount system is affected by its three natural frequencies ω_1 , ω_2 and ω_3. The value of frequency ω_1, obtained analytically is 9.24 Hz but experimentally obtained value of this frequency is 9.76 Hz. The value of ω_2 is 14.35 Hz from analytical results whereas from the experimental results it comes out 14.24 Hz. ω_3 is equal to 21.34 Hz from the analytical results whereas it comes out equal to 21.47 Hz from experimental observations.

The observations from experiments and the analytical results come about close. The difference that persists can be attributed to the coupling up of various modes. The analytical modelling assumes that vertical plane about which the engine is symmetrical is decoupled from the rest of the planes. But in actual case coupling up of various modes exist because the C.G. of the power pack lies slightly off centered. Moreover the damping in the system adds to the coupling up of various modes.

CHAPTER 6

PROPOSED MODIFICATIONS IN DESIGN

6.1 INTRODUCTION:

From previous chapters, it is clearly seen that three natural frequencies, ω_1, ω_2 and ω_3 equal to 9.24 Hz, 14.35 Hz and 21.34 Hz, of the engine mount system, are important. As the vehicle speeds up from an engine idling speed of 14.25 Hz to its maximum speed, ω_2 is encountered first. It being very close to the idling speed (within 1%) causes large vibrations at idling also resulting in pronounced vibrations of vehicle even when it is not moving. On further increase of engine speed ($\cong$ 20 Hz), corresponding to vehicle moving at about 10 kmph, ω_1 is encountered. ω_1 corresponds to the firing frequency of the four stroke engine at the engine speed of $2\omega_1$. It is largely responsible for the rocking of the engine thereby causing failure of exhaust pipe. The third frequency ω_3 though is observed in the experimental observations will also have its resonating effect around 21 Hz, but being a higher order frequency its effect is not pronounced. Besides it is not even observed visually. ω_3 is not much of concern. Thus the desired goal would be to have an engine mount whose natural frequencies (notably ω_1 and ω_2) lie outside the domain of engine operating frequency. But as will be discussed later in this chapter, the above desired design is not feasible with the low speed 4-stroke diesel engine presently used in the three wheeler Vikram, with the rubber isolators available from Dunlop Company and space constraints from the chassis.

6.2 IDENTIFYING THE POSSIBLE SOLUTION ZONES:

The geometrical constraints of the availability of space for the engine-mount system lead to two solution zones.

(i) When isolators are mounted below the channel and central torque tube of the chassis (Solution Zone 1).

(ii) When the isolators are mounted above the chassis (Solution Zone 2).

6.2.1 Solution Zone 1:

In this case the isolators have been placed below the chassis. The relevant geometrical variables are (Fig.3.1):

θ : inclination angle of front isolators with respect to X axis ($\theta = \theta_5 = \theta_6 = \pi - \theta_2 = \pi - \theta_3$)

a : vertical distance below C.G of engine from center of front rubber isolators. ($a = | a_i |$, $i = 2, 3, 5$ &,6)

b : horizontal distance of C.G of engine from center of the front rubber isolator. ($b = b_2 = b_3 = - b_5 = - b_6$)

The geometrical constraints under which the Solution Zone 1 are as follow,

b_{min} = 180 mm (restricted by mounting point on the engine).
b_{max} = 230 mm (restricted by the outer frame).
a_{min} = 130 mm (restricted by the channel).
a_{max} = 160 mm (restricted for fear of unstability).
θ_{min} = 30° (restricted to prevent isolators from excessive shear loading).
θ_{max} = 90°

While searching for a solution, the ideal goal is to choose the geometrical parameters such that all the above said frequencies, fall outside the engine operating speed (14 - 50 Hz). The natural frequencies of the present design are very close to the exciting speed as compared to the maximum engine speed. Thus to get the frequencies out of the operation range, lowering the natural frequencies below the engine idling limit would be advisable as compared to raising it past 50 Hz. In the later case the system would become very rigid and engine forces coming on the structure will be large. Thus it is convenient to decrease natural

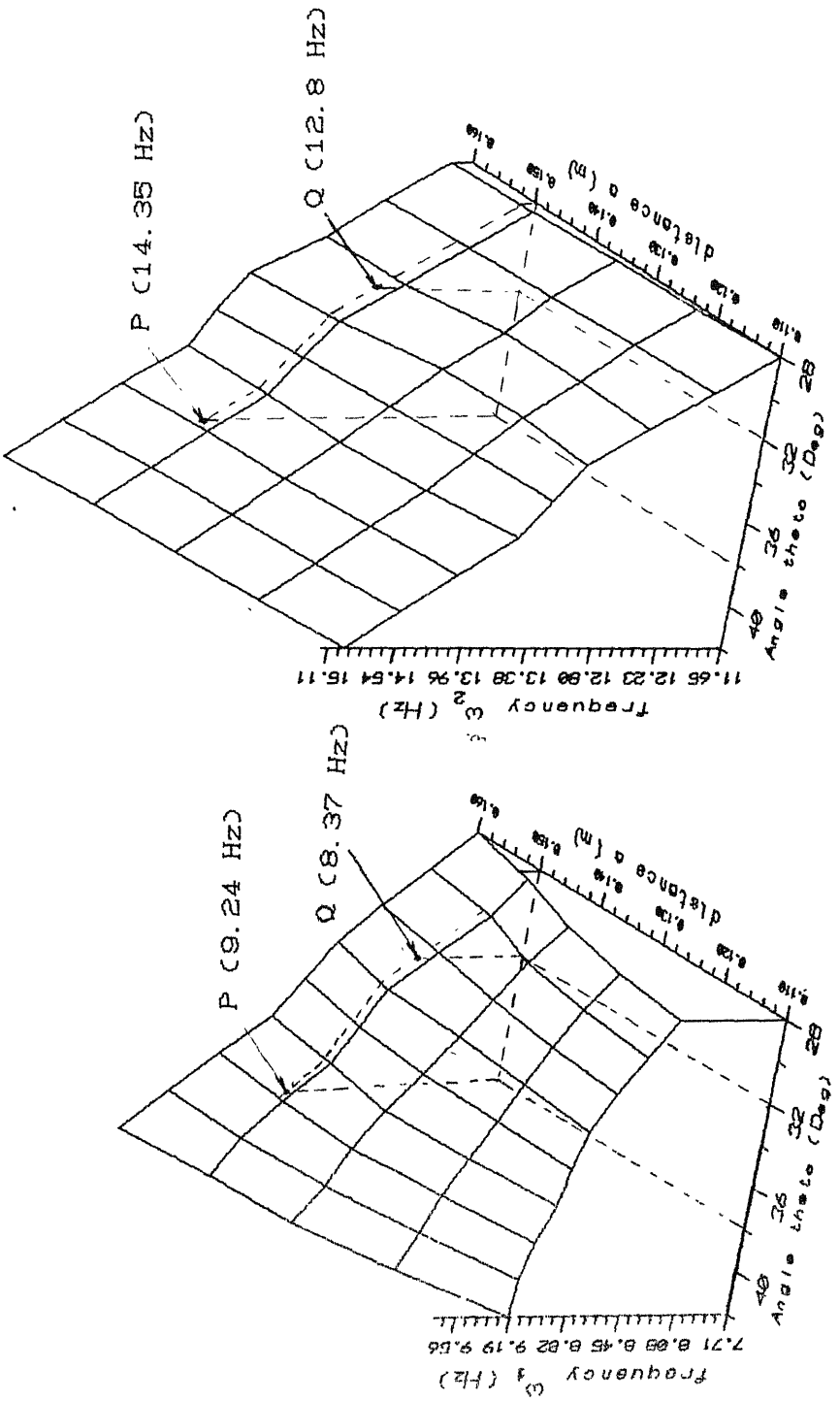

Fig.6.1a Surface Curve of ω_1 for b = 190 mm

Fig.6.1b Surface Curve of ω_2 for b = 190 mm

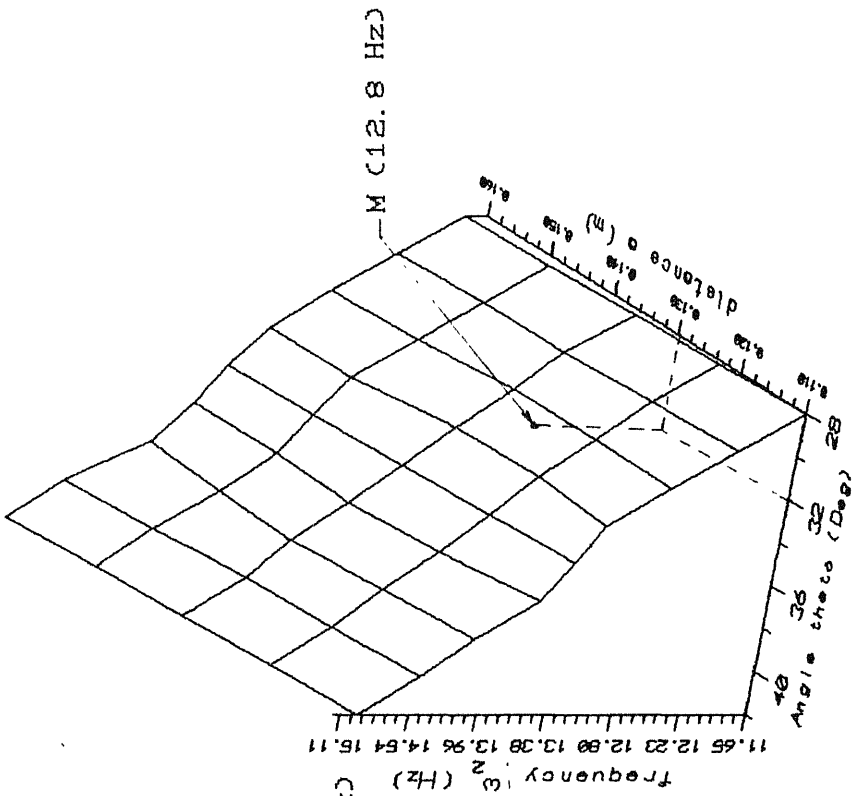

Fig. 6.2b Surface Curve of ω_2 for b = 200 mm

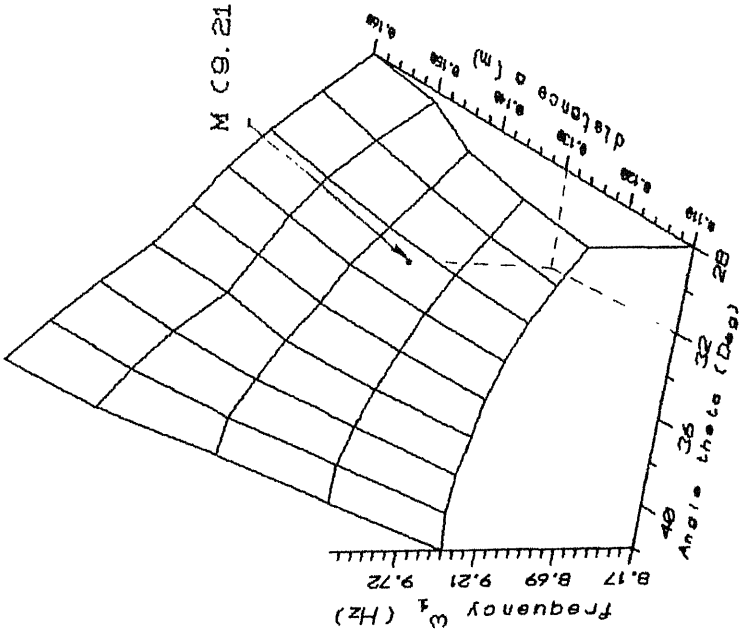

Fig. 6.2a Surface Curve of ω_1 for b = 200 mm

frequencies below idling, ω_1 has to be decreased to around 6 Hz (12 < 14.25) while ω_2 have to brought to around or below 13 Hz.

As will be seen later in this section, only one frequency at a time can be brought below idling. As a first case, the possibility of decreasing ω_2 below the idling speed is discussed. Through repeated trials, the optimum solution that has been obtained, Design 1, is as follows.

Design 1:

Design 1 proposes a location, that brings ω_2 down the idling speed (marked N in Fig.6.2).

The inclination angle of the front isolators	θ	=	32°
The vertical height of C.G from rubber mounts	a	=	130 mm.
The horizontal distance of the C.G from rubber mount	b	=	200 mm.

With the above location, ω_2 = 12.8 Hz (below engine idling speed) and ω_1= 9.21 Hz is obtained.

From the chapter 4, θ was found to be the controlling parameter for ω_2. From Fig.6.1, it is observed that as θ is reduced from 38°, for the present mounting location (marked P in Fig.6.1b), to around 32°(marked Q), value of ω_2 comes down from 14.35 Hz to 12.8 Hz (below engine idling). But simultaneously value of ω_1 falls from 9.24 Hz (marked P in Fig.6.1a) to 8.75 Hz (marked Q) i.e $2\omega_1$ stays above idling. To get $2\omega_1$ down the idling speed, while maintaining ω_2 below idling requires further reduction in θ to 25° with a subsequent change in b (= 180 mm) and a (= 160 mm). Mounting isolators at $\theta = 25^\circ$ is unsafe as the isolator will be loaded to much in shear. $2\omega_1$ near the idling is not desirable as it will rock the engine at idling. So it is better to push ω_1 to its present value such that it is crossed over as the vehicle accelerates. In this process, from point Q (Fig.6.1), surface plots for different b's are searched, such that the value of ω_2 remain same while ω_1 is pushed to its present value of around 9.24 Hz. The above stated desired value of ω_1 and $\omega_2$is met by location

corresponding to point N (Fig.6.2). This gives the desired location for Design 1. The hardware requirement for placing the isolator at the location suggested by Design 1 is discussed in Hardware Configuration Of Design 1 (Sec.6.4).

6.2.2 Solution Zone 2:

In this case, the isolators are placed above the chassis. The geometrical constraints under which the Solution Zone lies are as follows (Fig.3.1).

b_{min} = 230 mm (restricted by the engine contour).
b_{max} = 260 mm (restricted by the outer frame).
a_{min} = -30 mm (restricted to accommodate the isolator stud).
a_{max} = -30 mm (restricted to prevent isolator from hitting air filter above).
θ_{min} = 55° (restricted by isolators mounting problem)
θ_{max} = 90°

Design 1 is unable to bring ω_1 below the firing frequency at idling. Thus for this purpose, the locations above the chassis are explored in the present Solution Zone 2. As constraints of minimum angle stands at 55°, ω_2 in any case would be above the idling speed. keeping with the above objective (pushing down the value of ω_1) under the space constraints, Design 2 is proposed.

Design 2:

Design 2 proposes the location, marked N in Fig.6.4, that enables the engine-mounting system to escape vibration in ω_1 natural frequency.

The inclination angle of the front isolators θ = 60°
The vertical height of C.G below rubber mounts a = 30 mm.
The horizontal distance of the C.G from rubber mount b = 250 mm.

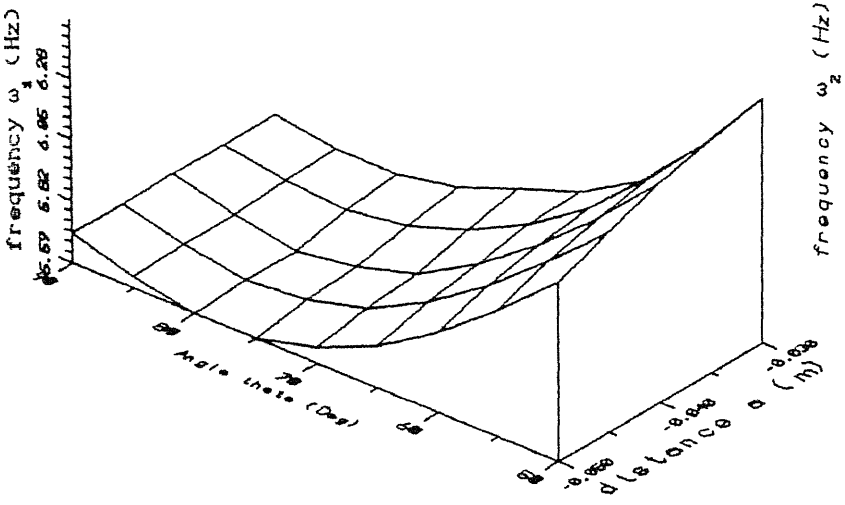

Fig. 6.3a Surface Curve of ω_1 for

b = 240 mm

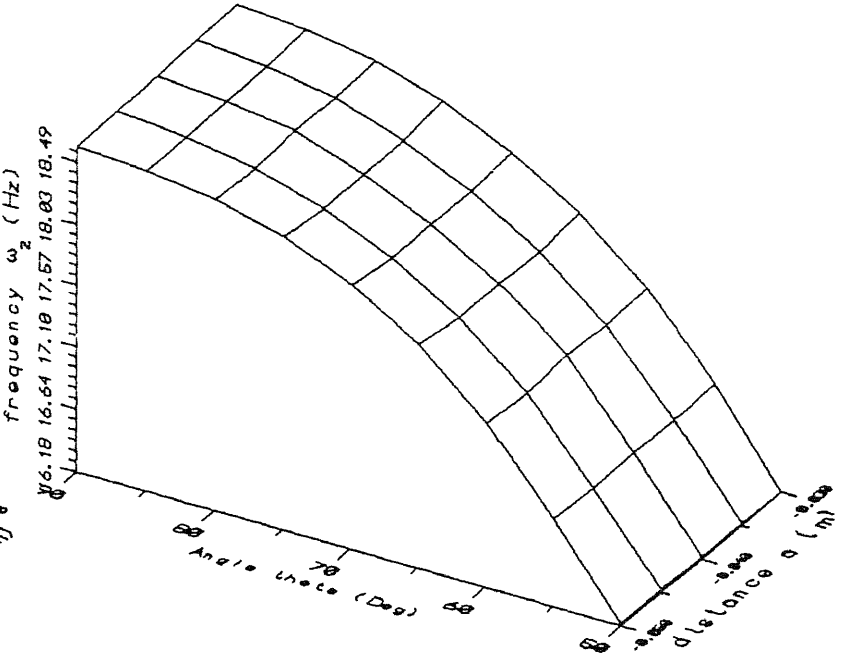

Fig. 6.3b Surface Curve of ω_2 for

b = 240 mm

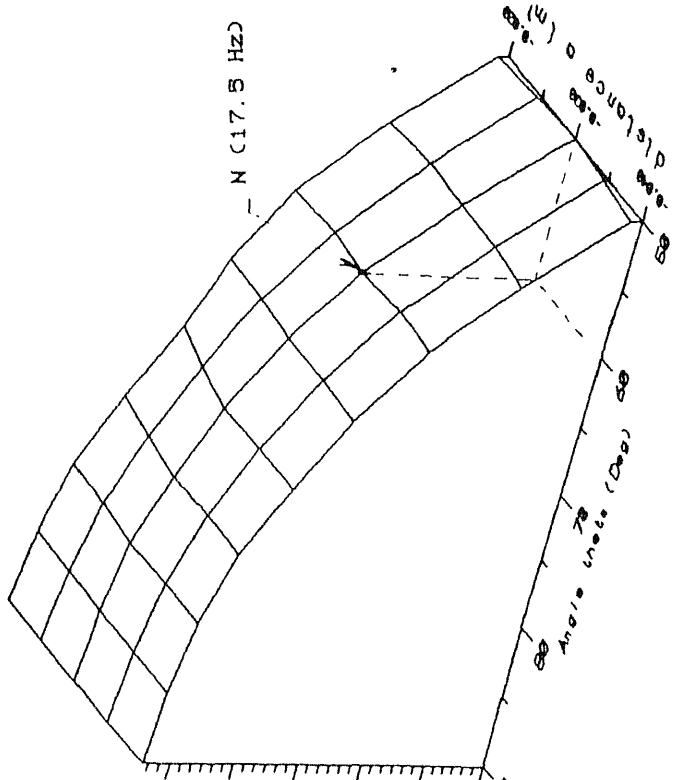

Fig. 8.4a Surface Curve of ω_2 for b = 260 mm

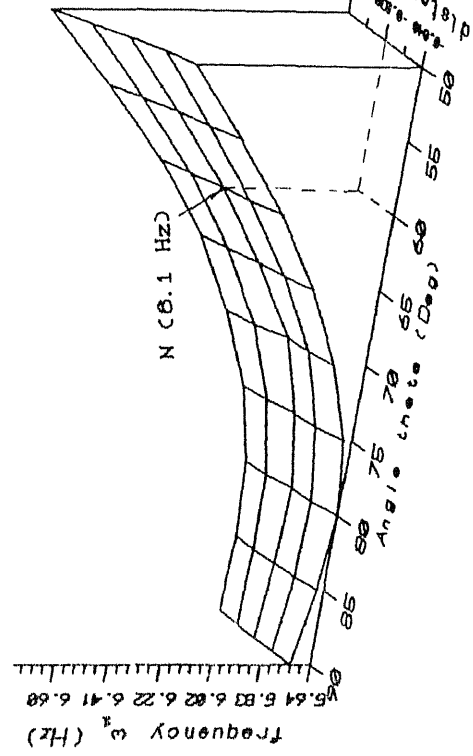

Fig. 8.4a Surface Curve of ω_1 for b = 260 mm

With the above location, ω_1 = 6.10 Hz (below the firing speed at idling) and ω_2 = 17.5 Hz is obtained.

The para below explains the basis of selecting the above location for Design 2.

The geometrical constraints stated in this Section restricts the angle θ to be below 55°. This means ω_2 can not be below the idling speed. From Figs. 6.3 and 6.4, it is observed that ω_1 through out has a value below 6.5 Hz when mounted just above C.G. and therefore falls below the firing speed at idling ($2\omega_1$ less than idling). With change in a, not much change in value of ω_1 and ω_2 is observed. With increase in b, ω_1 marginally goes up. Due to presence of a channel and a central tube, and thus the space limitation the idea of placing the isolators below C.G to eliminate rocking of engine is ruled out.

Thus to eliminate rocking vibrations of the engine, isolators are to be placed above the channels and the central tube. On the channel side of the engine mounting, the rubber cannot be mounted at a height of more than 25 mm from the channel as then it would be obstructed by the air filter projecting out from the engine, while the engine vibrates during running condition. On the lower side of the isolators there is a stud projecting out, for which space should be available and also for the nut that has to be tightened on it. So it would be better if stud projects out of channel. For which b has to be greater than 260 mm.

From the above discussion, an improved location N (Fig.6.4) is suggested, in keeping with the space restriction imposed by the engine and the vehicle's body.

These isolators project out enough to be accommodated inside the outer steel sheet body of the three wheeler. θ equal to 60°, besides giving ω_1 value equal to 6.02 Hz will give a softer and stable mounting as compared to those angle greater than 60°. While b equal to 260 mm allows the stud to stay away from the channel, so that it can be screwed on easily. ω_2 is around 17.5 Hz and will be crossed over as the vehicle begins to accelerate.

The hardware requirement for the Design 2 is discussed in hardware Configuration of Design 2 (Sec.6.5).

6.3 Comparision Of The Two Design:

The solutions are rather independent in nature i.e both have different functional utility.

(i) Design 1 aims at reducing drastically the vibrations at idling thereby giving only rocking mode to the engine-mount system as it accelerates. This results in a comfortable ride for the passengers but the problem of the breakage of the exhaust pipe stays on.

(ii) Design 2 aims at eliminating the rocking mode of engine vibrations. The vibrations at idling are also reduced. As the vehicle accelerates, the other resonant frequencies are easily crossed.

6.4 HARDWARE CONFIGURATION OF DESIGN 1:

Figure 6.5a shows the present engine mount design. As we see that not much of change in location and orientation has been recommended in the Design 1, the present mount design can be slightly redesigned. The redesigned engine mount is shown in Fig.6.5b. As the change required for obtaining a vibration free idling condition, is not much, S.I.L Lucknow would find it easy to make the required changes.

6.5 HARDWARE CONFIGURATION OF DESIGN 2:

Figure 6.6 shows, the proposed Hardware Configuration Of Design 2, conforming with the location as suggested in Design 2. In this design, three things need to designed are:

(i) Channel Rest

(ii) Bottom Rest

(iii) Bracket

The structure above the channel, on which isolators rest are called as Channel Rest while the structure above the central tube used for the similar purpose is called Tube Rest. The third thing that needs to designed is the bracket, which connects the engine to the rubbers.

6.5.1 DESIGN OF CHANNEL REST:

The Channel Rest is the structure, above the channel, on which the rubber isolators rests. In the present vehicle, the maximum normal dynamic load on the isolator is approximately 1350 N. In the present vehicle, the plate on which the isolator rest has an overhang of 60 mm (Fig.6.5a). But in the proposed Design 2, the overhang is small about half of the present one. Thus this 3 mm thick plate will serve the purpose (Fig.6.6) of lowering of forces due to increase in moment arm. However the mounting has to be reinforced so that it becomes rigid. Further reinforcement has to be provided by welding a triangular plate at each ends of the rest, part of which is also welded to the channel.

6.5.2 DESIGN OF TUBE REST:

The Tube Rest is the structure, above the tube, on which the rubber isolators rests. As shown in Fig.6.6, the part is again made of a 3 mm plate, the thickness being again decided on the same ground as the Channel Rest. Another plate is welded in between to serve as reinforcement. Here again triangular plate has to be provided at the two ends of the curved plate, which are welded to the channel also.

6.5.3 DESIGN OF BRACKET:

The bracket is the part that connects the engine to the rubber isolators. This is a very critical member of the engine mounting

system. While mounting the engine, it may so happen that for a fraction of time, the whole of the engine weight may come on one bracket, along with some impact. This part takes a substantial amount of dynamic loads also.

The bracket in the present vehicle is 6 mm thick and is 174 mm wide. The width of the designed mount has to remain same keeping with the location requirement of engine and the space availability. The length is primarily decided by the location of isolator (Fig.6.6). Thus, as the width and length are nearly specified, the thickness remains the variable at hand. With a high safety margin, the thickness is calculated equal to 11 mm. The thickness being decided by assuming the bracket as a cantilever with a force acting at it's free end. Hence the bracket comes out as a curved bent plate at an angle of 60°, made out of 386 X 174 X 11 mm size plate. This plate needs to be further reinforced to make it more stiffer.

6.6 CLOSURE:

In this chapter, two solution zones for the engine mounting locations were searched and a improved location under space constraints, were suggested.

The two solution, Design 1 and Design 2 were proposed.

The actual design of the engine-mount for the Design 1 will drastically reduce vibrations at idling.

Design 2 takes care of the engine rocking thereby tackling the problem of breakage of exhaust pipe, along with less vibrations at idling.

CHAPTER 7

FEM ANALYSIS OF THE CHASSIS VIBRATIONS

7.1 INTRODUCTION:

In the previous chapters for the sake of simplicity the engine mountings have been assumed to be supported on fixed supports. However, in reality they are fixed to the chassis which is a flexible elastic structure. It is the aim of this chapter to investigate the modes of the chassis and check whether the vibration modes of the chassis match with the excitation from the engine. In such a situation the engine vibration are transmitted to the chassis which will make the whole vehicle vibrate to the discomfort of the passengers. The present investigation uses the finite element analysis of the chassis to determine the natural frequencies and mode shapes.

7.2 BASICS OF FINITE ELEMENT FORMULATION:

In finite element methodology the domain of the problem is divided into a number of sub domains known as elements interconnected at nodal points. Equilibrium equations are derived for each element and assembled to make global equilibrium equations. Those equations are derived here using virtual work principle.

The principle of virtual work states that if a general structure in dynamic equilibrium is subjected to a system of small infinitesimal displacements, within a compatible state of deformation, the virtual work of external actions is equal to virtual strain energy of internal stresses.

Applying the above principle to a finite element,

$$\delta U_e = \delta W_e$$

where,

δU_e is virtual strain energy of internal stresses and

δW_e is virtual work of external action on the element.

For a single element, this work balance, excluding damping, comes out as,

$$\int_V \{ u \}^T \{ F \} dV + \int_S \{ \delta U \}^T \{ \phi \} dS + \sum_{i=1}^{n} \{ \delta u \}_i^T \{ P \}_i = \int \{ \delta \varepsilon \}^T \{ \sigma \} + \{ \delta u \}^T \rho \{ \ddot{u} \} \qquad (7.1)$$

where,

$\{ \delta u \}$ and $\{ \delta \varepsilon \}$ are respectively infinitesimal arbitrary displacements and their corresponding strains, $\{ F \}$ are the body forces, $\{ \phi \}$ are prescribed surface tractions, $\{ P \}$ are concentrated load that act at a total n points on the element. ρ is the mass density of the material and volume element is carried out over the elemental volume V_e.

If the displacement $\{ u \}$ are expressed in terms of nodal displacement as

$$\{ u \} = [N] \{ q \}, \quad \{ \dot{u} \} = [N] \{ \dot{q} \} \quad \& \quad \{ \ddot{u} \} = [N] \{ \ddot{q} \}$$

where, $[N]$ are shape function of space only and nodal displacements $\{ q \}$, are functions of time.
Equation 7.1 leads to,

$$\{ q \}^T \left[\int_V [B]^T \{ \sigma \} dV + \int_V \rho [N]^T [N] dV \{ \ddot{q} \} - \int_V [N]^T \{ F \} dV - \int_S [N]^T \{ \phi \} dS - \sum_{i=1}^{n} \{ P \} \right] = 0 \qquad (7.2)$$

Since $\{ \delta d \}$ is arbitrary, the above equation can be written as,

$$[m] \{ \ddot{q} \} + [r^{int}] = [r^{ext}] \qquad (7.3)$$

where,

$$[\ m\ ] = \int_{V_e} \rho\ [\ N\ ]^T [\ N\ ]\ dV$$

and the element internal force and external load vector are defined as,

$$\{\ r^{int}\ \} = \int_{V_e} [\ B\ ]^T \{\ \sigma\ \}$$

$$\{\ r^{ex}\ \} = \int_{V_e} [\ N\ ]^T \{\ F\ \} dV + \int_{S} [\ N^T\ ]\ \{\ \phi\ \} dS + \sum_{i=1}^{n} \{\ P\ \}_i \qquad (7.4)$$

Structure Matrices [M] and { R^{int} } are constructed by the conceptual expansion of element matrices [m] and { r^{int} } to ' structure size '.

The consistent mass matrix [m] are positive definite because ρ is positive. The internal force vector, represents loads at nodes caused by straining of material.

For linearly elastic material behavior,

$$\{\ \sigma\ \} = [\ E\ ]\ [\ B\ ]\ \{\ q\ \} \qquad (7.5)$$

where [E] is matrix relating time - varying stresses in $\{\sigma(t)\}$ to strain in $\{\ \varepsilon(t)\ \}$.

and equation 7.4 becomes,

$$\{\ r^{int}\ \} = [\ k\ ]\ \{\ q\ \} \qquad (7.6)$$

where the usual definition of stiffness matrix holds i.e

$$[\ k\ ] = \int_{V_e} [\ B\ ]^T\ [\ E\ ]\ [\ B\ ]\ dV \qquad (7.7)$$

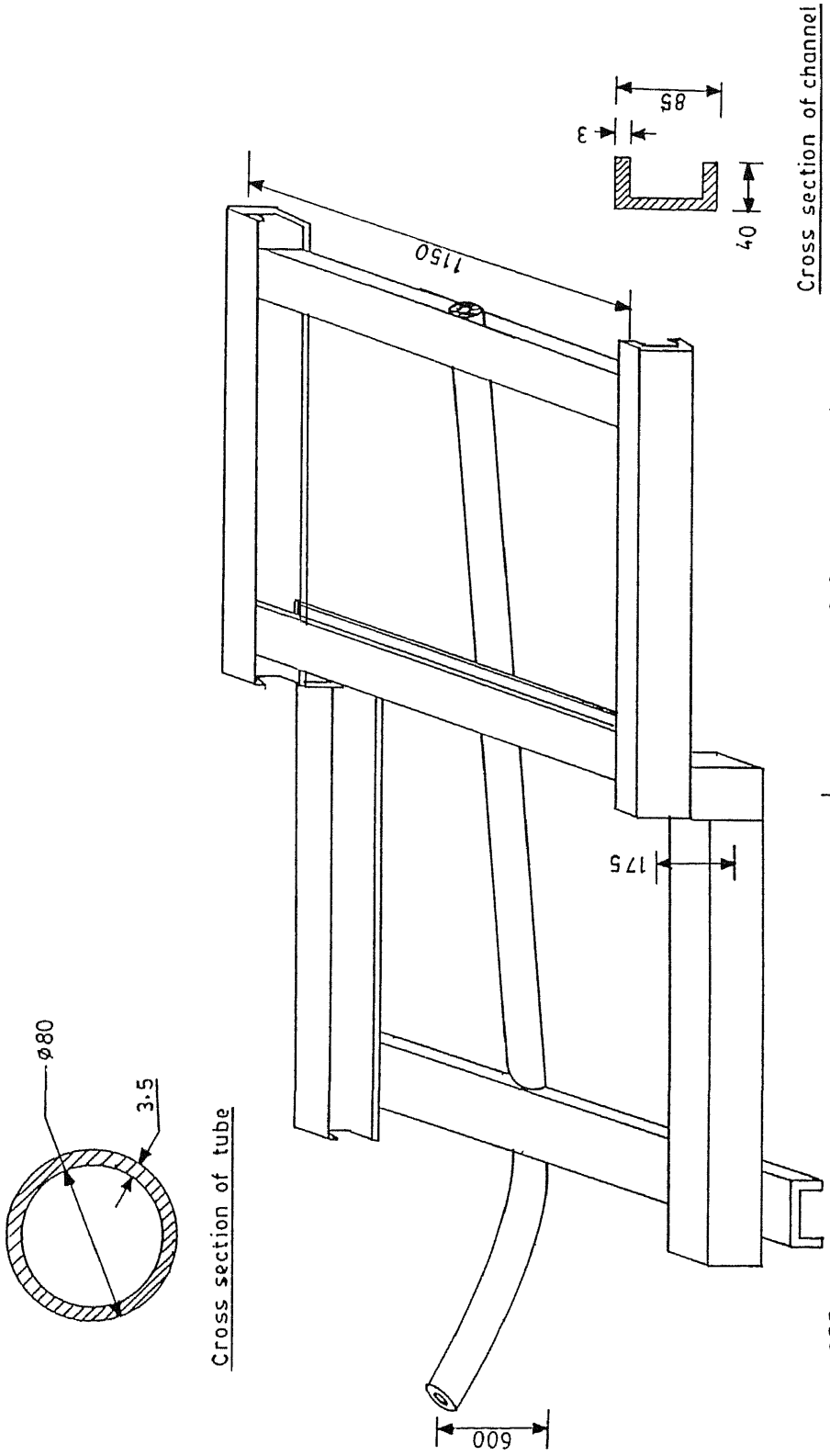

Fig. 7.1 Schematic diagram of chassis of vikram

leads equation 7.2 to the form

$$[\ m\ ]\ \{\ \ddot{q}\ \} + [\ k\ ]\ \{\ q\ \} = \{\ r^{ext}\ \} \qquad (7.8)$$

For the assembled structure, we get

$$[\ M\ ]\ \{\ \ddot{Q}\ \} + [\ K\ ]\ \{\ Q\ \} = \{\ R^{ext}\ \} \qquad (7.9)$$

where $\{\ R^{ext}\ \}$ corresponds to loads $\{\ R\ \}$ of a static problem but is in general a function of time.

7.3 ELEMENT STIFFNESS AND MASS MATRIX:

The present chassis can be looked upon as a space frame consisting of general beam elements (frame element) of which the location of joints and direction of member are completely arbitrary, and the structure is designed to carry forces that are general in space. Each node is has three components of translation and three components of rotational degrees of freedom. The stiffness and mass matrix are determined from axial, torsional and flexural considerations. Such members are first expressed in local directions and then transformed to global direction by rotation of axes. The $[\ k\ ]$ and $[\ m\ ]$ matrices are given in Appendix C. Then these transformed elemental matrices are assembled up to build up stiffness and mass matrices of the whole structure.

7.4 ANALYSIS OF THE PRESENT CHASSIS:

7.4.1 Introduction to Chassis Structure:

Figure 7.1 shows the chassis of the three wheeler *'VIKRAM'*. It is made of a central tube through out the length of vehicle. This tube can be called the central main element of the entire vehicle. Two channels running parallel to the tube are mounted to the tube through cross members, which are perpendicular to the tube attached to the tube. These cross members are also channel sections having the same crossectional area as that of side channel. The crossection of the channel and the tube is shown in Fig. 7.1.

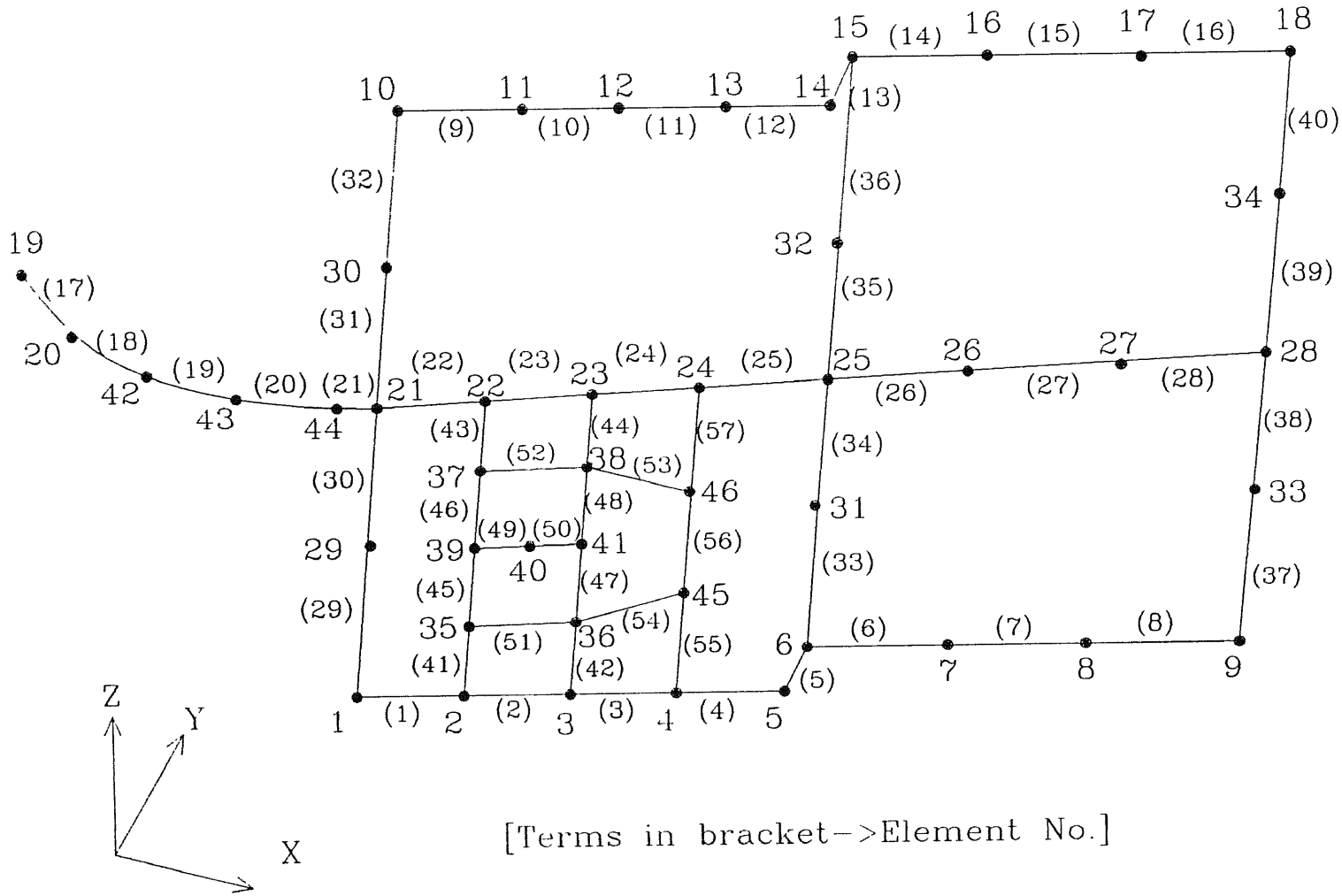

[Terms in bracket->Element No.]

Fig 7.2 Discretized Chassis

7.4.2 Discreatization of the Chassis Structure:

For the finite element analysis, the chassis is discretized into 57 frame elements as shown in Fig. 7.2. The mass of the structure is 570 kg was distributed equally on each node. The engine weight of 130 kg and, as the C.G. lies in the plane of the nodes 35, 36, 37, 38, 44 and 45, was distributed at six supports i.e amongst these six nodes. The payload that the vehicle carries when fully loaded is equal to 700 kg. This load is distributed amongst the nodes on the channels.

7.4.3 Results:

The elemental mass matrices [m] and the stiffness matrices [k] are determined by using the data of inertia's of elements, areas of element, connectivity amongst elements, density of element and orientation and location in space along with the necessary boundary conditions. As the aim is to find the different natural frequencies and its mode shape, the chassis is assumed to be supported at six nodes by springs of very small stiffness. In other words, it is assumed to be unrestrained with springs being added to the system for the sake of obtained solution which, otherwise make [K] singular. The element matrices were transformed and assembled. The mass and stiffness matrices were used to determine natural frequencies and the mode shape using subroutines of NAG library.

For the present chassis, the natural frequencies determined, are as follows:

0.00038	Hz	0.007	Hz	0.010	Hz	
0.03	Hz	0.04	Hz	0.05	Hz	
9.55	Hz	11.73	Hz	12.45	Hz	
12.98	Hz	14.03	Hz	15.04	Hz	
16.78	Hz	18.32	Hz	20.46	Hz	etc

The present vehicle, by nature of its use stays at idling while loading and unloading passengers. The idling speed of engine

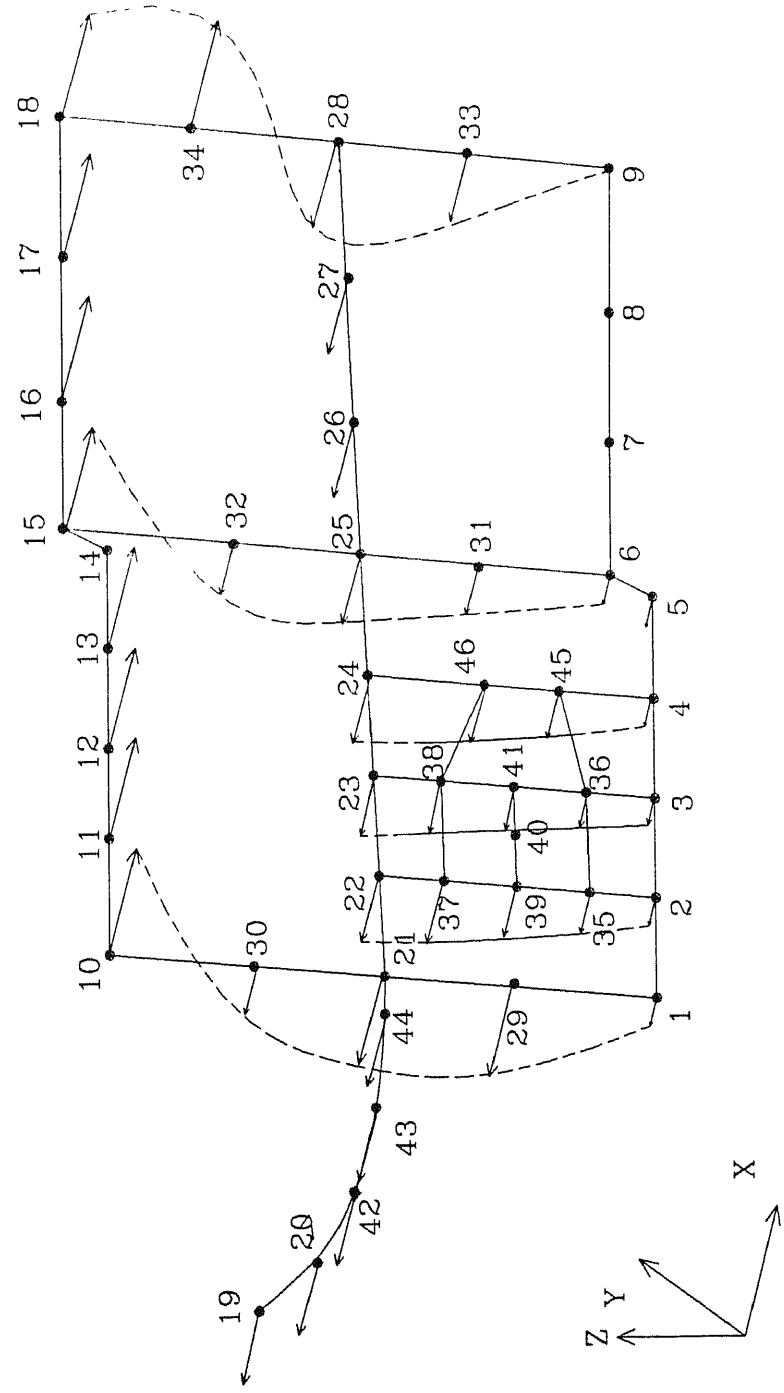

Fig 7.3(a) Mode Shape in X Direction at 14.03 Hz

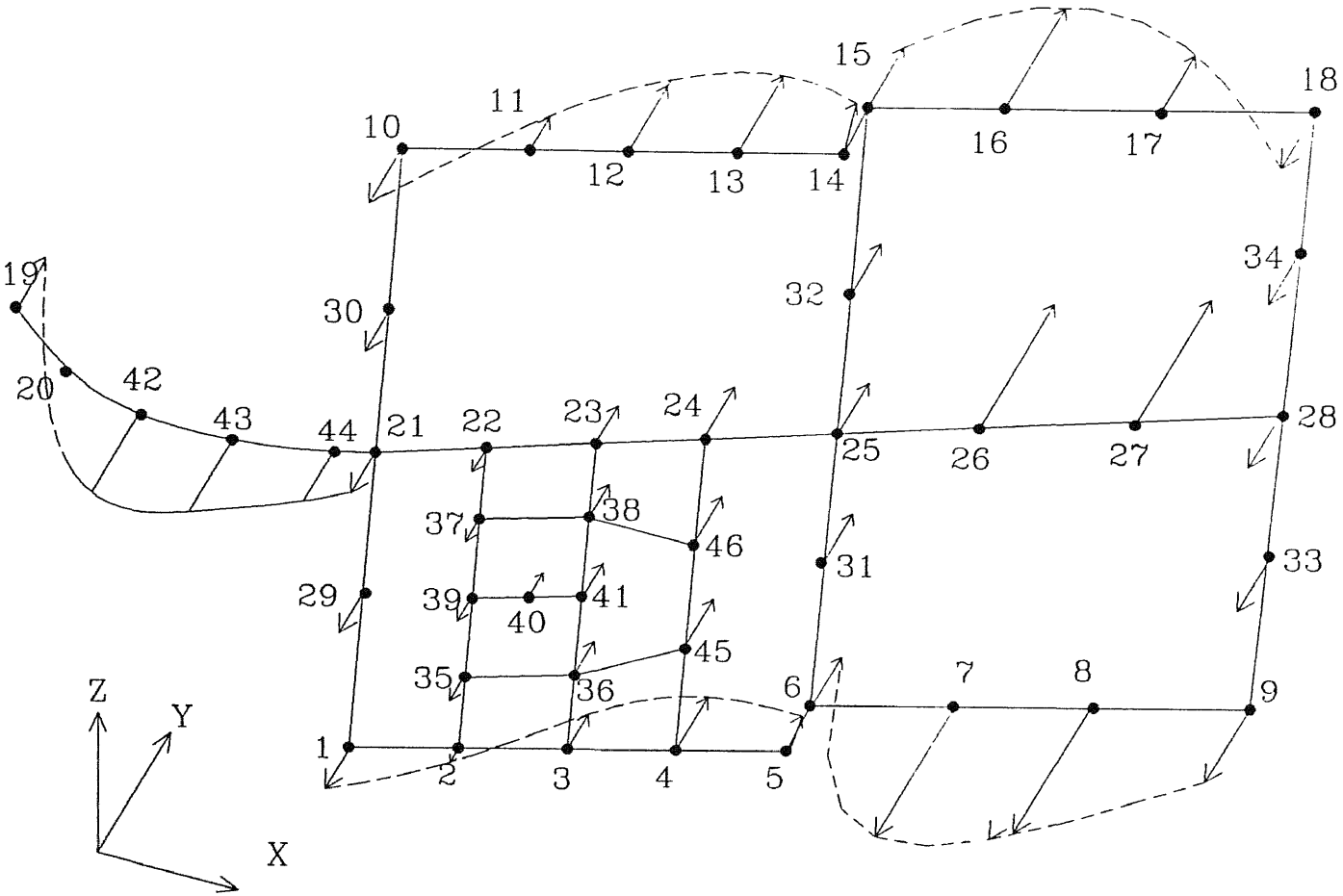

Fig 7.3(b) Mode Shape in Y Direction at 14.03 Hz

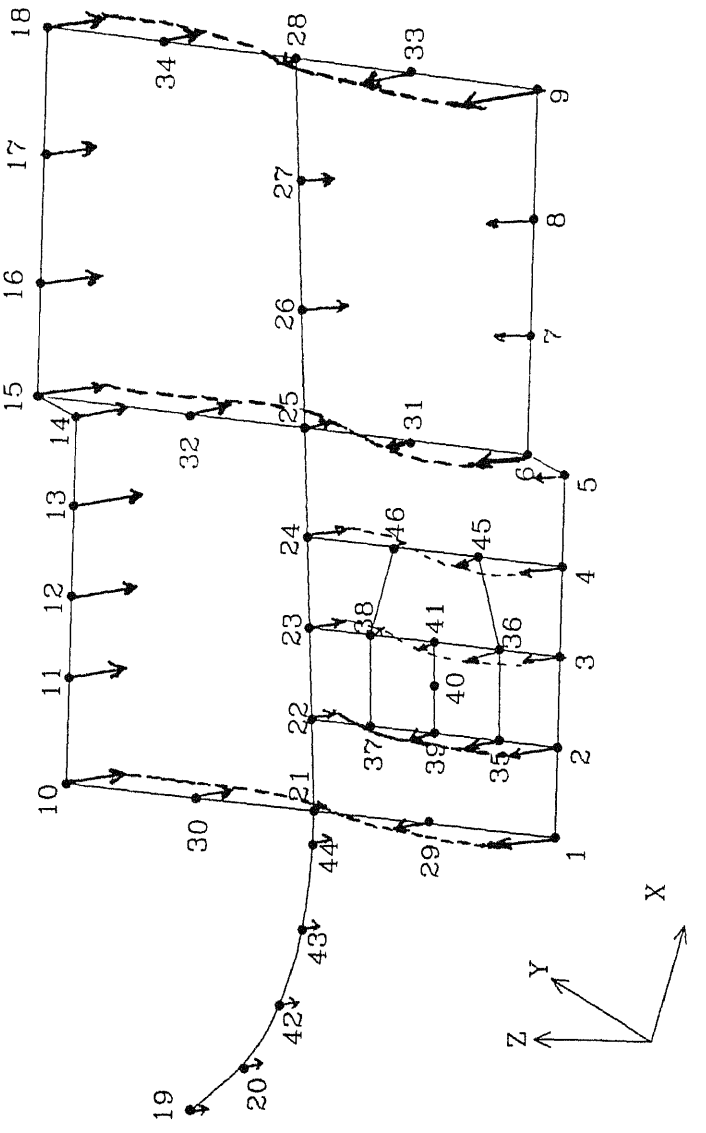

Fig 7.3(c) Mode Shape in Z Direction at 14.03 Hz

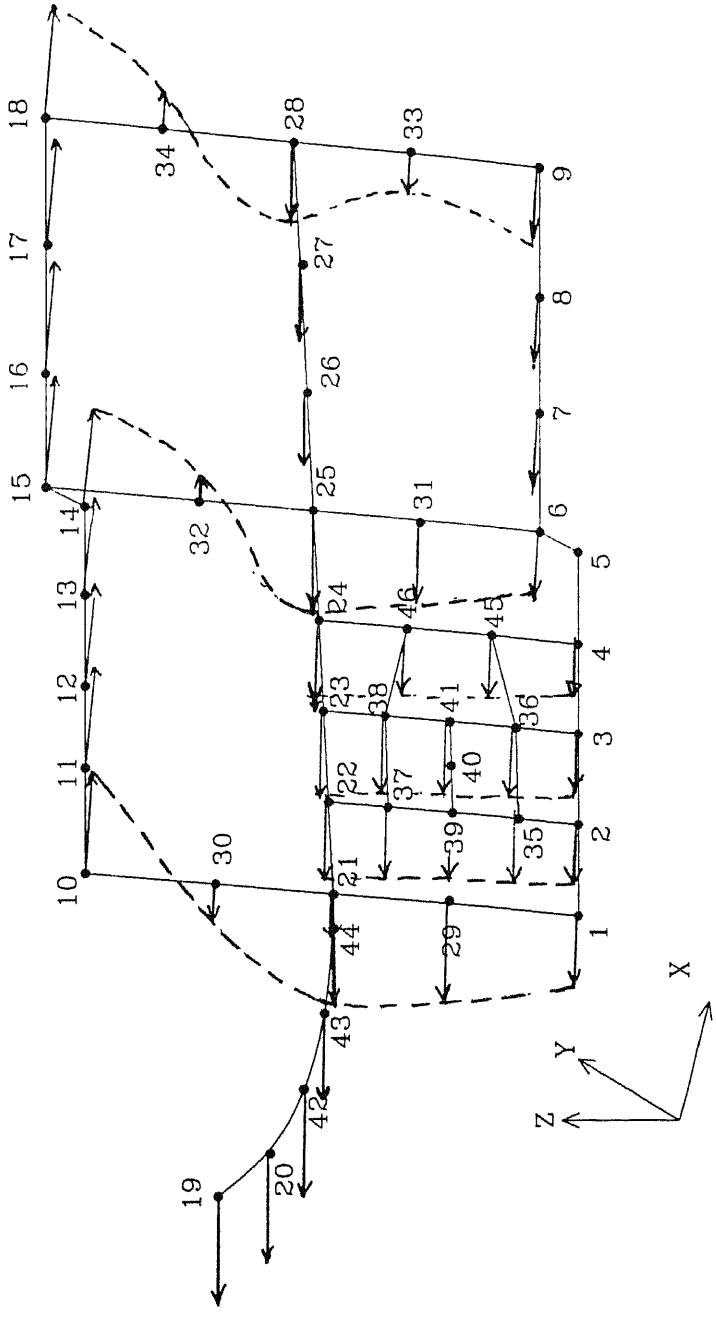

Fig 7.4(a) Mode Shape in X Direction at 15.05 Hz

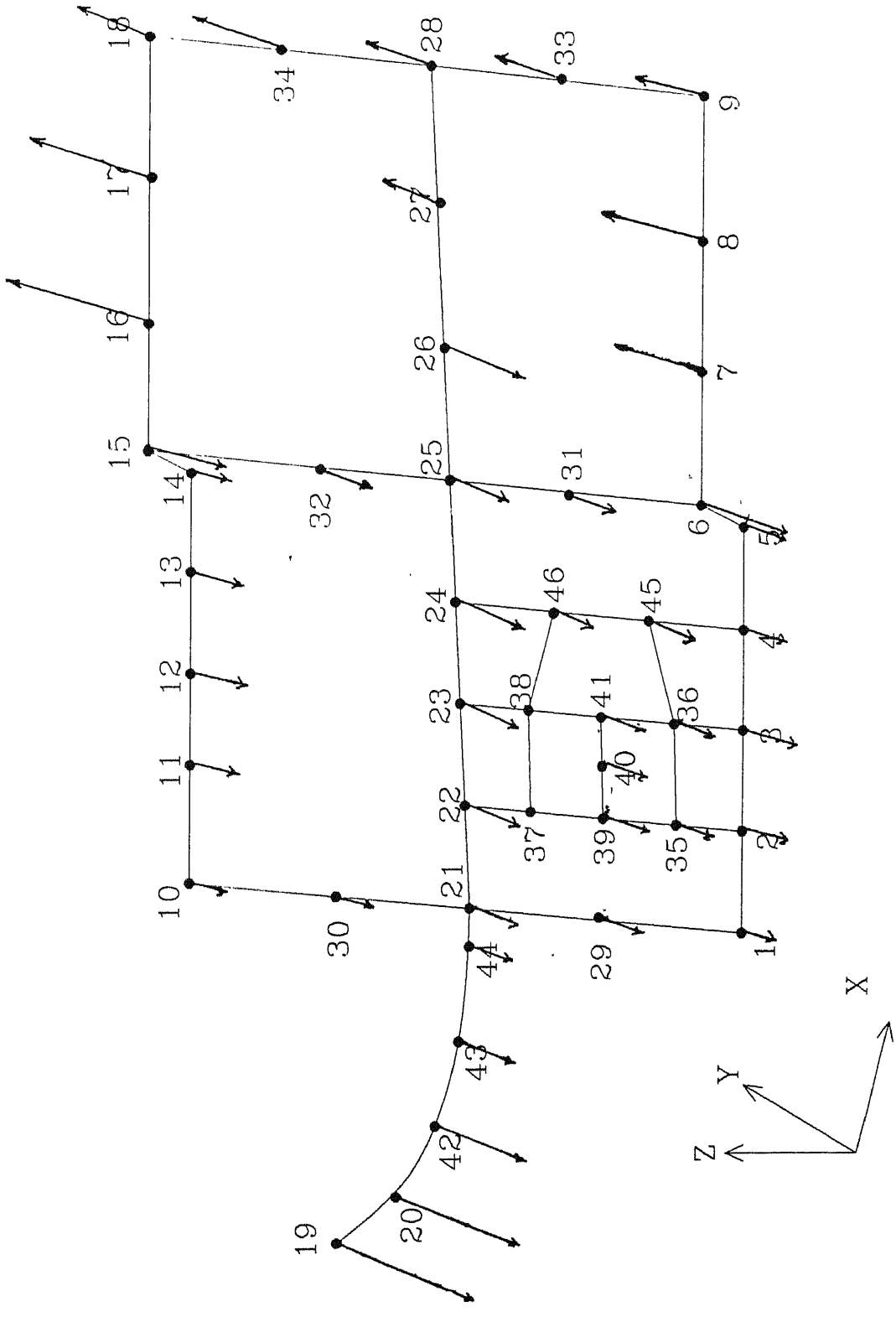

Fig 7.4(b) Mode Shape in Y Direction at 15.05 Hz

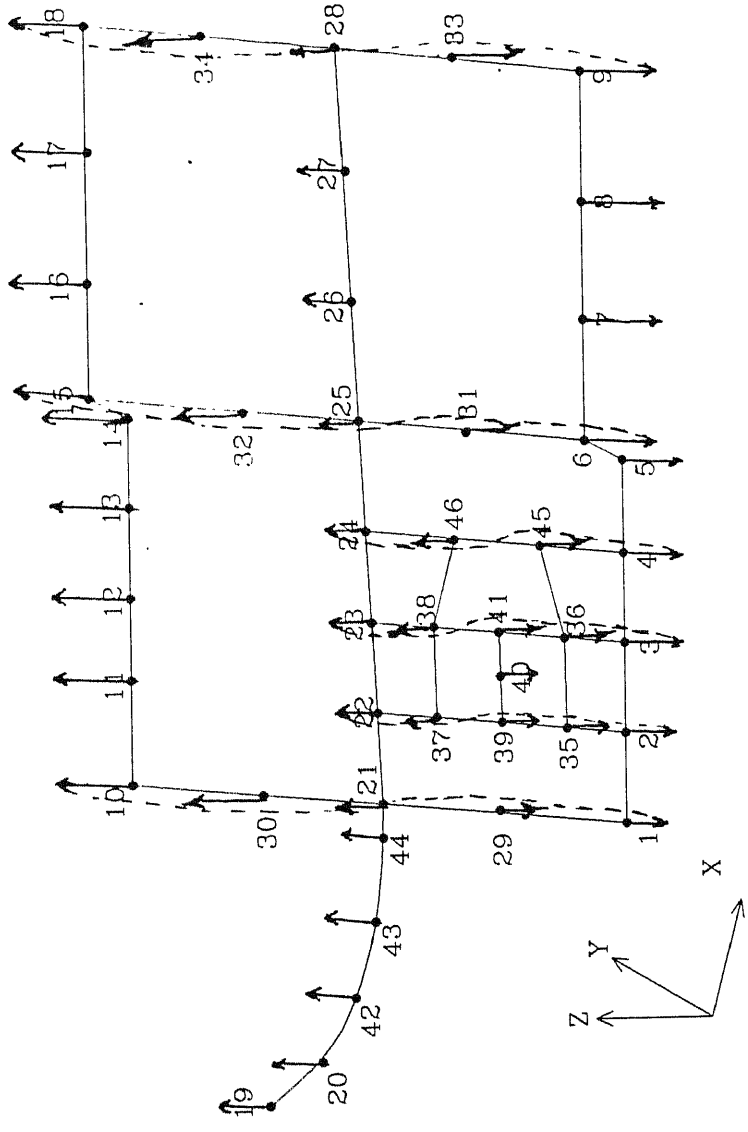

Fig 7.4(c) Mode Shape in Z Direction at 15.05 Hz

(Sec.5.1) is 14.25 Hz. The natural frequency of the engine-mount system around idling is 14.35 Hz (Sec.5.3). When the vehicle is idling, engine goes into vibration corresponding to mode of natural frequency of 14.356 Hz. There are two structural natural frequencies of the chassis close to idling speed. They are frequency of 14.03 Hz and 15.05 Hz. These two frequencies will get excited around the idling only if the mode o vibrations of the engine is similar to the mode shape of the vibrating structure. Hence to ascertain the nature of vibrations of the structure, the mode shape at frequency of 14.03 Hz and at frequency of 15.05 Hz needs to be looked into.

Figures 7.3 and 7.4 shows the mode shape for X, Y and Z directional deflection of the structure, at natural frequency of 14.03 Hz and 15.05 Hz respectively. From Fig.7.3c, Node 35, 36, and 45 go up in vertical direction, correspondingly nodes 37, 38, and 46 come down therefore it is observed from vibrations of nodes, that the engine mounting nodes are going in a rocking mode of vibrations about Z axis. From Fig.7.4c, for the structural natural frequencies of 15.03 Hz, the engine-mount nodes is again observed to have a rocking mode of vibration. That is around the idling, the two structural frequencies close by, have rocking vibrations of engine mounting nodes.

From Sec.5.4, the engine-mount analysis at frequency of 14.35 Hz was found to be vertical. But from the chassis analysis vibration mode of engine mounting nodes on the structure is rocking about Z axis. As these two modes of vibration happens to be different, a cumulative build up of excitation at this frequency is ruled out.

Thus in absence of matching of modes of vibration of engine and its mounting structure, the chassis would not go into enhanced vibrations, as a result of vibrations of the engine. Concluding from the above analysis, the existing chassis is found to be satisfactory vis a vis the excitation of its nodes at idling speed. The proposed designs of chapter 6 too do not have engine-mount natural frequencies close to the idling speed. As a result the existing chassis would work well with the proposed design also.

The finite element analysis undertaken in the present chapter can be done with an increased number of elements and figuring out the mode shape more closely. With a better knowledge of the exciting force as function of time and including damping, a study of higher modes of excitation can be done to ascertain whether any higher harmonics are exciting the structure or not as the engine force might comprise of some force that is exciting the structure into steady state vibrations at its frequency which stands out different from the presently considered forcing from the engine, which runs at engine speed.

CHAPTER 8

CONCLUSION AND SCOPE FOR FUTURE WORK

The aim of the present work is to develop a model of the engine-mount system of the three wheeler Vikram and analyze it. The hardware parameters required were determined. Two natural frequencies ω_1 and ω_2, responsible for the resonant phases encountered by the present vehicle, are identified. As these frequencies are dependent on the location and orientation of the isolators, parametric study was undertaken. From these studies, two locations are identified for improvement in design.

The first location leads to DESIGN 1, which will bring down the value of ω_2 below the engine idling speed. The result is drastic reduction in vibrations at the idling. The second location leads to DESIGN 2, which will bring down value of ω_1 such that it is never encountered during the entire engine travel. The result is no rocking mode encountered by the engine mount system i.e less breakage of the exhaust pipe.

The finite element study of the chassis structure reveals that at idling the chassis does not go into enhanced vibrations as a result of engine excitation. Hence the present structure of chassis is satisfactory.

In the present work, methods have been suggested to bring only one of the resonating frequencies below the idling speed. However by trying out different isolators it should be possible to bring both of these frequencies below the idling speed (with the space constraints imposed) as that would come out as a better design of the engine-mount.

With the knowledge of exciting force as a function of time and the damping present, a realistic response of the vibrating engine and the structure at resonance condition can be predicted.

REFERENCES

1. Hull E.H. & Stewart W.C. " Elastic Supports for Isolating Rotating Machinery ". Trans. A.I.E.E, Vol. 50-No 3, September 1931. pp 1063-1068.

2. Crede C.E. " Vibration and Shock Isolation ". John Wiley and Sons, New York 1951.

3. Crede C.E. & Walsh J.P. " The Design of Vibration Isolating Bases or Machinery ". Journal of Applied Mechanics, Vol.14-No.1, March 1947. pp A-7 - A-14.

4. Hull E.H. " The Use of Rubber in Vibration Isolation ". Trans. A.S.M.E (Journal of App. Mechanics, Vol. 4-No.3), September 1937. pp A-109 - 114.

5. Downie Smith J.F. " Rubber Mountings ". Journal of Applied Mechanics, Vol. 5-No.1, March 1938. pp A-13 - A-23.

6. Crede C.E. " Determining Moment of Inertia ". Machine Design, Vol. 20.-No.8, August 1948. pp 138.

7. Crede C.E. & Harris C.M. " Shock and Vibration Handbook Mcgraw-Hill book Company, INC. 1961.

11. Krishnamoorthy C.S. " Finite Element Analysis Thory and Programming ". Tata Mcgraw-Hill Publishing Company Limited N. Delhi, 1988.

12. Weaver W. & Johnston P.R. " Structural Dynamics by Finite Elements ". Prentice-Hall, INC., New Jersey, 1987.

APPENDIX A

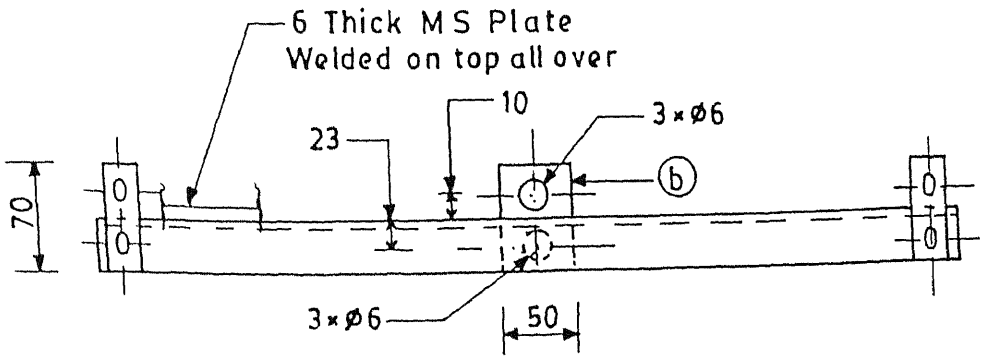

ELEVATION

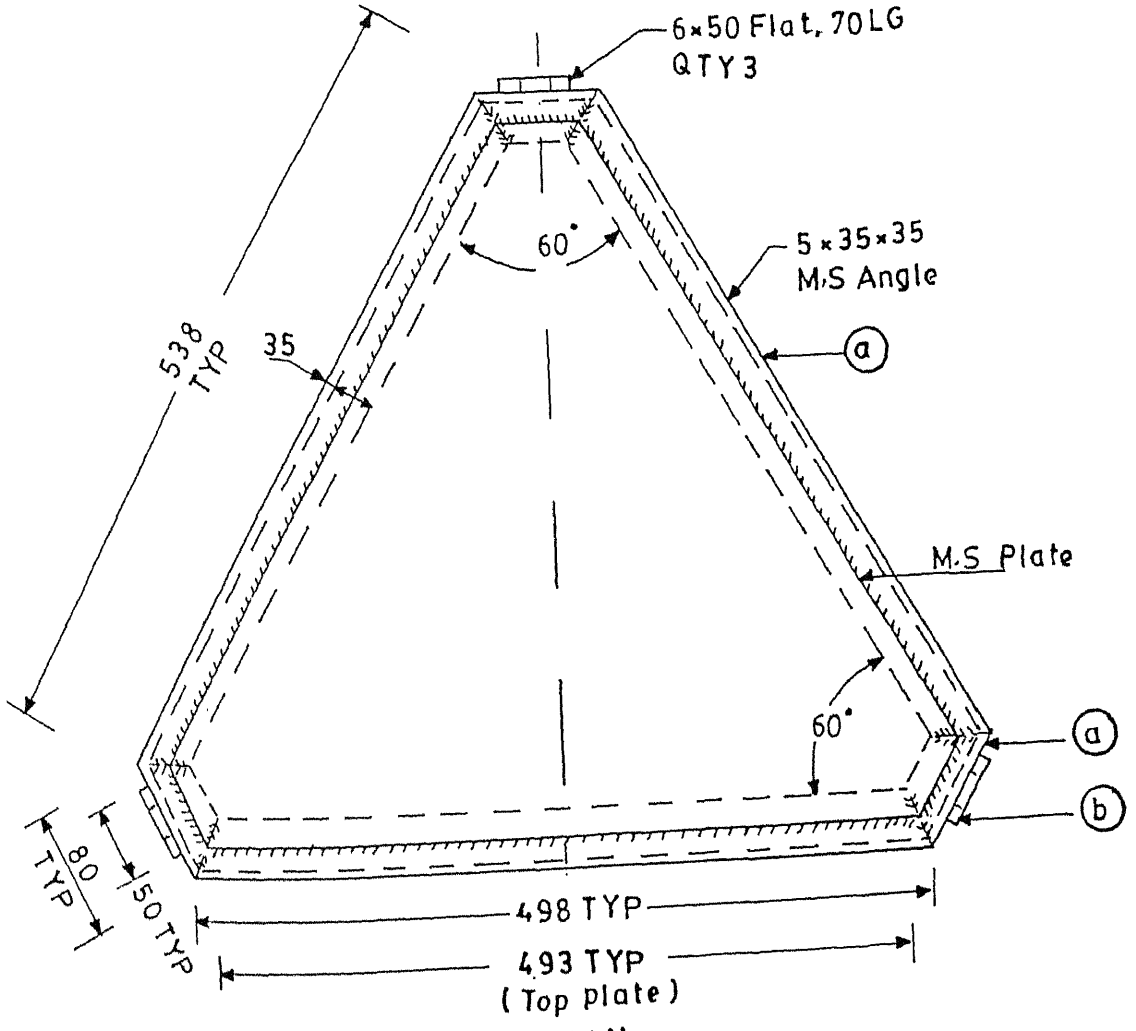

PLAN

Fig. A.1 BASE FRAME

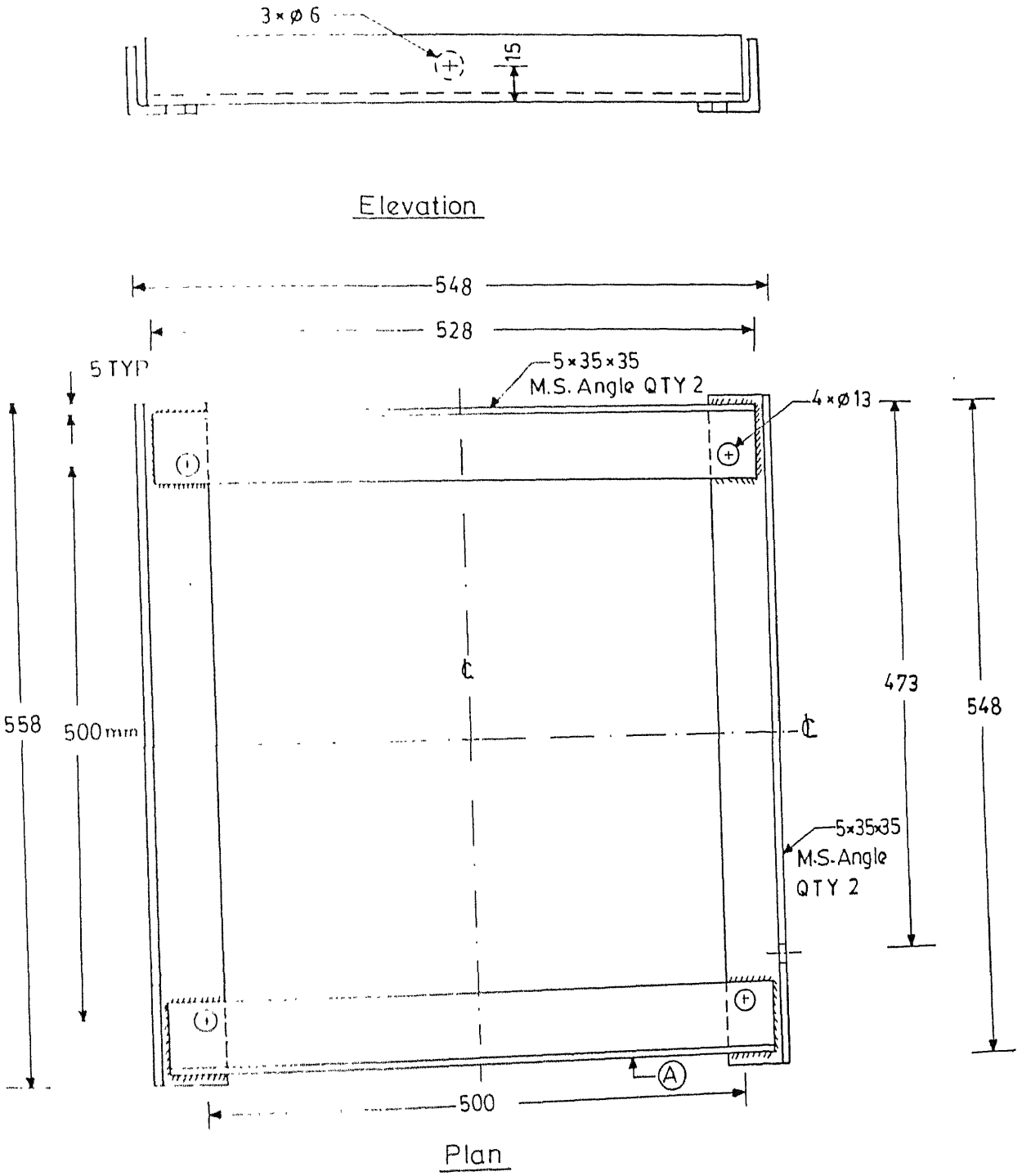

Fig.A2 Roof Frame

APPENDIX B

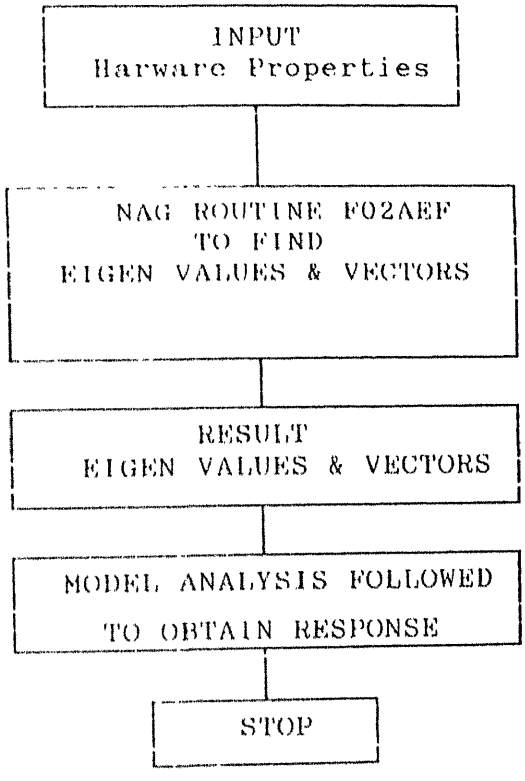

Fig. A.3 Flow Chart For Vibrational Analysis of Modelled Engine

APPENDIX C

$$
[k] = \begin{bmatrix}
\frac{EA}{L} & 0 & 0 & 0 & 0 & 0 & -\frac{EA}{L} & 0 & 0 & 0 & 0 & 0 \\
 & \frac{12EI_z}{L^3} & 0 & 0 & 0 & \frac{6EI_z}{L^2} & 0 & -\frac{12EI_z}{L^3} & 0 & 0 & 0 & \frac{6EI_z}{L^2} \\
 & & \frac{12EI_y}{L^3} & 0 & -\frac{6EI_y}{L^2} & 0 & 0 & 0 & -\frac{12EI_y}{L^3} & 0 & -\frac{6EI_y}{L^2} & 0 \\
 & & & \frac{GI_x}{L} & 0 & 0 & 0 & 0 & 0 & -\frac{GI_x}{L} & 0 & 0 \\
 & & & & \frac{4EI_y}{L} & 0 & 0 & 0 & \frac{6EI_y}{L^2} & 0 & \frac{2EI_y}{L} & 0 \\
 & & & & & \frac{4EI_z}{L} & 0 & -\frac{6EI_z}{L^2} & 0 & 0 & 0 & \frac{2EI_z}{L} \\
 & & & & & & \frac{EA}{L} & 0 & 0 & 0 & 0 & 0 \\
 & & & & & & & \frac{12EI_z}{L^3} & 0 & 0 & 0 & -\frac{6EI_z}{L^2} \\
 & & & & & & & & \frac{12EI_y}{L^3} & 0 & \frac{6EI_y}{L^2} & 0 \\
 & & & & & & & & & \frac{GI_x}{L} & 0 & 0 \\
 & & & & & & & & & & \frac{4EI_y}{L} & 0 \\
 & & & & & & & & & & & \frac{4EI_z}{L}
\end{bmatrix}
$$

Elemental Mass Matrix.

$r_g^2 = \frac{I}{A}$, where I is the polar moment of inertia of the element

$$[m] = \frac{\rho A L}{420}$$

$$\begin{bmatrix}
140 & & & & & & & & & & & \\
0 & 156 & & & & & & & & & & \\
0 & 0 & 156 & & & & & & & & & \\
0 & 0 & 0 & 140r_q^2 & & & & \text{symmetric} & & & & \\
0 & 0 & -22L & 0 & 4L^2 & & & & & & & \\
0 & 22L & 0 & 0 & 0 & 4L^2 & & & & & & \\
70 & 0 & 0 & 0 & 0 & 0 & 140 & & & & & \\
0 & 54 & 0 & 0 & 0 & 13L & 0 & 156 & & & & \\
0 & 0 & 54 & 0 & 13L & 0 & 0 & 0 & 156 & & & \\
0 & 0 & 0 & 70r_q^2 & 0 & 0 & 0 & 0 & 0 & 4L^2 & & \\
0 & 0 & 13L & 0 & 3L^2 & 0 & 0 & 0 & 22L & 0 & 4L^2 & \\
0 & 13L & 0 & 0 & 0 & 3L^2 & 0 & -22L & 0 & 0 & 0 & 4L^2
\end{bmatrix}$$